High Temperature Superconductors (I)

Dag Winkler
Microtechnology and nanoscience, MC2
Chalmers
Göteborg

Superconductivity and Low Temperature Physics 2007

High Temperature Superconductors (I)

Dag Winkler Chalmers

winkler@fy.chalmers.se www.chalmers.se +46 31-7723474

Contents:

Brief history and introduction

The material

Electronic properties

Other properties

Anisotropy and consequences

Other bits and pieces in the puzzle…

What do we know?

What don't we know

J R Waldram: Superconductivity of metals and cuprates, (Institute of Physics, Bristol, 1996)

Brief history and introduction

Superconductivity

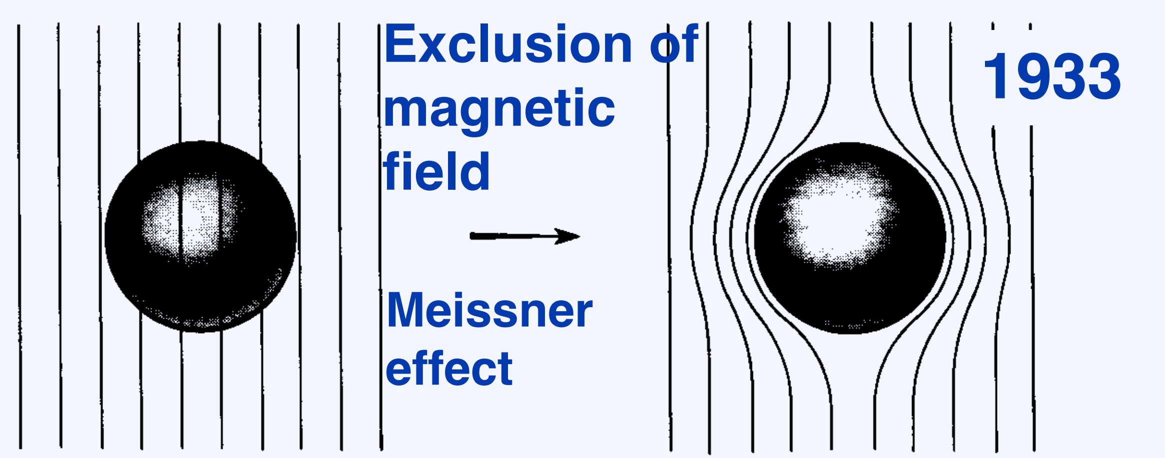

Figure 2 Meissner effect in a superconducting sphere cooled in a constant applied magnetic field; on passing below the transition temperature the lines of induction **B** are ejected from the sphere.

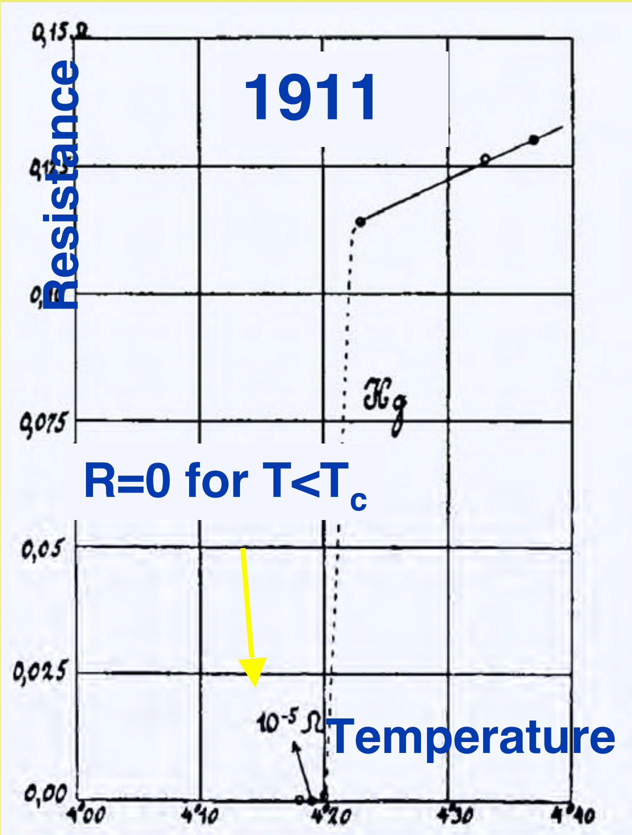

Figure 1 Resistance in ohms of a specimen of mercury versus absolute temperature. This plot by Kamerlingh Onnes marked the discovery of superconductivity.

The Meissner effect

1933 Walter Meissner and Robert Ochsenfeld

Heike Kamerlingh-Onnes

Leiden

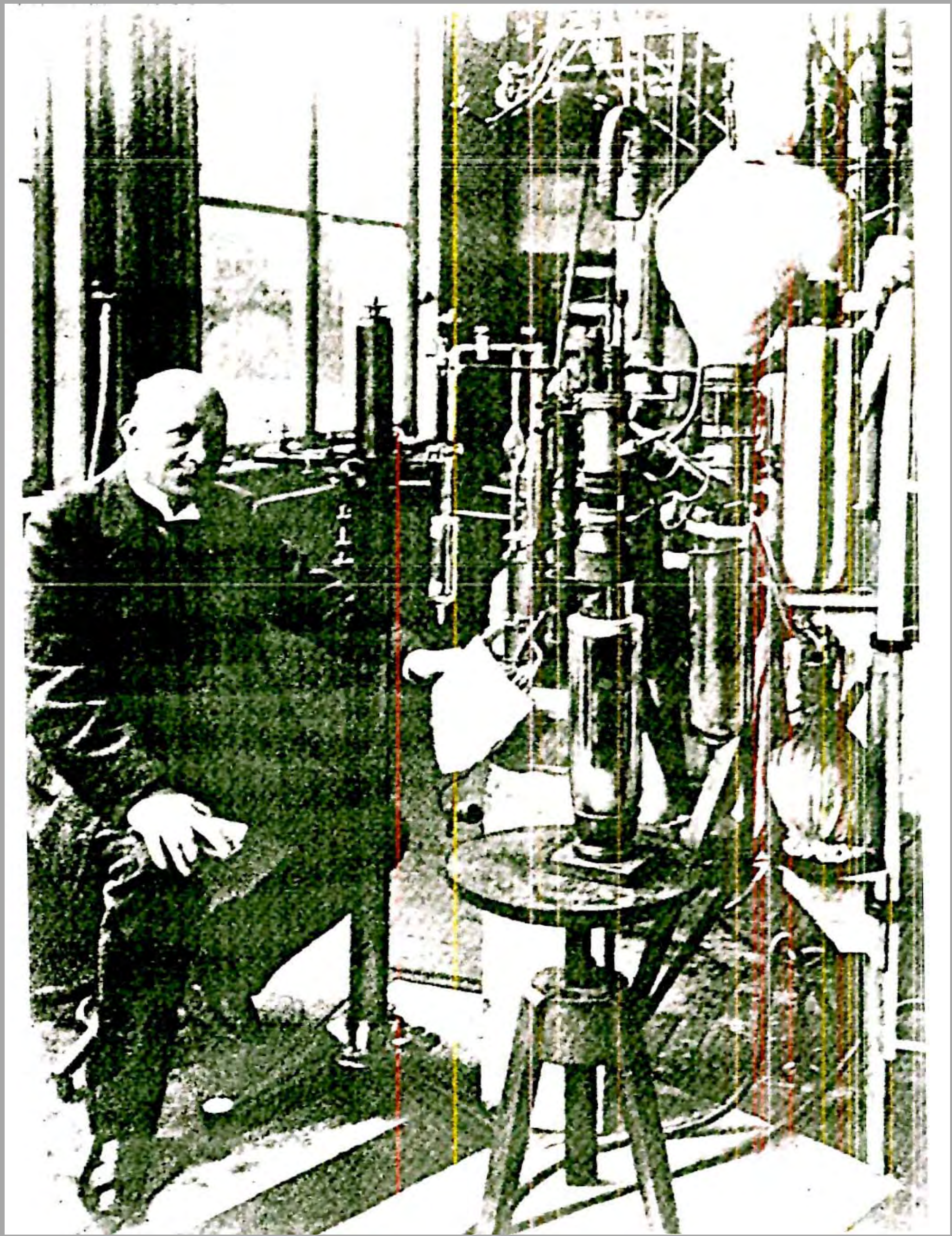

Bardeen, Cooper och Schrieffer - BCS

John Bardeen, Leon Cooper and J. Robert Schrieffer

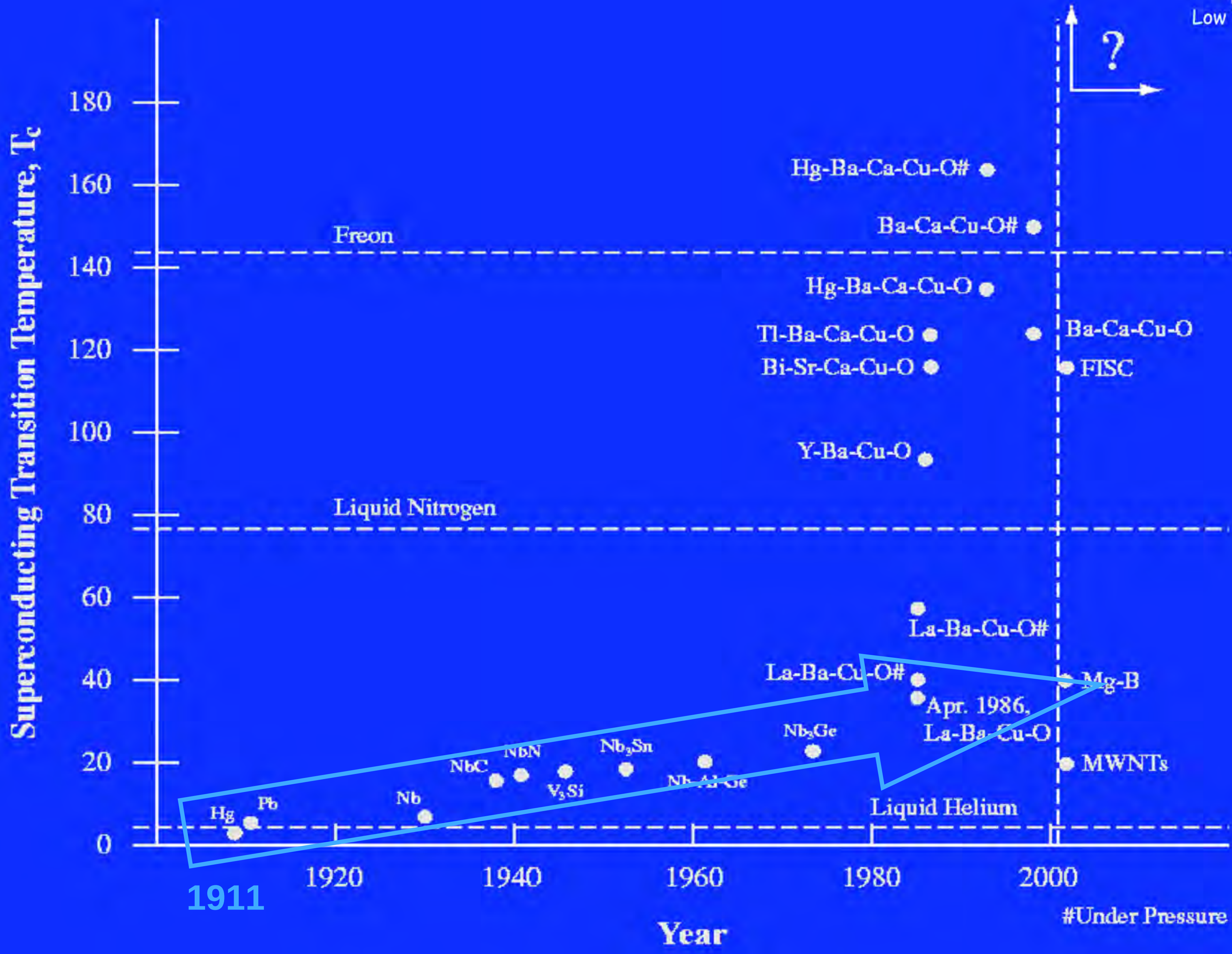
?
Superconducting Transition Temperature, T_c
180
160
140
120
100
80
60
40
20
0
Freon
Liquid Nitrogen
Liquid Helium
Hg-Ba-Ca-Cu-O#
Ba-Ca-Cu-O#
Hg-Ba-Ca-Cu-O
Tl-Ba-Ca-Cu-O
Bi-Sr-Ca-Cu-O
Ba-Ca-Cu-O
FISC
Y-Ba-Cu-O
La-Ba-Cu-O#
La-Ba-Cu-O#
Apr. 1986,
La-Ba-Cu-O
Mg-B
MWNTs
Hg
Pb
Nb
NbC
NbN
V_3Si
Nb_3Sn
Nb-Al-Ge
Nb_3Ge
1911
1920
1940
1960
1980
2000
Year
#Under Pressure

250W/W
@ LHe

TME

APS 1987

By MICHAEL D. LEMONICK

"May. 11, 1987 They began lining up outside the New York Hilton's Sutton Ballroom at 5:30 in ^ the afternoon; by the time the doors opened at 6:45, recalls Physicist Randy Simon, a member of TRW's Space and Technology Group, "it was a little bit frightening. There was a surge forward, and I was in front. I walked into the room, but it wasn't under my own power." Recalls Stanford Physicist William Little: "I've never seen anything like it. Physicists are a fairly quiet lot, so to see them elbowing and fighting each other to get into the room was truly remarkable." Thus began a session of the American Physical Society's annual meeting that was so turbulent, so emotional and so joyous that the prestigious journal Science felt compelled to describe it as a "happening." AT&T Bell Laboratories Physicist Michael Schluter went even further, calling it the "Woodstock of physics." Indeed, at times it resembled a rock concert more than a scientific conference. Three thousand physicists tried to jam themselves into less than half that number of seats set up in the ballroom; the rest either watched from outside on television monitors or, to the dismay of the local fire marshal, crowded the aisles. For nearly eight hours, until after 3 a.m., the assembled scientists listened intently to one five-minute presentation after another, often cheering the speakers enthusiastically. Many lingered until dawn, eagerly discussing what they had heard and seen. What stirred all the excitement at that tumultuous meeting in March was a discovery that could change the world, a startling breakthrough in achieving an esoteric phenomenon long relegated to the backwaters of science: superconductivity. That discovery, most scientists believe, could lead to incredible savings in energy; trains that speed across the countryside at hundreds of miles per hour on a cushion of magnetism; practical electric cars; powerful, yet smaller computers and particle accelerators; safer reactors operating on nuclear fusion rather than fission and a host of other rewards still undreamed of. There might even be benefits for the Strategic Defense Initiative, which could draw on efficient, superconductor power sources for its space-based weapons. ..."

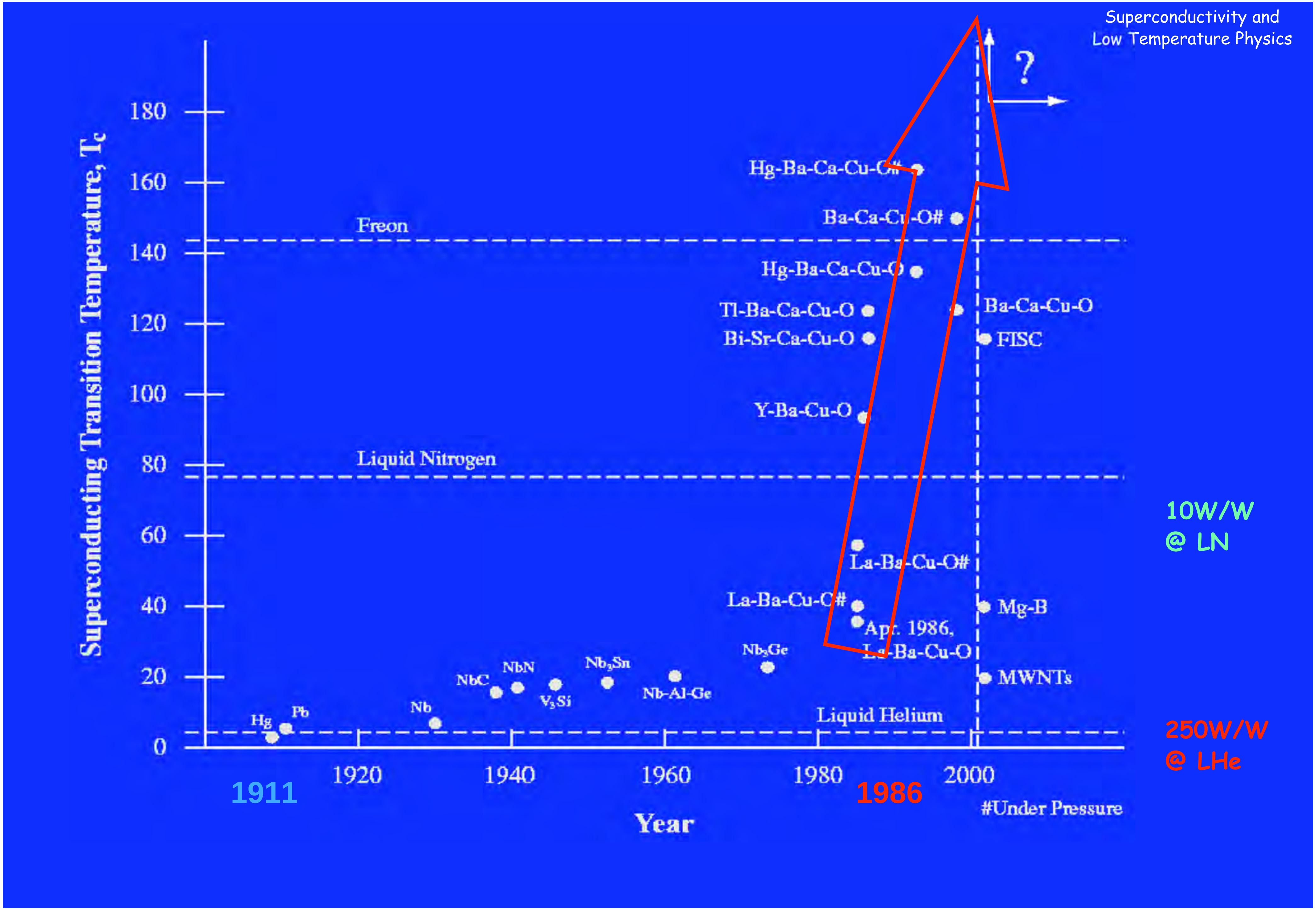
Superconductivity and
Low Temperature Physics
Superconducting Transition Temperature, T_c
180
160
140
120
100
80
60
40
20
0
Freon
Liquid Nitrogen
Liquid Helium
Hg-Ba-Ca-Cu-O#
Ba-Ca-Cu-O#
Hg-Ba-Ca-Cu-O
Tl-Ba-Ca-Cu-O
Bi-Sr-Ca-Cu-O
Ba-Ca-Cu-O
FISC
Y-Ba-Cu-O
La-Ba-Cu-O#
La-Ba-Cu-O#
Apr. 1986,
La-Ba-Cu-O
Mg-B
MWNTs
Nb_3Ge
Nb_3Sn
Nb-Al-Ge
NbN
NbC
V_3Si
Nb
Hg
Pb
?
1911
1920
1940
1960
1980
1986
2000
Year
#Under Pressure
10W/W
@ LN
250W/W
@ LHe

Superconductors

May 11, 1987

E-mail this « previous week's cover | following week's cover »


Superconducting Transition Temperature, T_c
180
160
140
120
100
80
60
40
20
0
1911
1920
1940
1960
1980
2000
1986
Superconductors
May 11, 1987
E-mail this
« previous week's cover | following week's cover »
TIME
Wiring the
THE SUPERCONDUCTIVITY REVOLUTION
Year
Freon
Liquid Nitrog
PEOPLE BEHIND REVOLUTIONARY DISCOVERIES IN SUPERCONDUCTIVITY
H. Kamerlingh Onnes (courtesy of Leiden University).
Georg Bednorz and Alex Müller, the day they obtained the Nobel Prize in 1987 (La Recherche).
Hg
Pb
Nb
NbC
NbN
V_3Si
Nb_3Sn
Nb_3Ge
Nb-Al-Ge
La-Ba-Cu
La-Ba-Cu-O
1986,
Ba-Cu-O
Mg-B
MWNTs
#Under Pressure
?
$dT_c/dt \sim 0,3$ K/year
$dT_c/dt \sim 60$ K/year
10W/W
@ LN
250W/W
@ LHe

H. Kamerlingh Onnes (courtesy of Leiden University).

Georg Bednorz and Alex Müller, the day they obtained the Nobel Prize in 1987 (La Recherche).

The Breakthrough 1986

Kritiska övergångstemperaturen, T_c
Kritiska magnetiska fältstyrkan, H_c
Maximal strömtäthet, j_c

•
•
•

Fram till 1986 är T_c - rekordet 23 K

1986 Bednorz och Müller hittar Ba-La-Cu-O med T_c kring 30 K (-243 ˚C).

Strax efteråt fick Paul Chu fram Y-Ba-Cu-O som var supraledande vid 98 K.

Idag är rekordet ~~125~~ 135 → 160 K K! (?)

(NB: Flytande helium 4.2 K
Flytande väte 20 K
Flytande kväve 77 K)

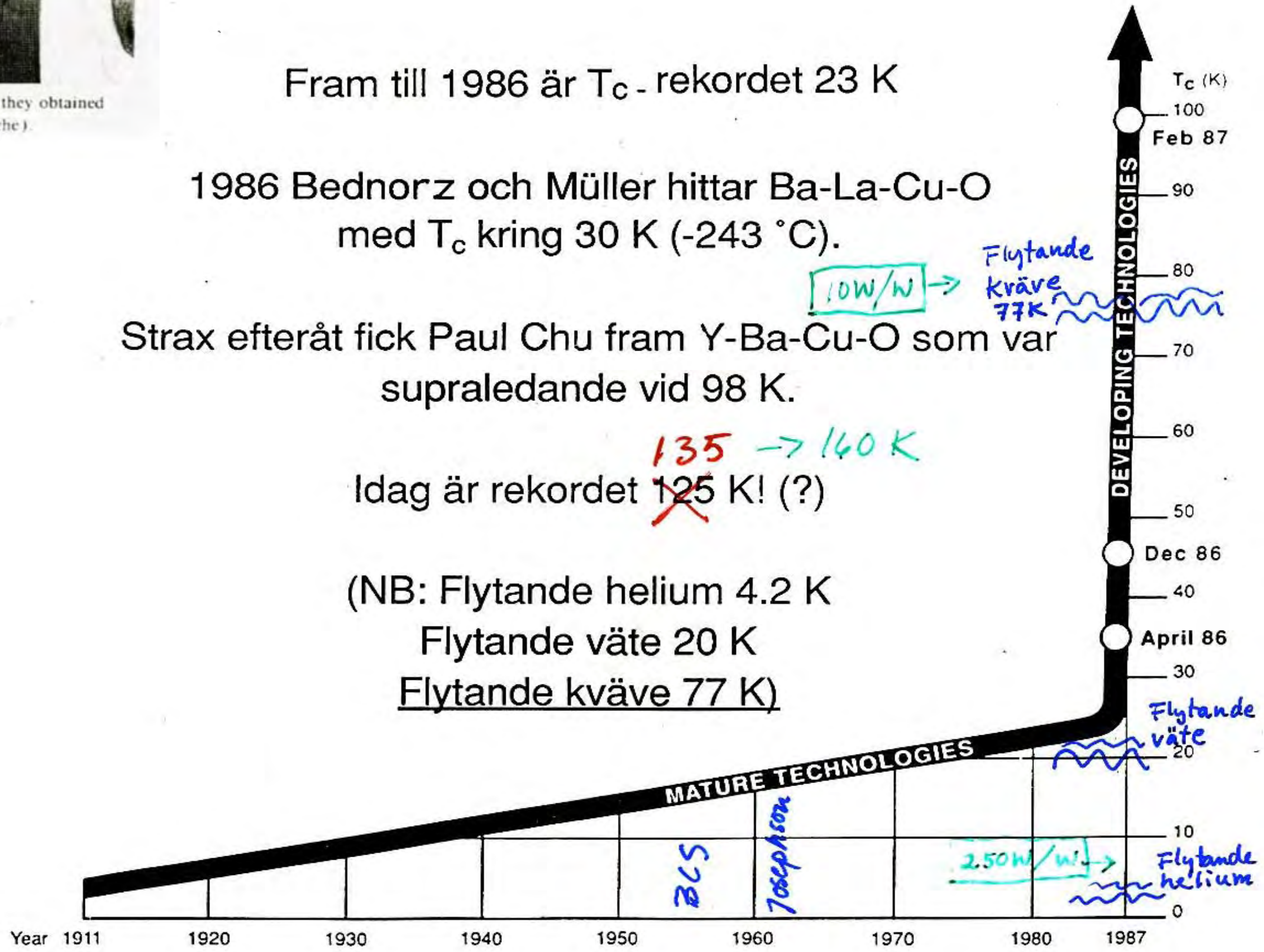

The Nobel price in physics 1987

Nobelpriset i fysik 1987

Tord Claeson och
Stig Lundqvist

Possible High T_c Superconductivity in the $Ba-La-Cu-O$ System

J.G. Bednorz and K.A. Müller
IBM Zürich Research Laboratory, Rüschlikon, Switzerland

Received April 17, 1986

Metallic, oxygen-deficient compounds in the $Ba-La-Cu-O$ system, with the composition $Ba_xLa_{5-x}Cu_5O_{5(3-y)}$ have been prepared in polycrystalline form. Samples with $x=1$ and 0.75, $y>0$, annealed below 900 °C under reducing conditions, consist of three phases, one of them a perovskite-like mixed-valent copper compound. Upon cooling, the samples show a linear decrease in resistivity, then an approximately logarithmic increase, interpreted as a beginning of localization. Finally an abrupt decrease by up to three orders of magnitude occurs, reminiscent of the onset of percolative superconductivity. The highest onset temperature is observed in the 30 K range. It is markedly reduced by high current densities. Thus, it results partially from the percolative nature, bute possibly also from 2D superconducting fluctuations of double perovskite layers of one of the phases present.

(Utdrag ur Z. Phys. B. – Condensed Matter 64, 189–193 (1986). som först presenterade de nya supraledarna)

Figur 1. Nobelpristagarna i fysik 1987. Georg Bednorz (t v) och Alex Müller.

Some stacking sequences

Table 12.1. The best known cuprate superconductors, showing the stacking of planes in the c direction.

$La_{2-x}Sr_xCuO_4$	$YBa_2Cu_3O_{6+x}$	$Bi_2Sr_2CaCu_2O_{8+x}$	$Tl_2Ba_2Ca_2Cu_3O_{10+x}$
La/Sr cuprate	YBCO 123	Bi 2212	Tl 2223
$T_c = 38$ K	$T_c = 93$ K	$T_c = 94$ K	$T_c = 125$ K
			CuO_2
	CuO_2	CuO_2	Ca
CuO_2	Y	Ca	CuO_2
	CuO_2	CuO_2	Ca
			CuO_2
(La/Sr)O	BaO	SrO	BaO
(La/Sr)O	CuO_x	$BiO_{1+x/2}$	$TlO_{1+x/2}$
	BaO	$BiO_{1+x/2}$	$TlO_{1+x/2}$
		SrO	BaO

Perovskites and cuprates

ABX_3

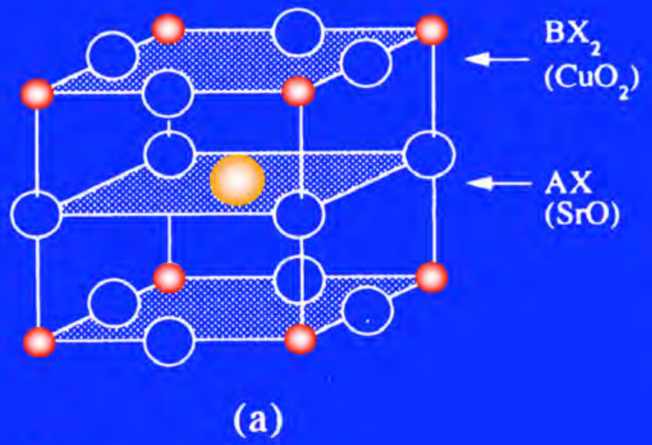

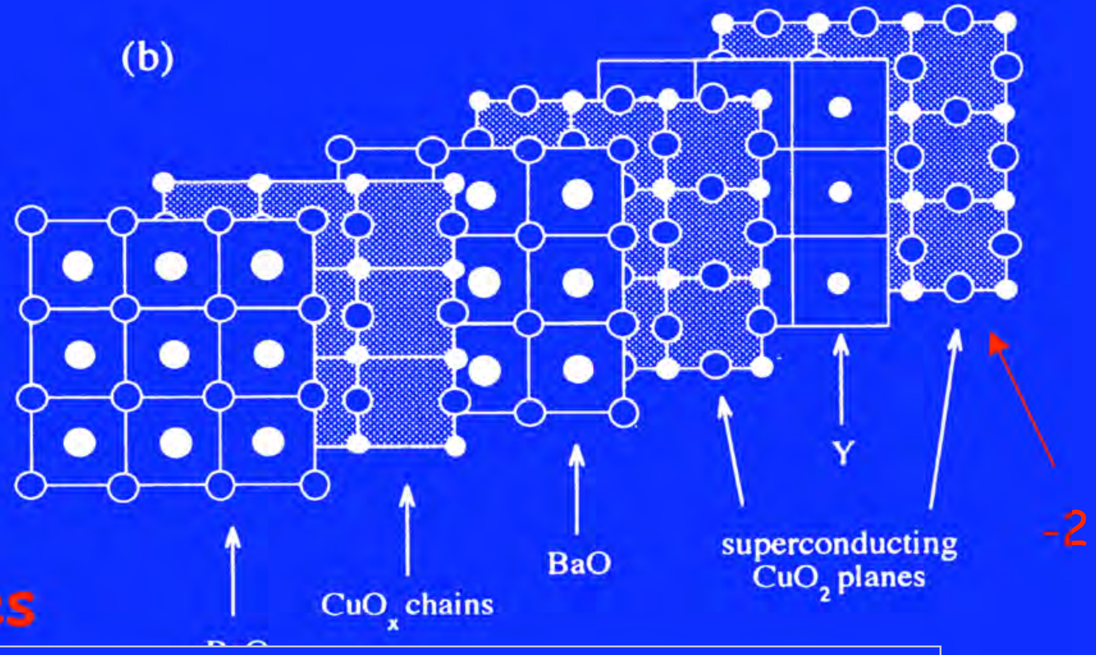

- A=Sr, Ba...
- B=Cu for the cuprates
- X=O

Just looking at the CuO_2 planes:

Figure 12.1. (a) The perovskite structure ABX_3, showing the BX_2 planes

s of the cu … rO or BaO … ertically, b … O chains in

The Cu configuration is $3d^9$ with one hole in the 3d shell

The O configuration is $2p^6$ with a complete p shell

Perovskites

Complex perovskites structures can be manipulated with regard to ions, charge doping, layering etc, to get new electronic, magnetic and superconducting properties.

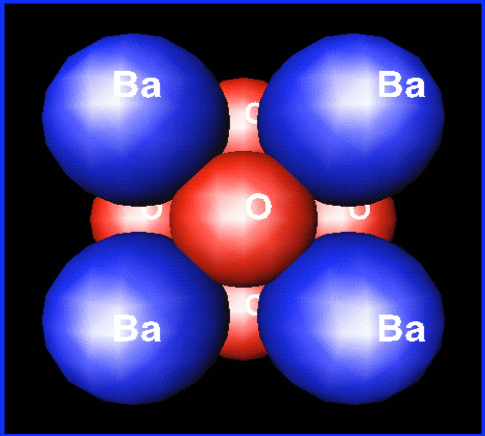

Perovskite structure

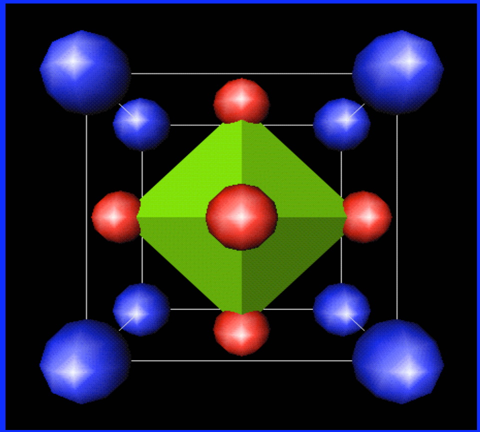

Ferroelectric

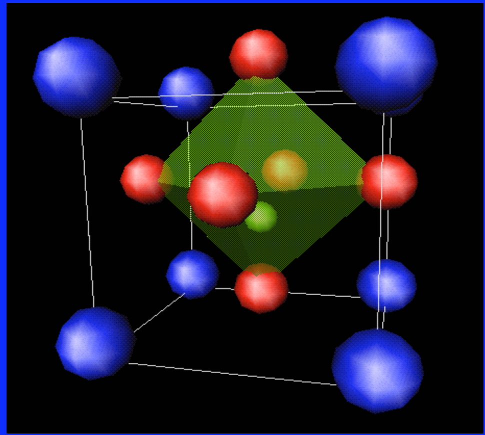

Ferroelectric

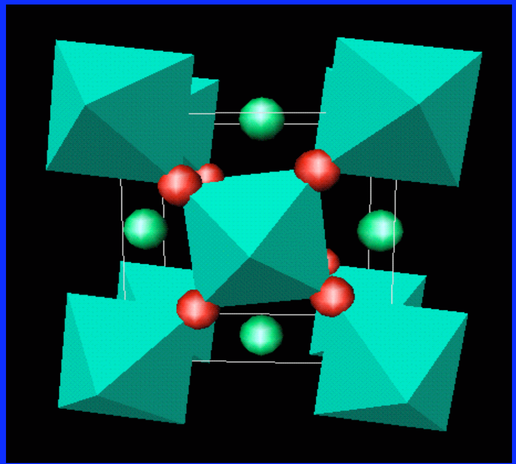

Anti-Ferroelectric

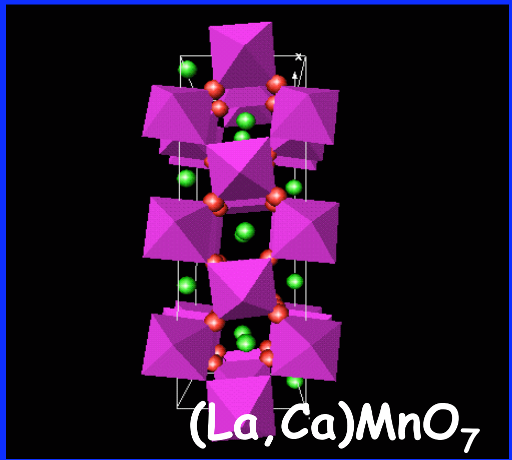

Giant Magneto-Resistive (GMR) oxides

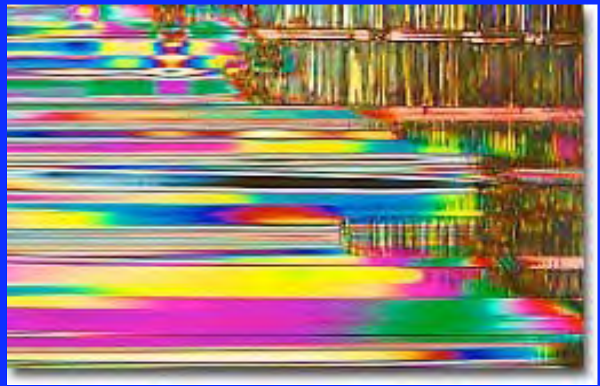

Lanthanum Aluminate
Low Magnification

http://www.ill.fr/dif/3D-crystals/index.html http://www.ill.fr/dif/3D-crystals/magnets.html

An example: $SrTiO_3$

Figure 1 Now you see it, now you don't. These micrographs of a SrTiO3 crystal show the effect of removing oxygen atoms, leaving vacancies in the crystal lattice: the glistening oxidized gem (top) is transformed into a dull blue, conductive crystal (bottom).

Semiconductor physics

The value of seeing nothing

Jochen Mannhart and Darrell G. Schlom

Ceramic superconductors

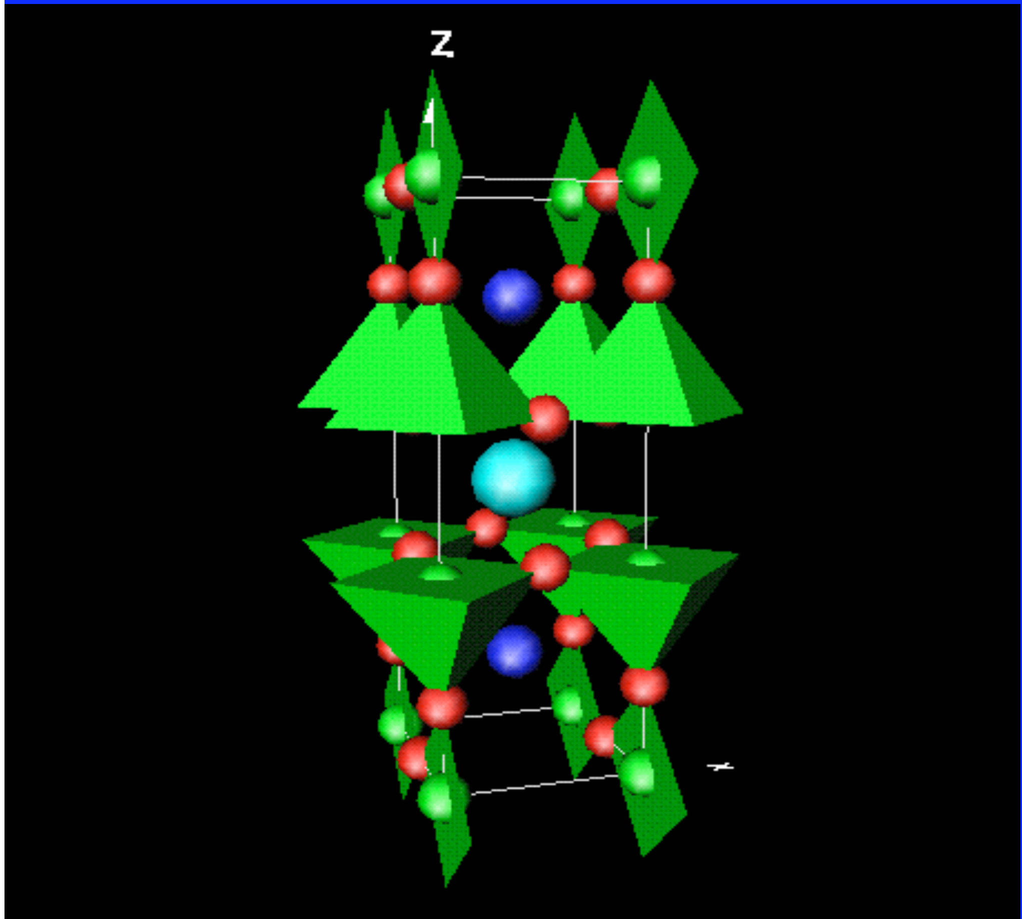

$YBa_2Cu_3O_7$

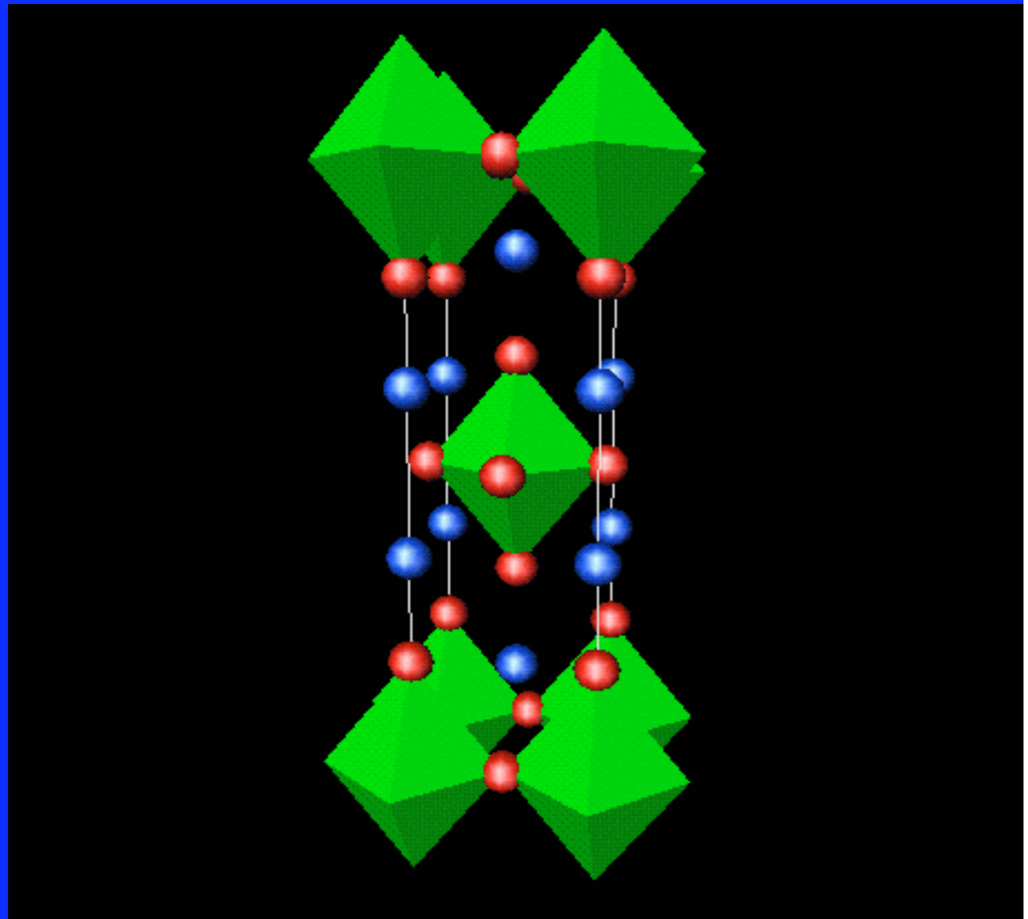

La_2CuO_4

http://www.ill.fr/dif/3D-crystals/superconductors.html

American Superconductors, and others, ...

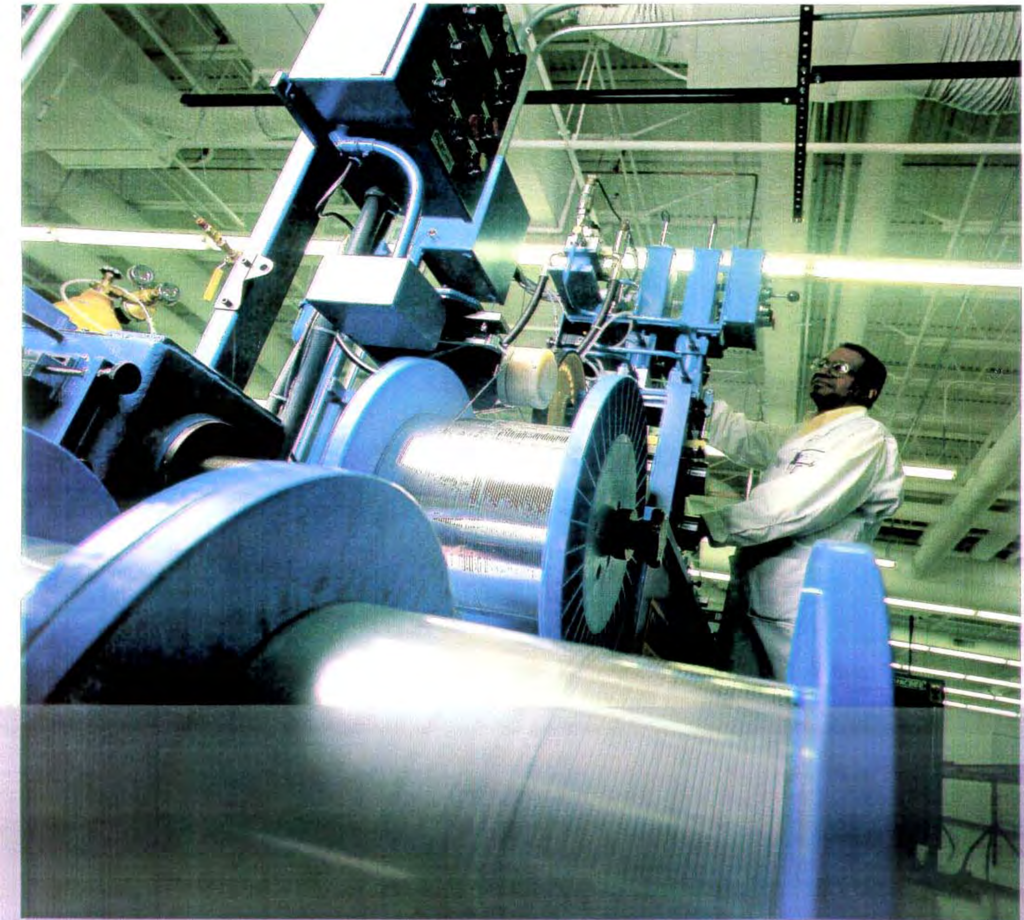

American Superconductor established the world's first pilot manufacturing line for HTS wires, a critical step in transitioning from its achievements in R&D to meeting the challenges of manufacturing. The company's manufacturing technologies, based on metal deformation processes such as wire drawing, are fully scalable to low-cost, high-volume production. The rolling mill, shown here, is used to create the internal architecture and external shape that is part of the process of transforming HTS material into usable wire. ASC currently produces approximately 900-foot lengths of wire on a day-to-day basis and has demonstrated lengths up to 3,800 feet.

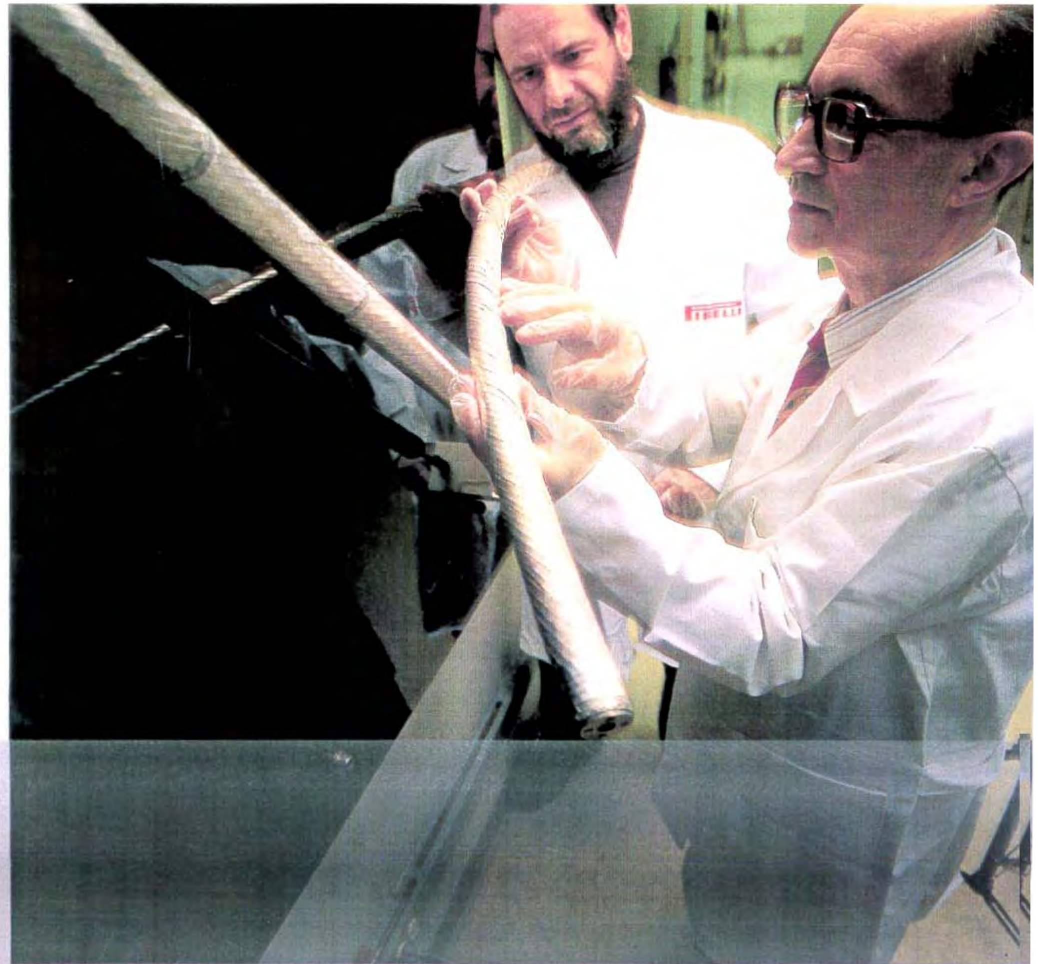

Strategic alliances have helped American Superconductor to accelerate the development of its HTS technology and to
relationships with prospective end-use customers. ASC is working closely with Pirelli Cavi SpA, one of the world's le
manufacturers of power transmission cables, on the development of HTS technology for superconducting power cable syst
The three-foot-long, 4,200 amp prototype HTS cable conductor shown above is a step toward reaching the goal of testing
scale prototype HTS power cables at electric utilities within the next three years.

Table I. Structurally or Chemically Distinct Copper Oxide Superconductors and Year of Discovery

Superconductor	Year	Superconductor	Year
$(La,M)_2CuO_4$	1986	$TlBa_2(Eu,Ce)_2Cu_2O_9$	1992
La_2CuO_{4+x}	1988		
$La_2CuO_4F_x$	1988	(Tl,Pb)SrCaCu variants of Tl, Ba, Ca compounds	1988
$(Nd,Sr,Ce)_2CuO_4$	1989		
$(Nd,Ce)_2CuO_4$	1989		
$Nd_2CuO_{4-x}F_x$	1989	$GaSr_2(Y,Ca)Cu_2O_7$	1991
Sr_2CuO_{3+x}	1993	$GaSr_2Ca_{n-1}Cu_nO_x$	1994
$Sr_2CuO_2F_{2+x}$	1994	$n = 3, 4$	
$(Ca,Na)_2CuO_2Cl_2$	1994	$AuSr_2CaCu_2O_7$	1997
$(Ca,Na)_3Cu_2O_4Cl_2$	1995	$NbSr_2(Nd,Ce)_2Cu_2O_{10}$	1992
(Sr,K) versions of previous two		$RuSr_2(Nd,Ce)_2Cu_2O_{10}$	1996
also are superconducting		and others in "1222" type with a mix of	
		Cu and M on first Cu site	
$(La,Sr)_2CaCu_2O_6$	1990	(e.g., Ti, V, Cr) also known	
$(Sr,Ca)_2(Sr,Ca)_{n-1}Cu_nO_x$	1993		
$(n = 2, 3, 4)$		$Cu(Eu,Ce)_2(Eu,Sr)_2Cu_2O_9$	1989
$PbBaSr(Y,Ca)Cu_3O_x$	1990	and others in this type with a mix of Cu and	
$Sr_{1-x}Nd_xCuO_2$	1991	M on first Cu site (e.g., Pb, Ga) also	
		known	
$YBa_2Cu_3O_7$	1987		
$YBa_2Cu_4O_8$	1988	$HgBa_2Ca_{n-1}Cu_nO_{2n+2}$	1993
$Y_2Ba_4Cu_7O_{15}$	1988	$n = 1, 2, 3, 4, 5, 6$	
$(Cu,M)Sr_2(Y,Ca)Cu_2O_7$	1988	$Hg_2Ba_2(Y,Ca)Cu_2O_8$	1994
M stabilized Sr 123		$(Hg_{0.5}Cr_{0.5})Sr_2CuO_5$	1995
M = Pb, Ga, Fe, B, SO_4, CO_3, Al, (Bi + Cd)		$(Hg_{0.5}Cr_{0.5})Sr_4Cu_2O_7CO_3$	1995
		$(Ba,Sr)_2Cu_{1+x}(CO_2)_{1-x}O_y$	1992
$Pb_2Sr_2(Y,Ca)Cu_3O_8$	1988	$(Cu_{1-x}(CO_2)_x)_m(Ba,Sr)_2Ca_{n-1}Cu_nO_y$	1994
$Pb_2(Sr,La)_2Cu_2O_6$	1988	$m = 1; n = 2, 3, 4, 5; x \neq 0$ or $x = 0$	
		$m = 2; n = 3, 4, 5; x \neq 0$	
"$Bi_2Sr_2CuO_6$"	1987		
$Bi_2Sr_2CaCu_2O_8$	1988	$Bi_2Sr_4Cu_2O_8CO_3$	1993
$Bi_2Sr_2Ca_2Cu_3O_{10}$	1988	$Bi_2Sr_5Cu_3O_{10}(CO_3)_2$	1994
$Bi_2Sr_2(Ln,Ce)_2Cu_2O_{10}$	1990	$(Tl,Pb)Sr_4Cu_2O_7CO_3$	1993
$Tl_2Ba_2Ca_{n-1}Cu_nO_{2n+4}$	1988	$Ca_{13.5}Sr_{.5}Cu_{24}O_{41}$	1996
$n = 1, 2, 3, 4$		(60 kbar (6 MPa) applied pressure only)	
$TlBa_2Ca_{n-1}Cu_nO_{2n+3}$	1988		
$n = 1, 2, 3$			

Robert J. Cava, "Oxide Superconductors" J. Am. Ceram. Soc., **83** [1] 5–28 (2000)

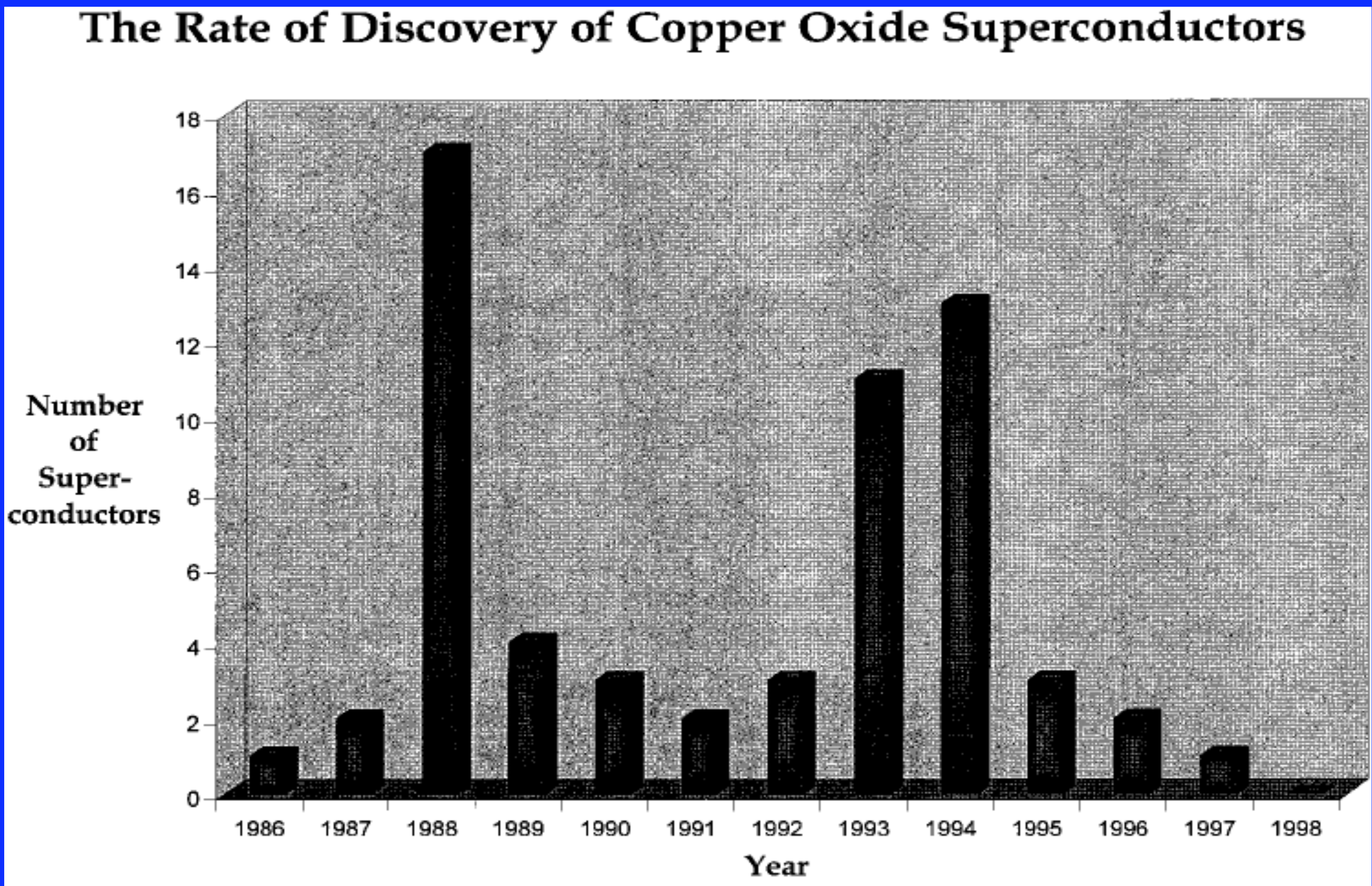

Fig. 23. Number of copper oxide superconductors discovered per year, 1986–present.

Robert J. Cava, "Oxide Superconductors" J. Am. Ceram. Soc., **83** [1] 5–28 (2000)

		T_c (K)	$B_c(0)$ (T)	$\lambda(0)$ (nm)	ξ_0 (nm)	NV (1)	$\frac{\Delta}{1.76kT_c}$ (2, 3)	$\frac{\Delta\sqrt{1.5\mu_0\gamma}}{k\pi B_c(0)}$ (2, 4)	$\frac{\Delta C}{1.43\gamma T_c}$ (3)
Non-transition elements									
Al	A1	1.175	0.010	50	1600	0.18	0.99	0.96	1.12
Sn	tetragonal	3.721	0.030	51	230	0.25	0.99	0.95	1.12
In	A1	3.405	0.028	64	440	0.30	1.01	1.02	
Pb	A1	7.19	0.080	39	83	0.39	1.21	1.05	1.85
Transition elements									
V	A2	5.4	0.125			0.23	0.97	0.95	1.10
Ta	A2	4.47	0.083			0.25	1.04	1.02	1.10
Nb	A2	9.25	0.127	44	40	0.30	1.04	0.99	1.45
A15 compounds									
Nb_3Ge	A15	23.0			3				
Nb_3Sn	A15	18.2			4				
Heavy-fermion compounds									
UBe_{13}		0.9							
UPt_3		0.45			18				
Organic compounds									
$(TMTSF)_2ClO_4$		1.2	0.003	500	140				
$(TMTSF)_2PF_6$		1.1(5)							
Ceramic cuprates									
$(La/Sr)CuO_4$		36	0.9	100	2.5				
$YBa_2Cu_3O_{7-\delta}$		93	1.0	130	1.5	0.66	1.3	1.25	2

Table 1.2. Typical superconductors with important parameters. For anisotropic materials the penetration depth λ and the coherence length ξ_0 are quoted for currents flowing in the highest conductivity direction. γ is the Sommerfeld constant (so γT is the electronic heat capacity per unit volume in the normal state). Notes: (1) The BCS coupling parameter NV is a nominal one obtained from T_c and the Debye temperature using the BCS weak-coupling formula (7.30). (2) These ratios have been computed using the tunnelling value for Δ where this is known. (3) These ratios should be 1.0 for an s-wave BCS weakly coupled superconductor. (4) This ratio should be 1.0 for any s-wave BCS superconductor if the gap parameter is independent of energy. (5) Measured at 8.5 kbar.

J R Waldram: Superconductivity of metals and cuprates, (Institute of Physics, Bristol, 1996)

The material

Perovskites and cuprates

ABX_3

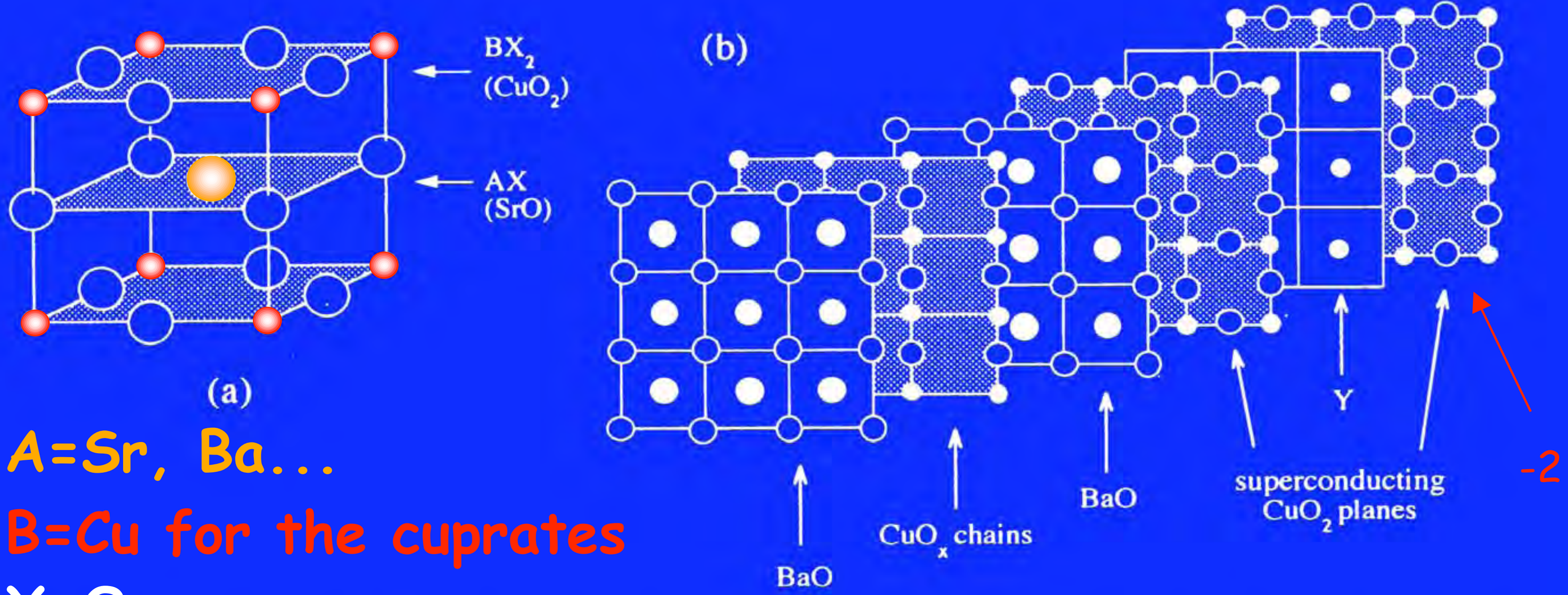

- A=Sr, Ba...
- B=Cu for the cuprates
- X=O

Figure 12.1. (a) The perovskite structure ABX_3, showing the BX_2 planes which correspond to the CuO_2 planes of the cuprate superconductors, and the AX planes, which correspond to the SrO or BaO planes. (b) Stacking of planes in YBCO: the planes are really stacked vertically, but have been displaced to make their structure visible. Note the Cu–O chains in the interleaving plane.

Fundamental Properties of HTS Important for Applications

Δ_0 ~ 30-50 meV

ξ_0 ~ few Å

highly anisotropic

d-wave order parameter symmetry

doping possible

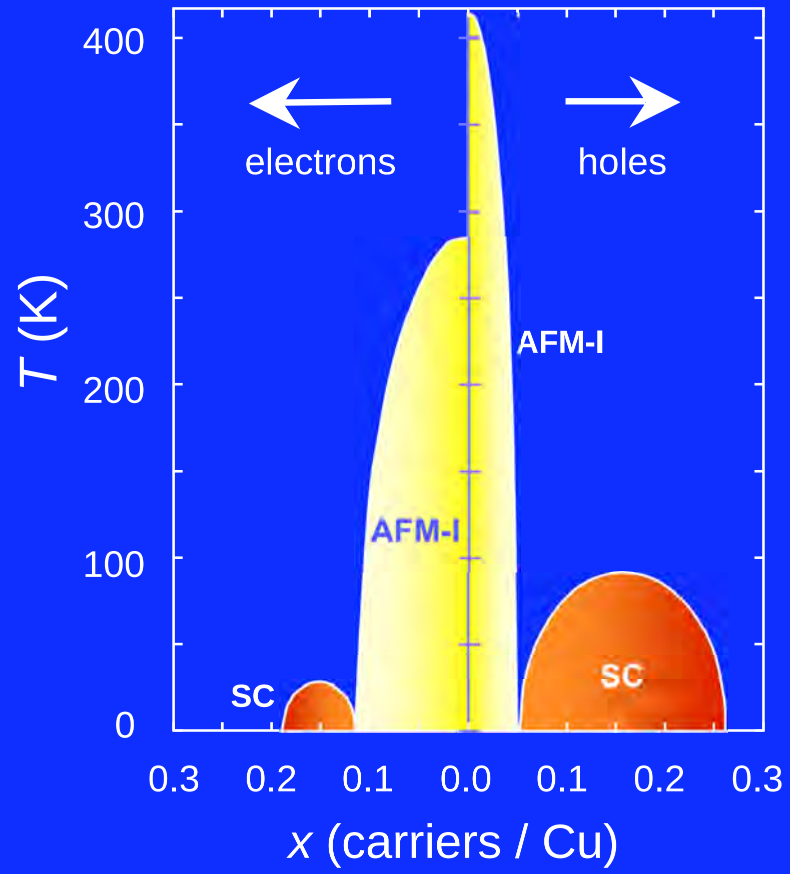

→ HTS device physics differs strongly from LTS

From Jochen Mannhart (Lecture Saas Fee)

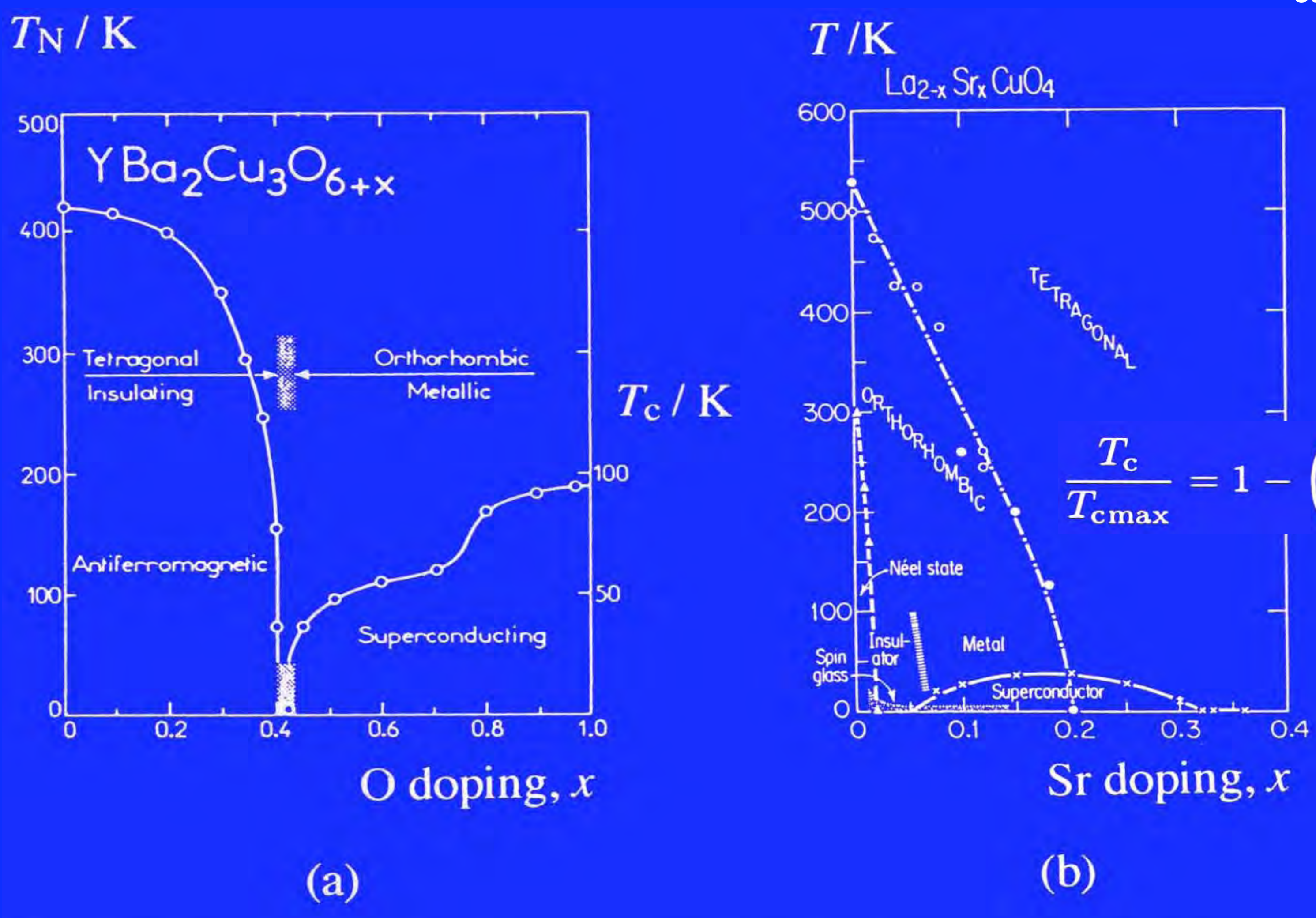

$$\frac{T_c}{T_{c\max}} = 1 - \left(\frac{n_d - 1.15}{0.10}\right)^2$$

Figure 13.2. Doping phase diagrams for YBCO (after Rossat-Mignod *et al* [9]) and for La/Sr cuprate (after Birgenau and Shirane [1]). T_c is always maximized at about 1.15 holes per unit cell in the CuO_2 planes, and an antiferromagnetic insulating phase always appears at one hole per unit cell. Note also in both materials the orthorhombic–tetragonal lattice transition, which is very slight and probably has little effect on the superconductivity.

J R Waldram: Superconductivity of metals and cuprates, (Institute of Physics, Bristol, 1996)

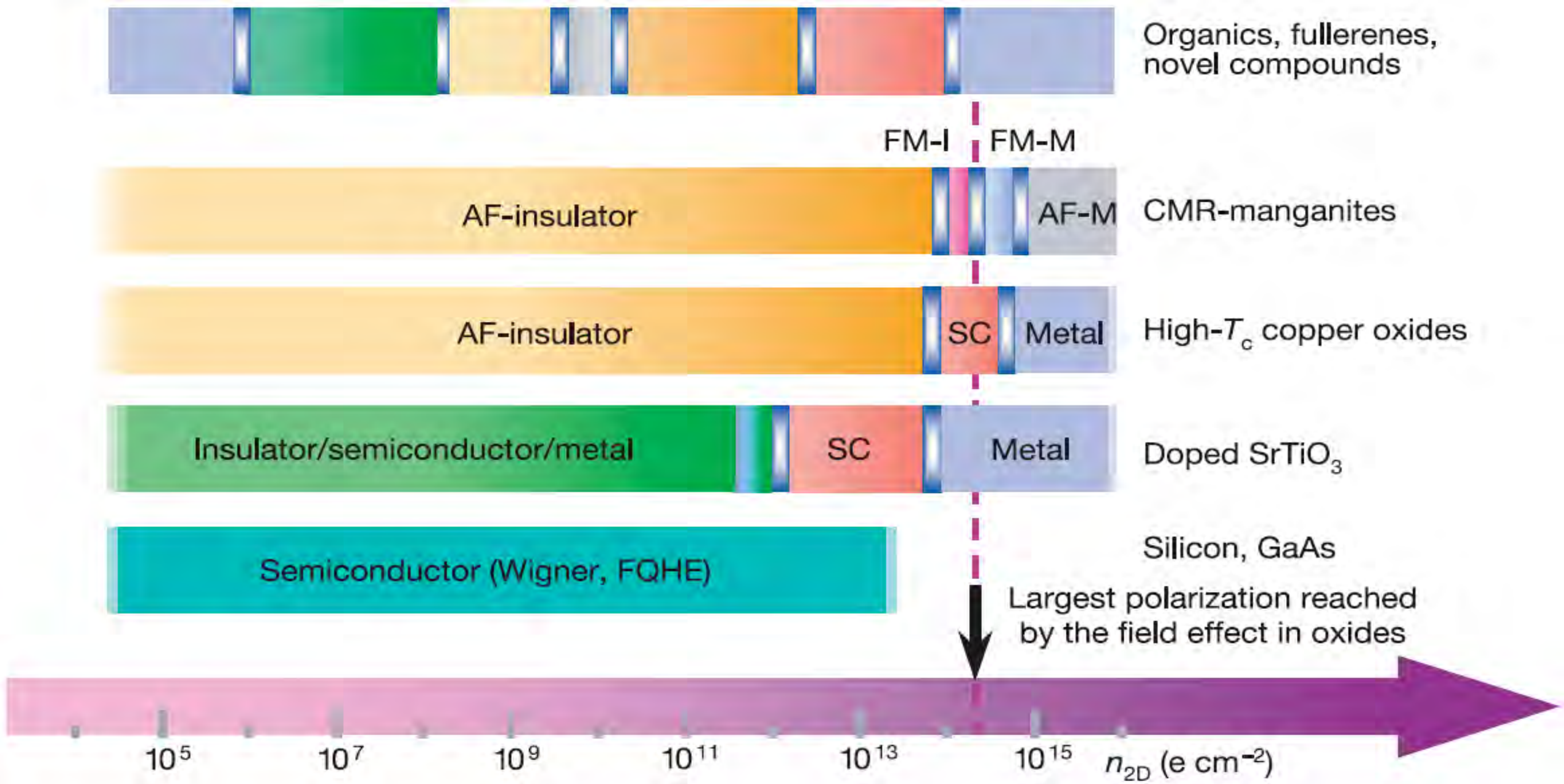

Figure 1 Illustration of the zero-temperature behaviour of various correlated materials as a function of sheet charge density (n_{2D}). Silicon is shown as a reference. The examples for high-T_c superconductors and for colossal magnetoresistive (CMR) manganites reflect $YBa_2Cu_3O_{7-\delta}$ and (La,Sr)MnO_3, respectively. The top bar has been drawn to illustrate schematically the richness of materials available for field-effect tuning and the spectrum of their phases. AF, antiferromagnetic; FM, ferromagnetic; I, insulator; M, metal; SC, superconductor; FQHE, fractional quantum Hall effect; Wigner, Wigner crystal.

Electric field effect in correlated oxide systems
C. H. Ahn, J.-M. Triscone & J. Mannhart

NATURE |VOL 424 | 28 AUGUST 2003 |www.nature.com/nature

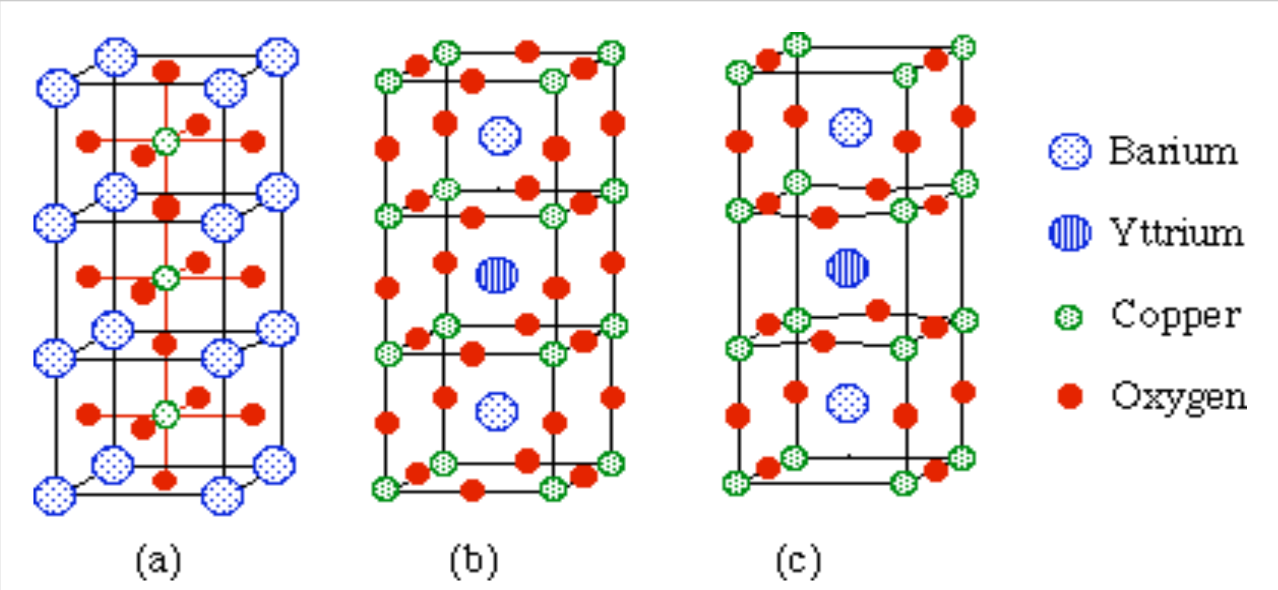

The idealized structure of $YBa_2Cu_3O_7$ shows evolution from the perovskite structure of Figure 4. (a) Stacking of 3 perovskite units; (b) Shift of the origin; (c) Removal of some of the oxygens to the give correct chemical composition.

http://chemiris.chem.binghamton.edu/chem445/HighTc/HighTc.htm

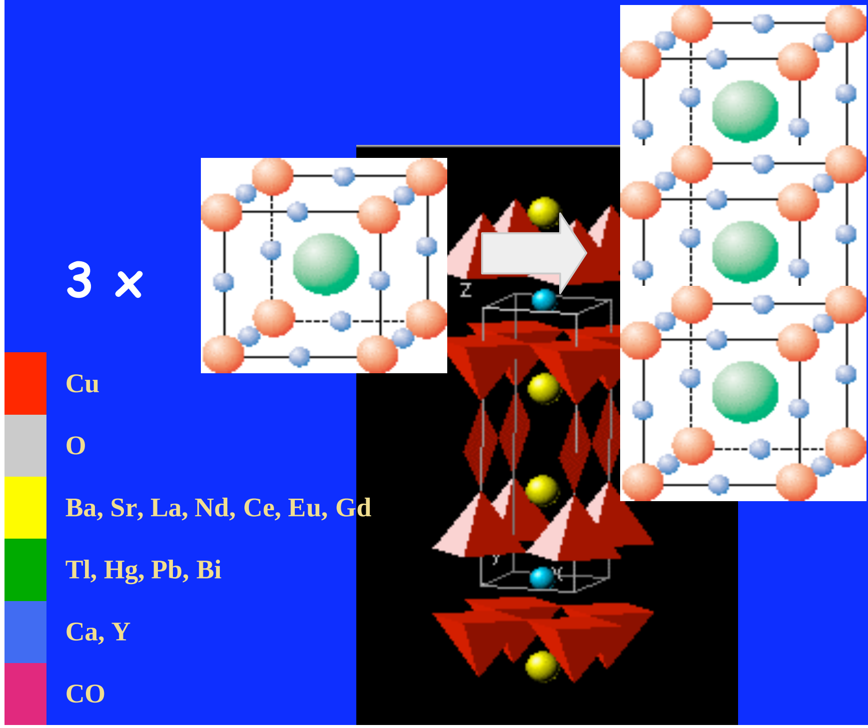

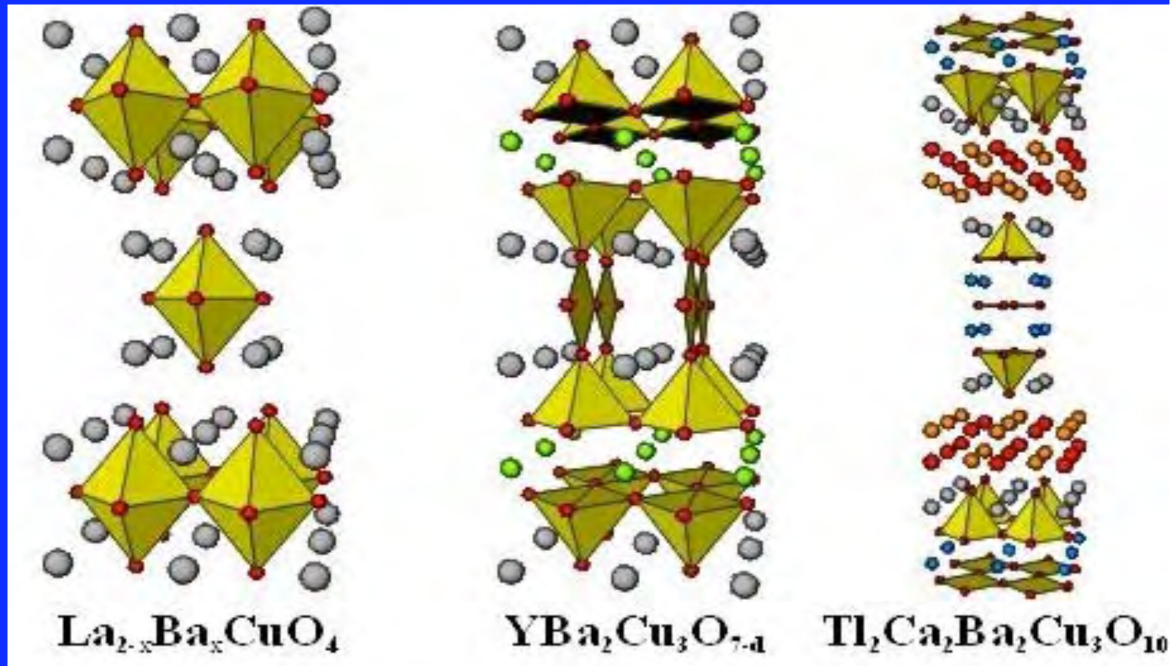

http://www.chem.northwestern.edu/~poeppel/SCBlurb.html

$YBa_2Cu_3O_{7-\delta}$

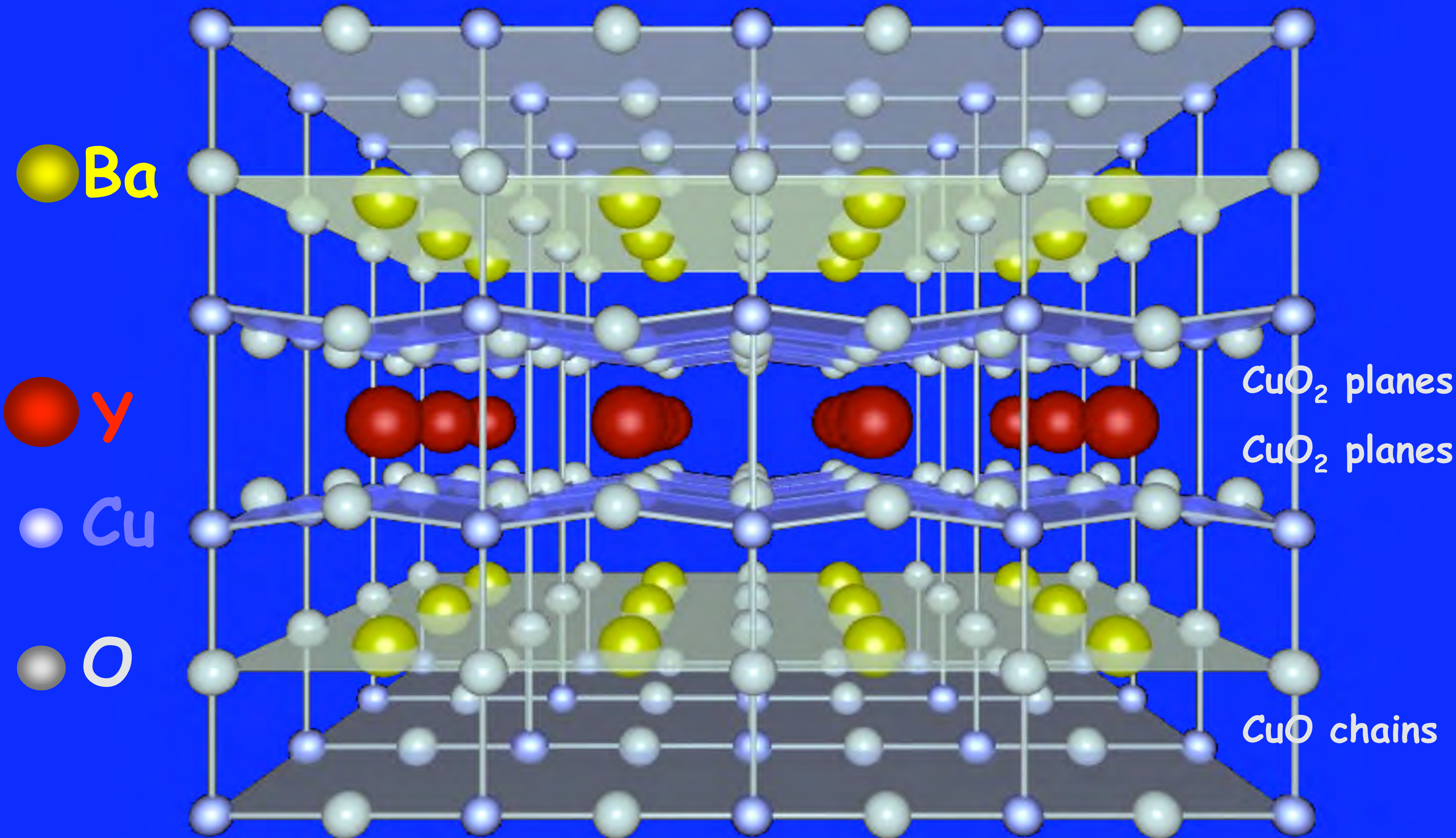

From Jochen Mannhart (Lecture Saas Fee)

A versatile structure…

Complex perovskites structures can be manipulated with regard to ions, charge doping, layering etc, to get new electronic, magnetic and superconducting properties.

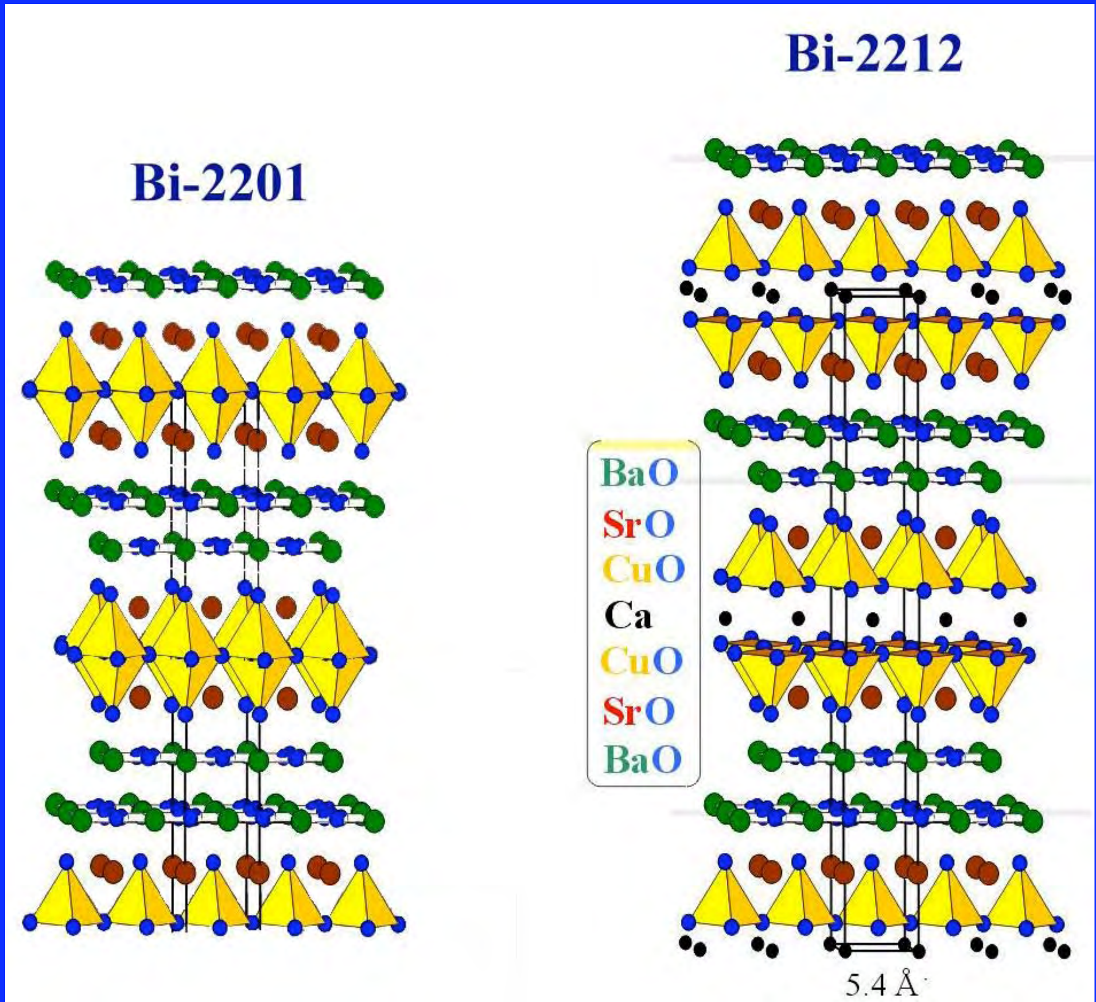

Cuprate superconductors

ABO_3

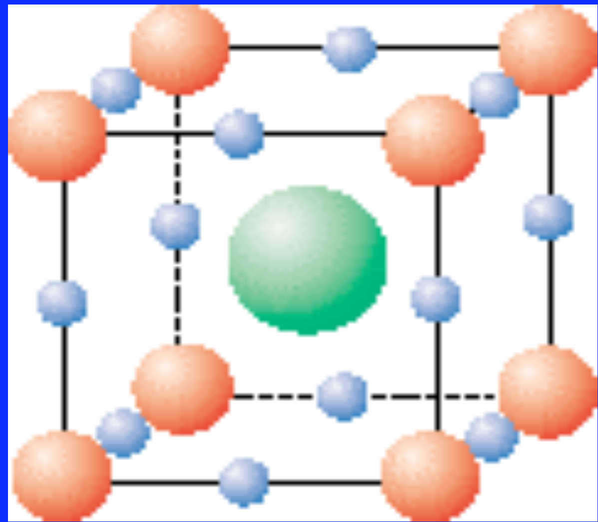

Sample	n	a (Å)	b (Å)	c (Å)	δ (Å)	d (Å)	Space Group	Ref.
$YBa_2Cu_3O_7$	2	3.8198(1)	3.8849(1)	11.6762(3)	8.3	3.36	Pmmm	[12]
$YBa_2Cu_3O_{6.66}$	2	3.8336(2)	3.8844(3)	11.7126(1)	8.4	3.36	Pmmm	[12]
$La_{1.9}Sr_{0.1}CuO_4$	1	3.7839(8)	3.7839(8)	13.211(4)	6.61	--	I4/mmm	[12]
$La_{1.85}Sr_{0.15}CuO_4$	1	3.7793(1)	3.7793(1)	13.2260(3)	6.61	--	I4/mmm	[12]
$La_{1.8}Sr_{0.2}CuO_4$	1	3.7675(1)	3.7675(1)	13.2220(6)	6.61	--	I4/mmm	[12]
$Nd_{1.85}Ce_{0.15}CuO_4$	1	3.9469(2)	3.9469(2)	12.0776(5)	6.04	--	P4/mmm	[12]
$Bi_2Sr_2CuO_6$	1	5.361(2)	5.370(1)	24.369(6)	7.5	--	Cmmm	[12,13]
$Bi_2Sr_2CaCu_2O_8$	2	5.411(2)	5.418(2)	30.89(2)	7.7	3.35	Fmmm	[12,13]
$Bi_2Sr_2Ca_2Cu_3O_{10}$	3	5.39	5.39	37.1	9.3	3.35	Fmmm	[12,13]
$Tl_2Ba_2CuO_6$	1	3.866(1)	3.866(1)	23.239(6)	7.76	--	I4/mmm	[12,14]
$Tl_2Ba_2CaCu_2O_8$	2	3.8550(6)	3.8550(6)	29.318(4)	7.52	3.2	I4/mmm	[12,14]
$Tl_2Ba_2Ca_2Cu_3O_{10}$	3	3.8503(6)	3.8503(6)	35.88(3)	7.61	3.2	I4/mmm	[12,14]

Table 1. Structural parameters for various cuprate materials, including the interplanar spacing, d, the intercell spacing, δ, and the number of CuO_2 planes per unit cell, n.

D. M. Ginsberg, Physical properties of high temperature superconductors (World Scientific, Singapore, 1994)

Electronic properties

Complex phase diagram

Complex perovskites structures can be manipulated with regard to ions, charge doping, layering etc, to get new electronic, magnetic and superconducting properties.

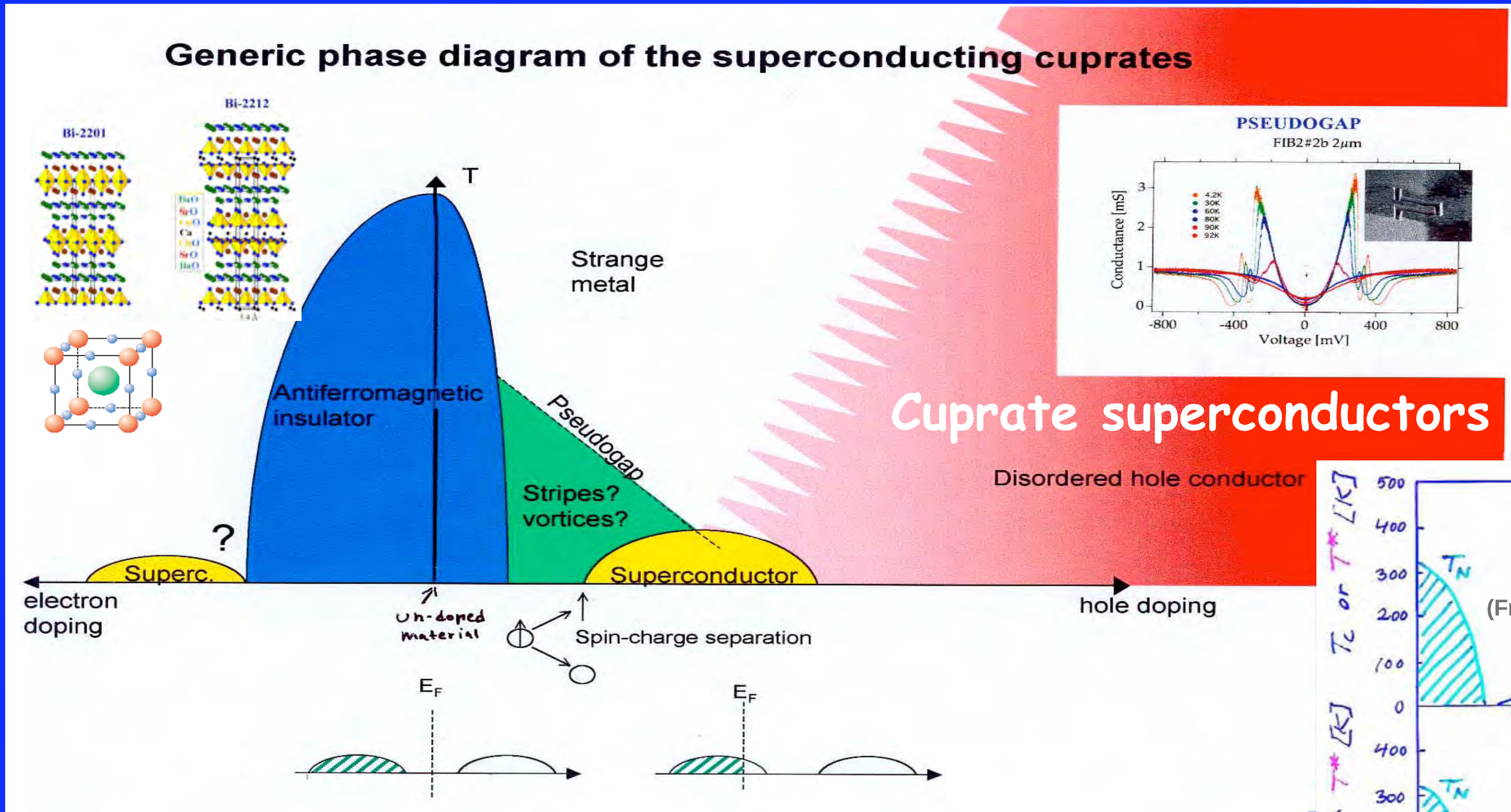

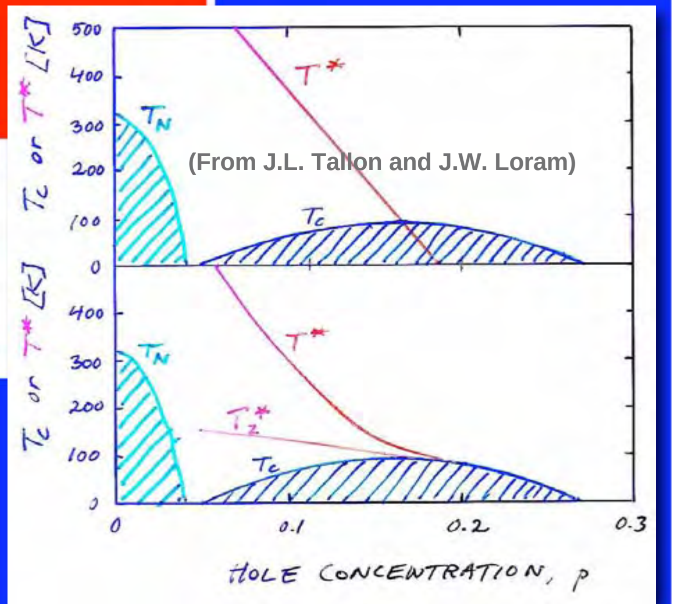

Perovskites and cuprates

ABX_3

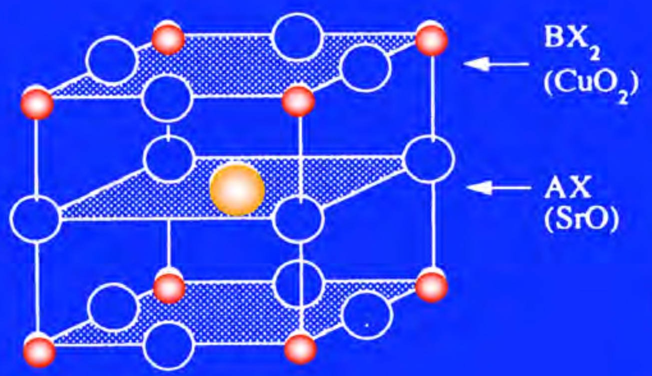

(a)

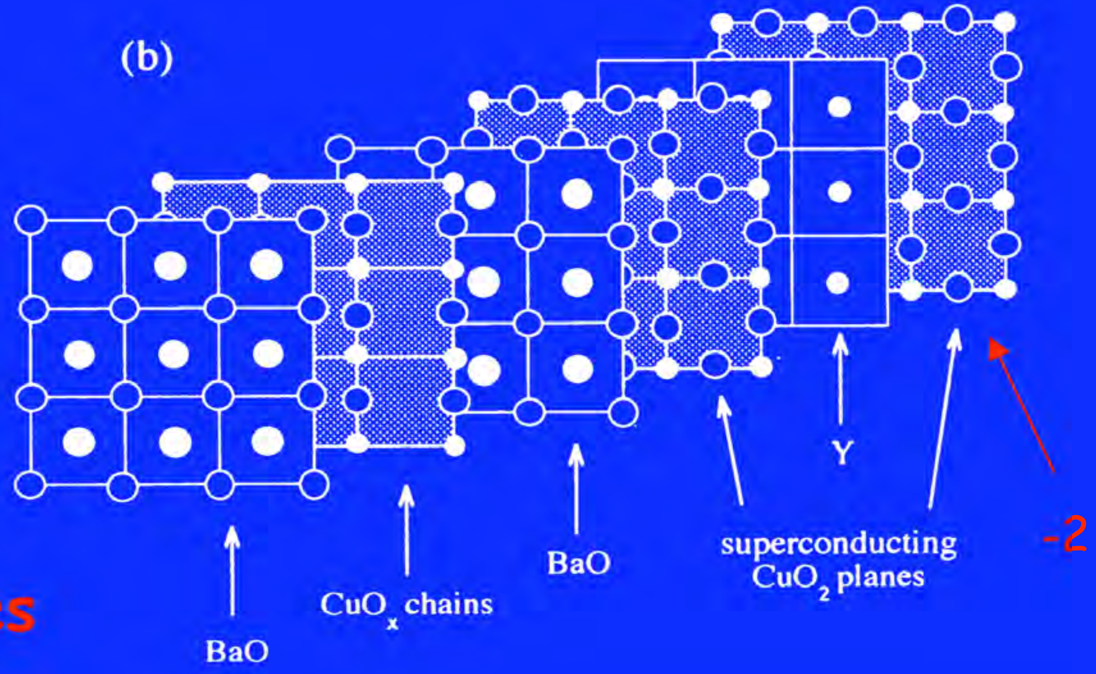

- A=Sr, Ba...
- B=Cu for the cuprates
- X=O

Coulomb interaction:

[redacted]

Zero point kinetic energy:

[redacted]

Orbitals...

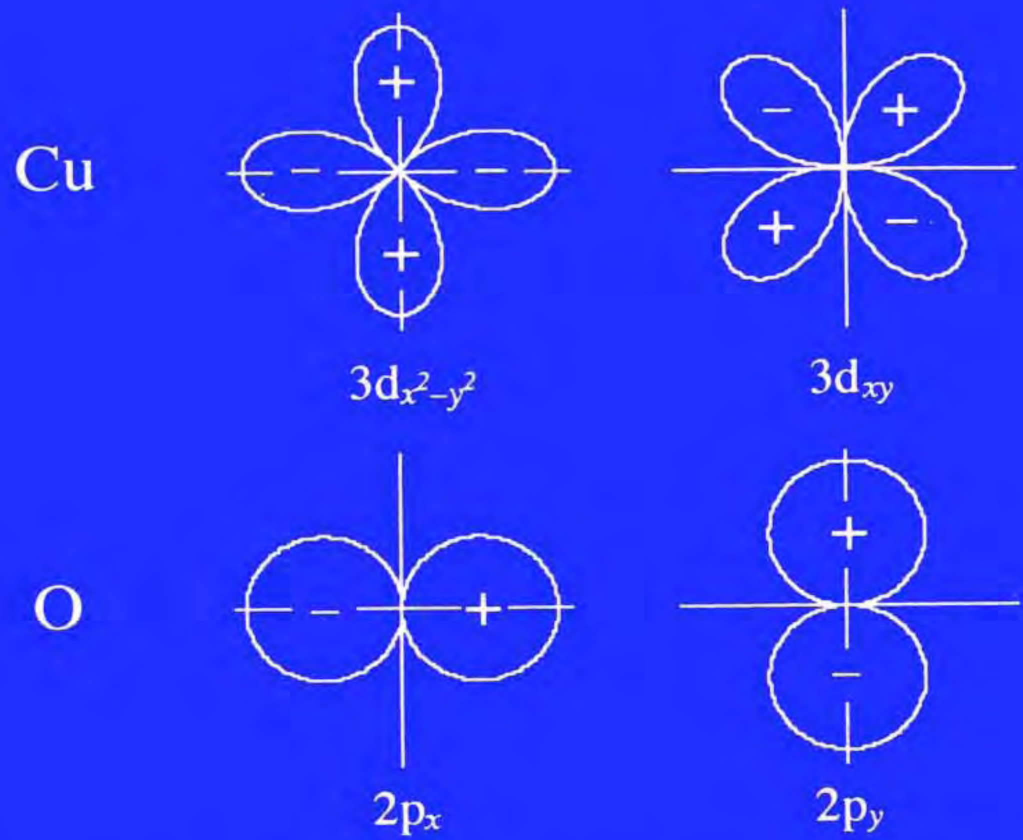

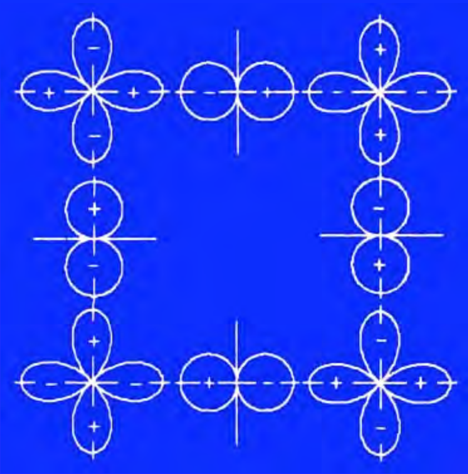

Figure 13.1. The highest-lying Cu and O orbitals likely to be associated with the mobile electrons in the CuO_2 planes and (in the 123 cuprates) in the CuO chains.

J R Waldram: Superconductivity of metals and cuprates, (Institute of Physics, Bristol, 1996)

Localized states and Mott insulators

Coulomb interaction:

- Coulomb interactions have the dominant effect for large *r*
- *At low densities the electrons behave more like classical particles and are trapped in localized states – Mott insulator*

Zero point kinetic energy:

- Zero point kinetic energy has the dominant effect for small *r*
- *At high densities the electrons have enough kinetic energy to tunnel through the barrier presented by their neighbors*

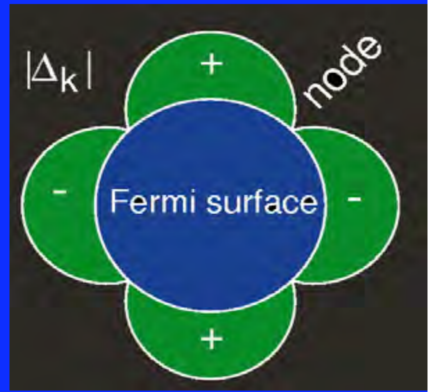

d-wave vs s-wave

$|\Delta_k|$

d-wave

s-wave

IBM Journal of Research & Development
© IBM Corporation

http://www.research.ibm.com/sup/kirtley.htm

SQUID microscope (IBM)

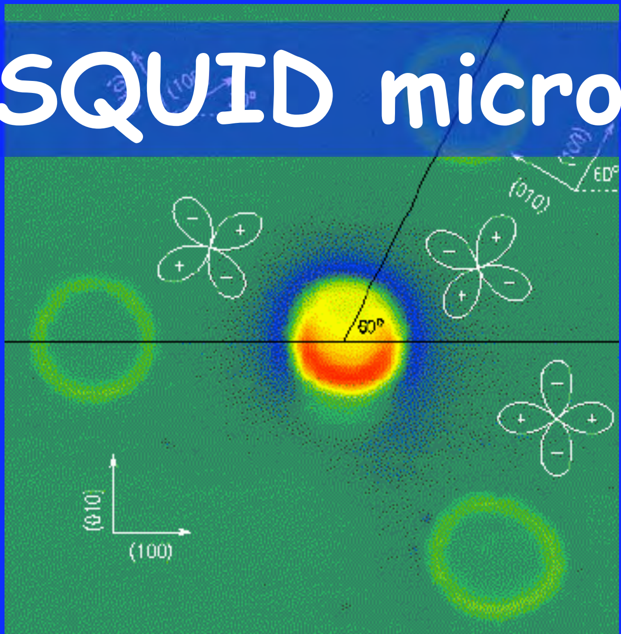

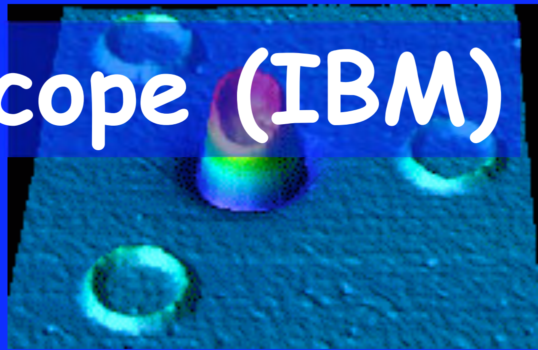

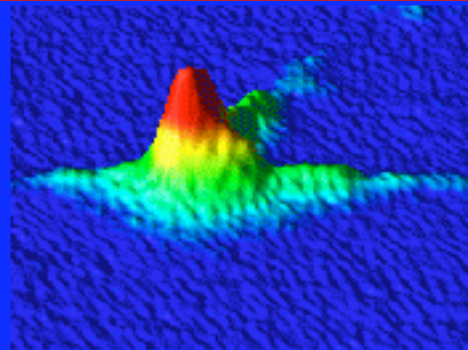

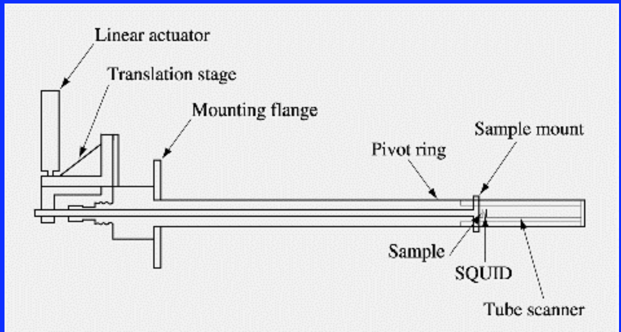

Figure 1

Schematic diagram of our scanning SQUID microscope [16].

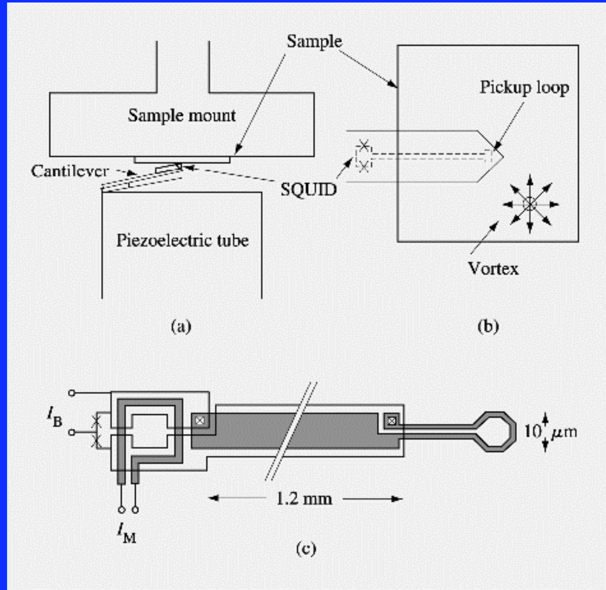

Figure 2

(a, b) Expanded views of the sample area; (c) schematic layout of the integrated magnetometer [16].

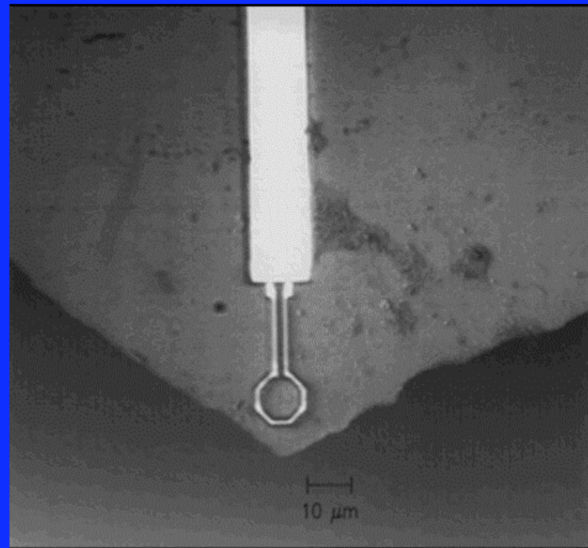

Figure 3

Optical image of the tip of a SQUID sensor after polishing.

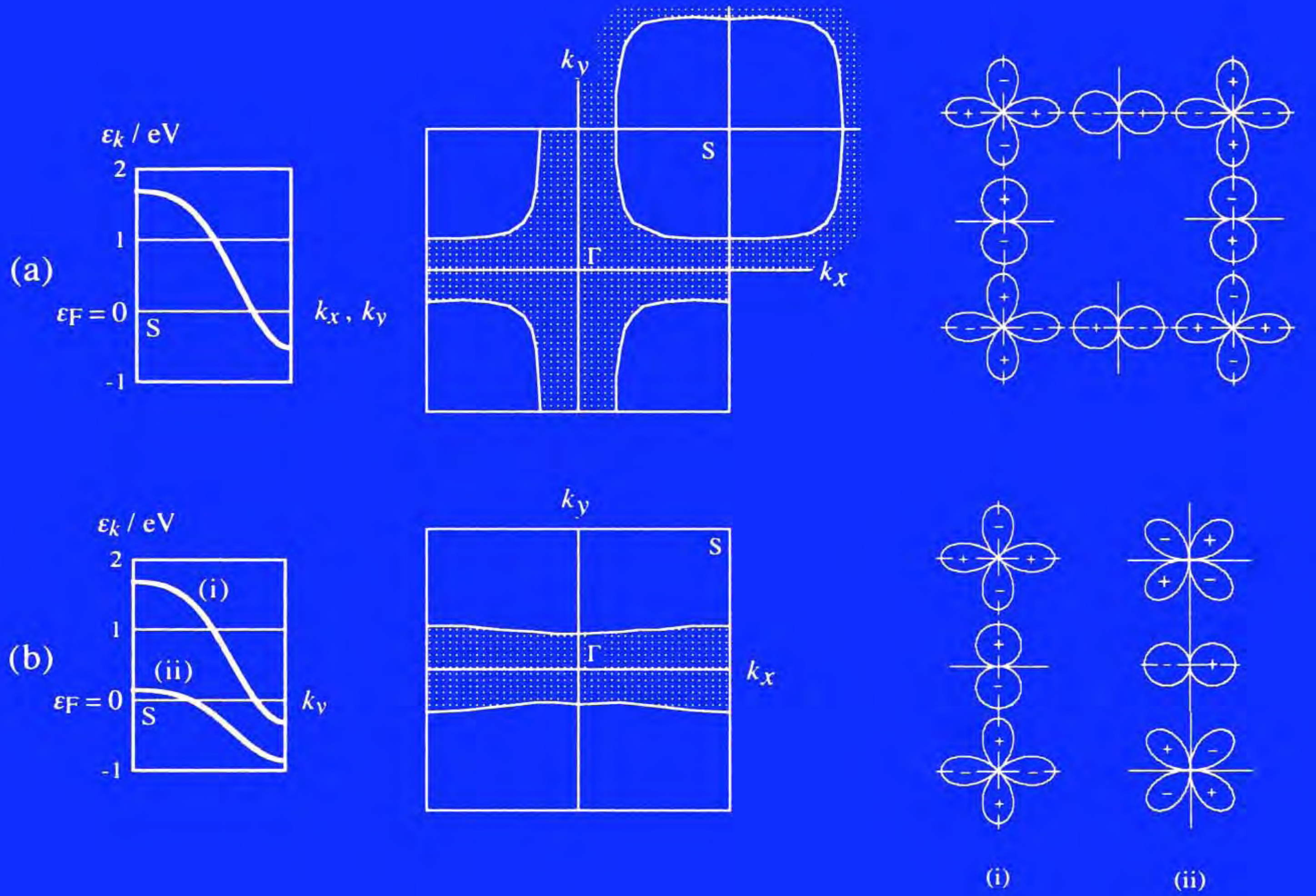

Figure 13.3. Simplified computed independent-electron band structure near the Fermi energy in cuprate superconductors. (a) The band for electrons moving in the CuO_2 planes, showing a nearly cylindrical hole surface centred on the Brillouin zone corner S; the figure shows how the orbitals form anti-bonding overlaps at S. (b) Bands for electrons moving on the CuO chains in 123 compounds such as YBCO, showing two essentially one-dimensional bands, also with anti-bonding overlaps at the top of the band. J R Waldram: Superconductivity of metals and cuprates, (Institute of Physics, Bristol, 1996)

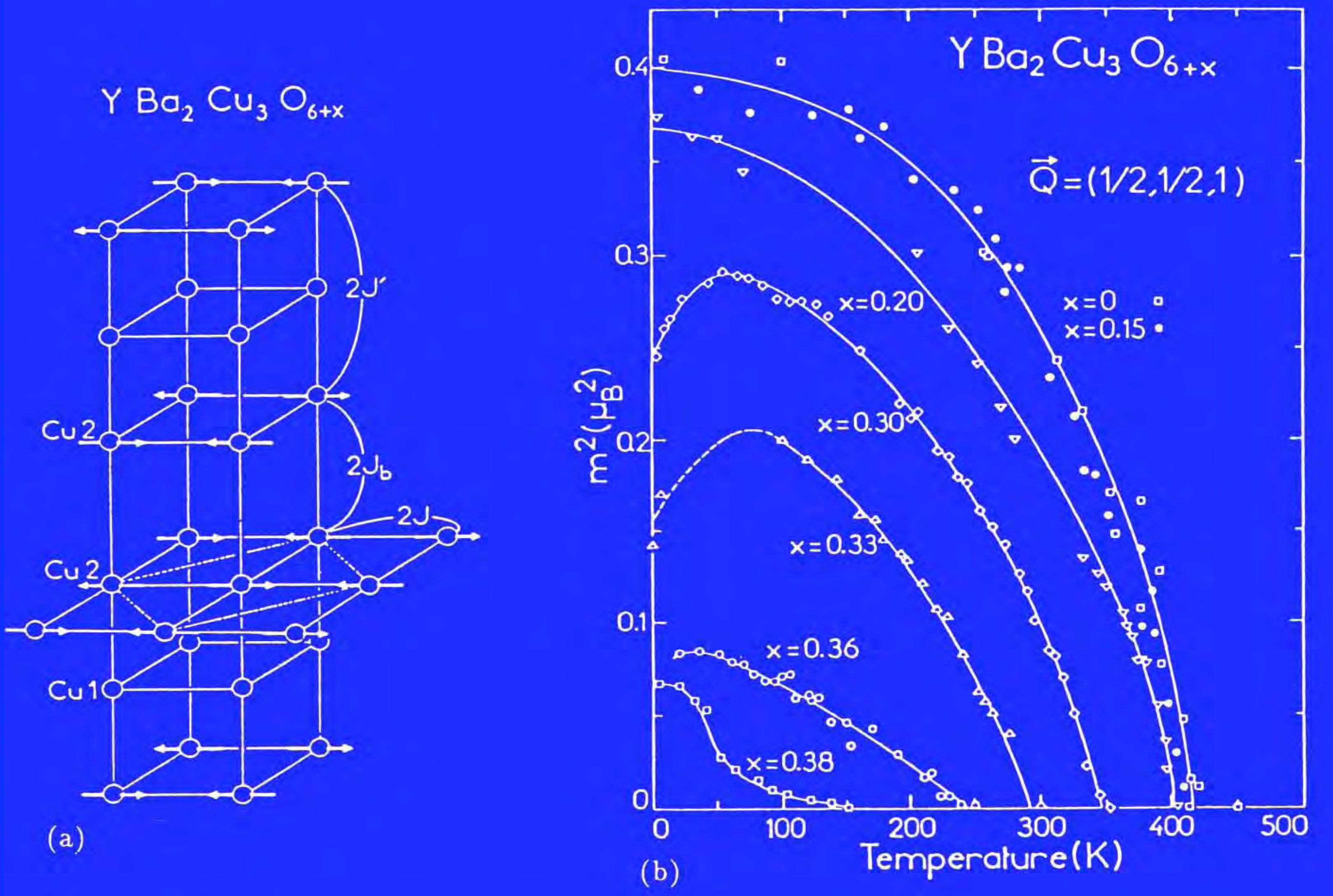

Figure 13.7. Antiferromagnetic properties of YBCO (from Rossat-Mignod *et al* [7] by permission): (a) spin arrangements on the Cu atoms; (b) magnetization as a function of doping and temperature.

J R Waldram: Superconductivity of metals and cuprates, (Institute of Physics, Bristol, 1996)

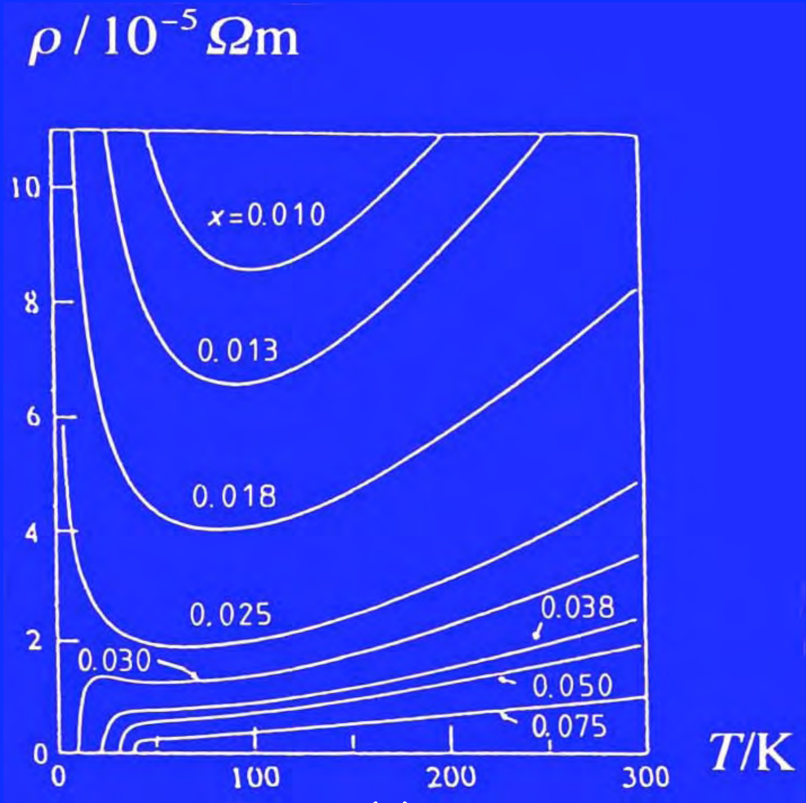

(a)

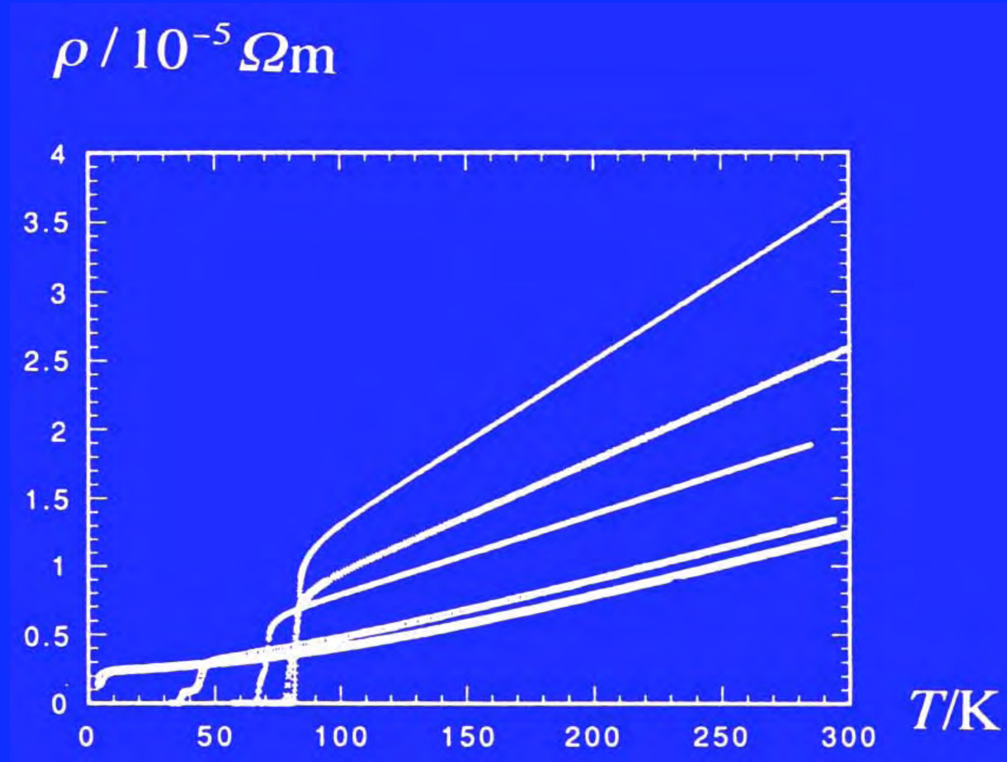

(b)

Figure 14.1. Typical resistivities $\rho(T)$ of cuprate superconductors for a wide range of dopings: (a) underdoped $(La_{2-x}Sr_x)CuO_4$ (after Takagi *et al* [4]); (b) overdoped $(Tl_{0.95}Cu_{0.05})2Ba_2CuO_{6+\delta}$ (after Cooper *et al* [5]), in which the overdoping increases from top to bottom. The T dependence is only linear close to the doping at which T_c is maximized.

J R Waldram: Superconductivity of metals and cuprates, (Institute of Physics, Bristol, 1996)

Anisotropy and consequences

Conduction in different directions

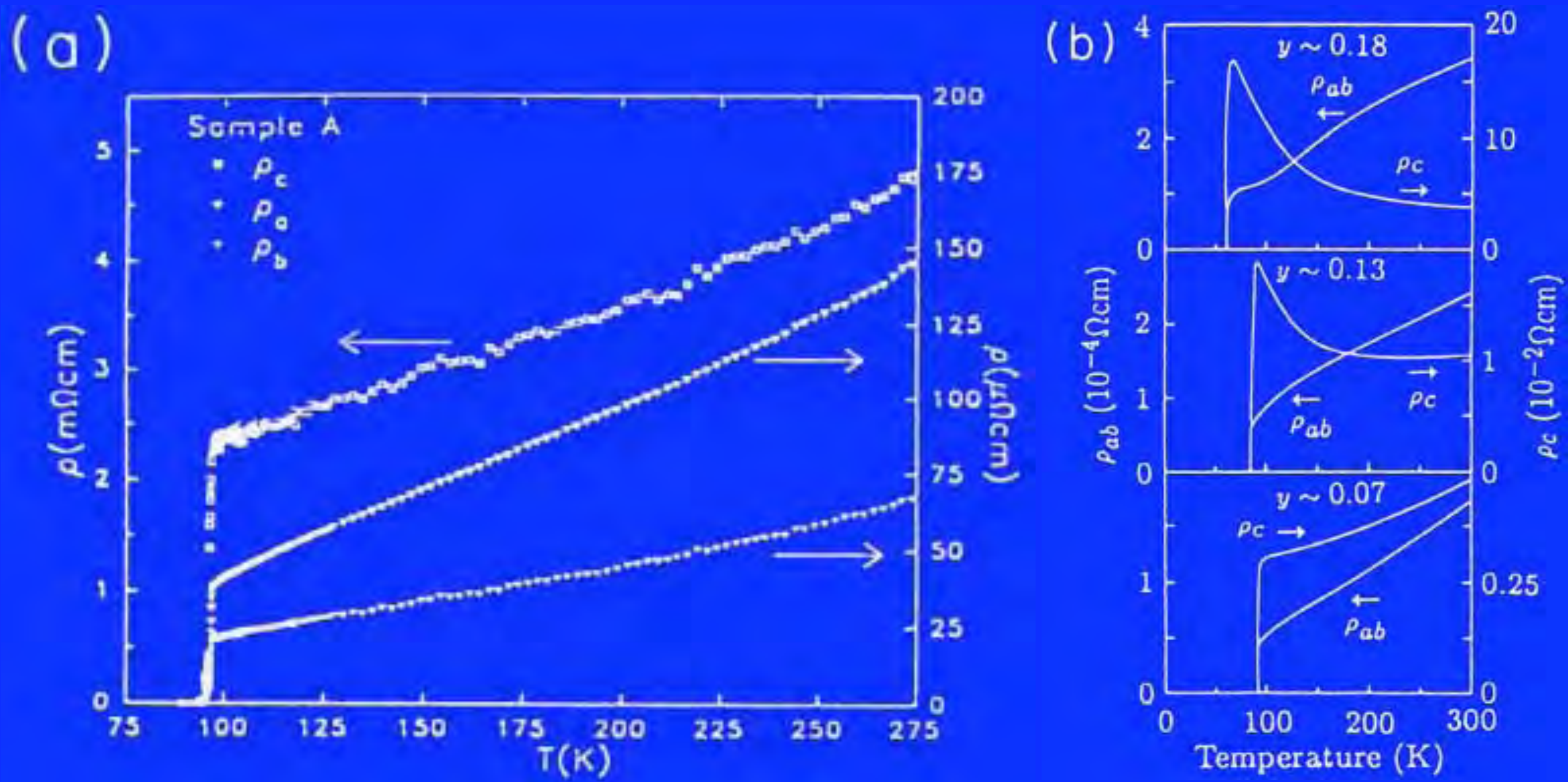

Fig. 4. (a) Temperature dependences of ρ_c, ρ_b, and ρ_a, in untwinned $YBa_2Cu_3O_7$ [from ref. 27]. (b) Temperature dependences of ρ_c and ρ_{ab} for several compositions of $YBa_2Cu_3O_{7-y}$ [from ref. 32].

D. M. Ginsberg, Physical properties of high temperature superconductors (World Scientific, Singapore, 1994)

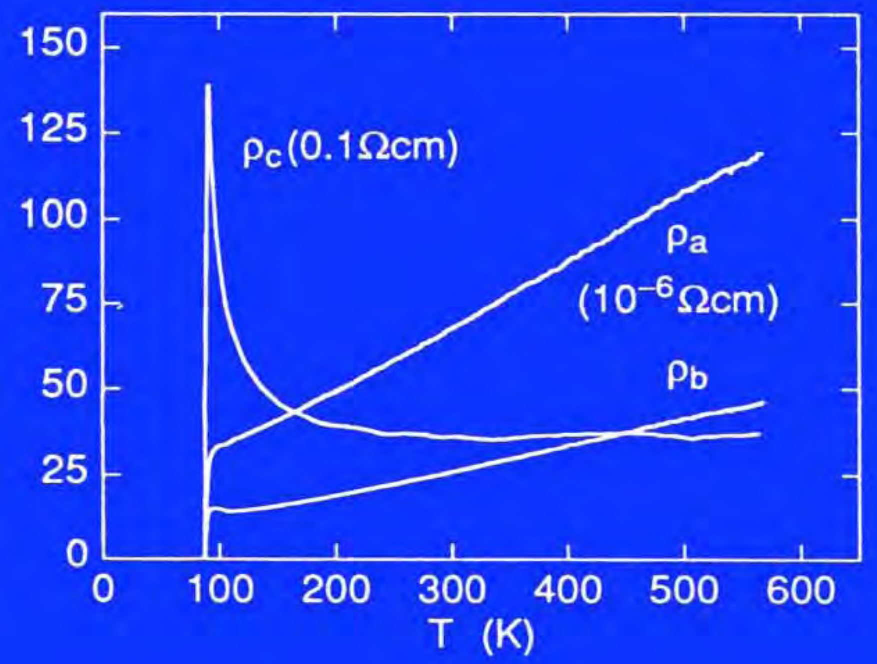

Fig. 6. Temperature dependences of ρ_c, ρ_a, and ρ_b in $Bi_2Sr_2CaCu_2O_8$ [from ref. 50].

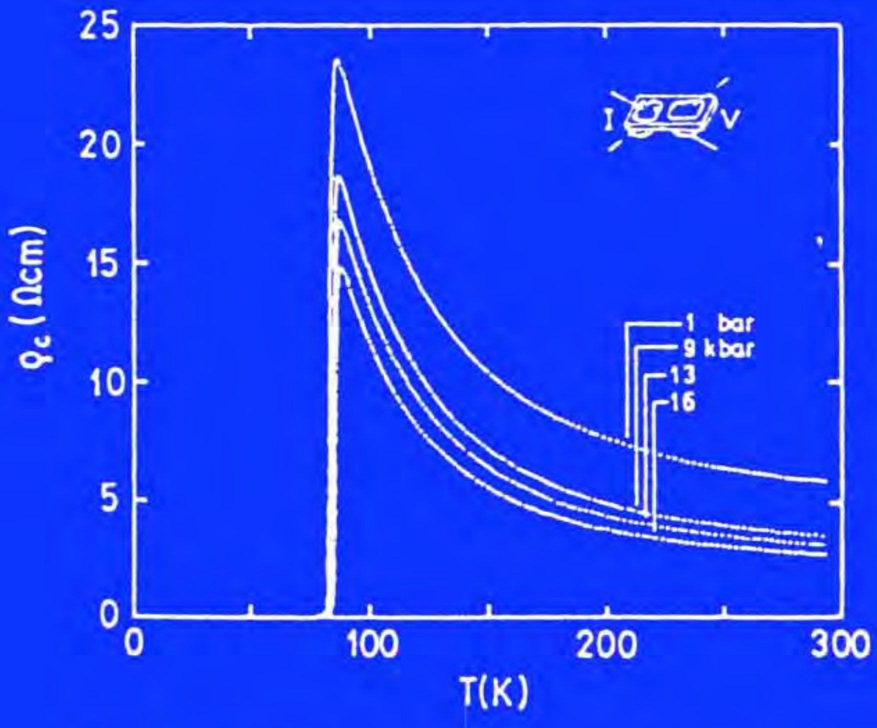

Fig. 7. Pressure dependence of ρ_c in $Bi_2Sr_2CaCu_2O_8$ [from ref. 55].

D. M. Ginsberg, Physical properties of high temperature superconductors (World Scientific, Singapore, 1994)

Sample	T_c (K)	$\rho_\perp (T_c)$ (mΩ-cm)	α ($\rho_c \sim T^{-\alpha}$)	$\rho_\perp/\rho_\parallel (T_c)$	Ref.
$YBa_2Cu_3O_{7-\delta}$ (untwinned)	90	2.3 - 3.4	-1	57-64 (ρ_c/ρ_a) 110-136 (ρ_c/ρ_b)	[27]
$YBa_2Cu_3O_{6.93}$	90	3	-1	70	[19,32]
$YBa_2Cu_3O_{6.93}$	90	4	-1	40	[33,35]
$YBa_2Cu_3O_{7-\delta}$	90	8	-1	40	[34]
$YBa_2Cu_3O_{7-\delta}$	90	9 - 11	~ 1	140	[38]
$YBa_2Cu_3O_{7-\delta}$	80-91	17.5	> 0	90	[37]
$YBa_2Cu_3O_{6.87}$	80	18	0 < α < 2	240	[19,32]
$YBa_2Cu_3O_{6.83}$	60	160	0 < α < 2	1600	[19,32]
$YBa_2Cu_3O_{7-\delta}$	60	150	> 1	1300	[18]
$YBa_2Cu_3O_{7-\delta}$	50	850	> 1	~ 4000	[42]
$Bi_2Sr_2CaCu_2O_8$	87	13,000	~ 1	$1 \times 10^5 - 8 \times 10^5$	[50,52]
$Bi_2Sr_2CuO_6$	6.5 - 8.5	16,000	0.52 - 1	$5 \times 10^4 - 2 \times 10^5$	[53]
$Tl_2Ba_2CaCu_2O_8$	105	75	< 0	250	[60]
$Tl_2Ba_2CuO_6$	75	100	~ 1.3	1500	[61]
$La_{1.9}Sr_{0.1}CuO_4$	26	600	> 0	1500	[30,31]
$La_{1.85}Sr_{0.15}CuO_4$	35	70	> 0	1000	[30,31]
$La_{1.8}Sr_{0.2}CuO_4$	30	25	> 0	500	[30,31]
$La_{1.7}Sr_{0.3}CuO_4$ (overdoped)	0	2	< 0	50-100	[30,31]
$Pr_{1.85}Ce_{0.15}CuO_4$	–	1000	> 0	–	[19]
$Nd_{1.84}Ce_{0.16}CuO_4$	–	1000-2000	< 0	$5 \times 10^3 - 2 \times 10^4$	[63,64]
2*H*-$NbSe_2$	7	--	< 0	10	[36]
4*Hb*-TaS_2	2.5	11.5	> 0	380 - 1000	[44]
2*H*-NbS_2	6	23	< 0	6600	[45]
$(TMTSF)_2ClO_4$	1	10	< 0	5000	[46]

Table 2. Transport parameters perpendicular ($\rho_\perp$) and parallel ($\rho_\parallel$) to the high conduction direction of various anisotropic materials.

D. M. Ginsberg, Physical properties of high temperature superconductors (World Scientific, Singapore, 1994)

Anisotropy and consequences

Intrinsic Josephson effect

KLEINER AND MÜLLER

VOLUME 68, NUMBER 15 PHYSICAL REVIEW LETTERS 13 APRIL 1992

Intrinsic Josephson Effects in $Bi_2Sr_2CaCu_2O_8$ Single Crystals

R. Kleiner, F. Steinmeyer, G. Kunkel, and P. Müller
Walther-Meissner-Institut, Walther-Meissner-Strasse 8, W-8046 Garching, Germany
(Received 21 August 1991; revised manuscript received 11 February 1992)

PHYSICAL REVIEW B VOLUME 49, NUMBER 2 1 JANUARY 1994-II

Intrinsic Josephson effects in high-T_c superconductors

R. Kleiner and P. Müller

FIG. 1. Superposition of the BSCCO crystal structure and a stack of Josephson junctions, whose electrodes are formed by CuO_2 double layers.

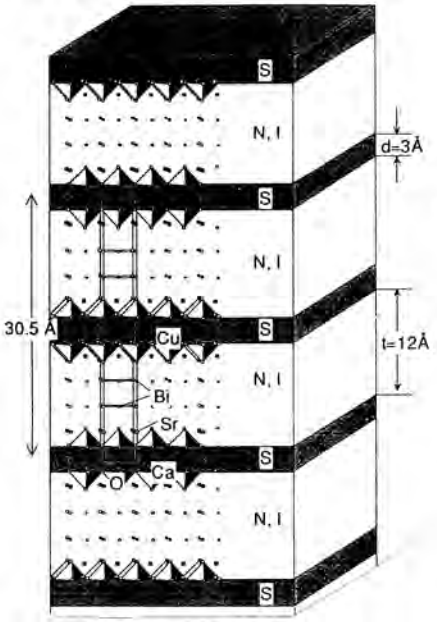

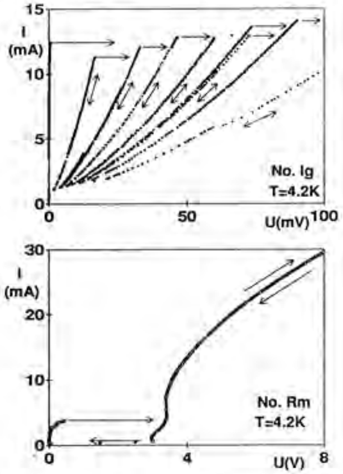

FIG. 5. *I-V* characteristics of Ar-annealed BSCCO crystals at different voltage scales. The multiple branches shown in the upper figure have not been traced out in the lower figure. The annealing conditions of the samples are 12 h, 600 °C (No. Ig) and 10 h, 550 °C (No. Rm). Contact resistances have been subtracted. Details of the *I-V* characteristics are described in the text.

VOLUME 68, NUMBER 15 PHYSICAL REVIEW LETTERS 13 APRIL 1992

2394 – 2397 **Intrinsic Josephson Effects in $Bi_2Sr_2CaCu_2O_8$ Single Crystals**

R. Kleiner, F. Steinmeyer, G. Kunkel, and P. Müller
Walther-Meissner-Institut, Walther-Meissner-Strasse 8, W-8046 Garching, Germany
(Received 21 August 1991; revised manuscript received 11 February 1992)

We have observed Josephson coupling between CuO double layers in $Bi_2Sr_2CaCu_2O_8$ single crystals by direct measurements of ac and dc Josephson effects with current flow along the *c* axis. The results show that a small $Bi_2Sr_2CaCu_2O_8$ single crystal behaves like a series array of Josephson junctions which can exhibit mutual phase locking.

PACS numbers: 74.50.+r, 74.60.Jg, 74.70.Jm

PHYSICAL REVIEW B VOLUME 49, NUMBER 2 1 JANUARY 1994-II
1327 – 1341

Intrinsic Josephson effects in high-T_c superconductors

R. Kleiner and P. Müller
Walther-Meissner-Institut, D-85748 Garching, Germany
(Received 19 July 1993)

We have investigated the coupling between CuO_2 layers in high-T_c superconductors by direct measurements of all dc and ac Josephson effects with current flow in the c-axis direction. The measurements have been performed on small single crystals of $Bi_2Sr_2CaCu_2O_8$, $(Pb_yBi_{1-y})_2Sr_2CaCu_2O_8$, $Tl_2Ba_2Ca_2Cu_3O_{10}$, and $YBa_2Cu_3O_{7-\delta}$ and on *a*-axis-oriented $YBa_2Cu_3O_7$ thin films. The results clearly show that all materials behave like stacks of superconductor-insulator-superconductor Josephson junctions. The current-voltage characteristics exhibit large hystereses and multiple branches, which can be explained by a series connection of highly capacitive junctions. From the modulation of the critical current in a magnetic field parallel to the layers, we infer a junction thickness of approximately 15 Å. In our microwave emission experiments we were able to prove explicitly that every pair of CuO_2 double or triple layers forms a working Josephson contact. An exception is $YBa_2Cu_3O_7$, where only flux-flow behavior has been observed.

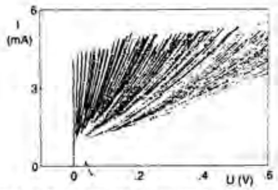

FIG. 1. *I-V* characteristic of sample *Fa* at *T* = 4.2 K. The contact resistance of 18 Ω is subtracted.

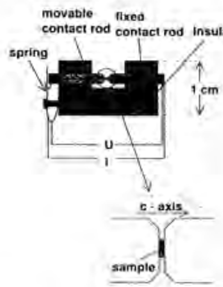

FIG. 4. Schematic view of the sample holder.

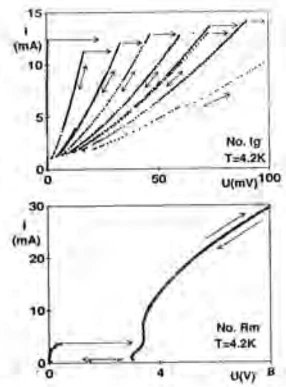

FIG. 5. *I-V* characteristics of Ar-annealed BSCCO crystals at different voltage scales. The multiple branches shown in the upper figure have not been traced out in the lower figure. The annealing conditions of the samples are 12 h, 600 °C (No. Ig) and 10 h, 550 °C (No. Rm). Contact resistances have been subtracted. Details of the *I-V* characteristics are described in the text.

Early measurements Kleiner & Müller

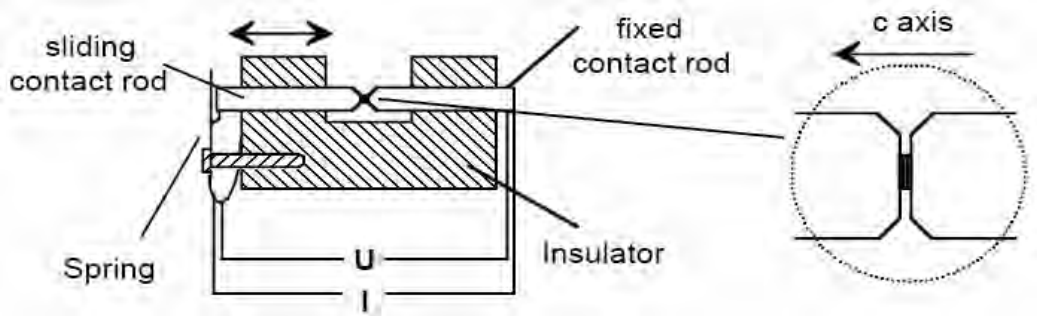

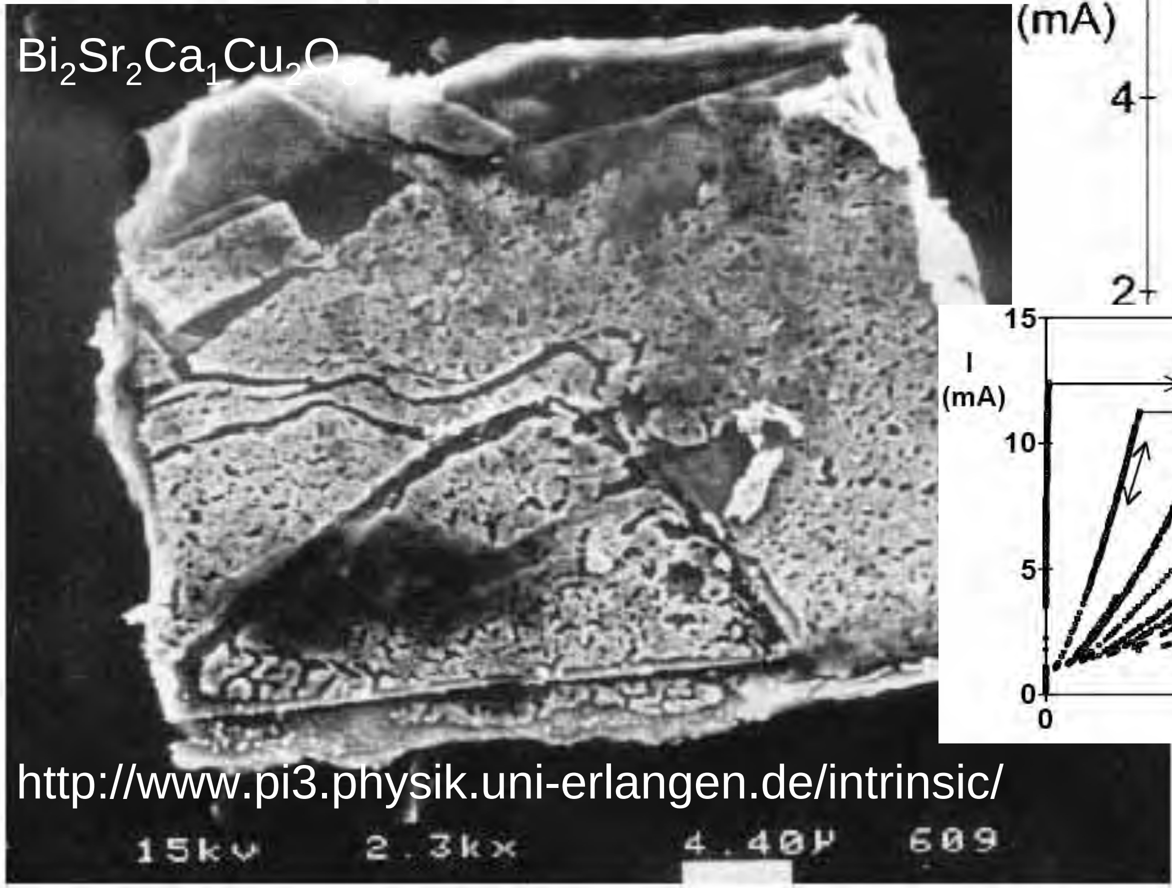

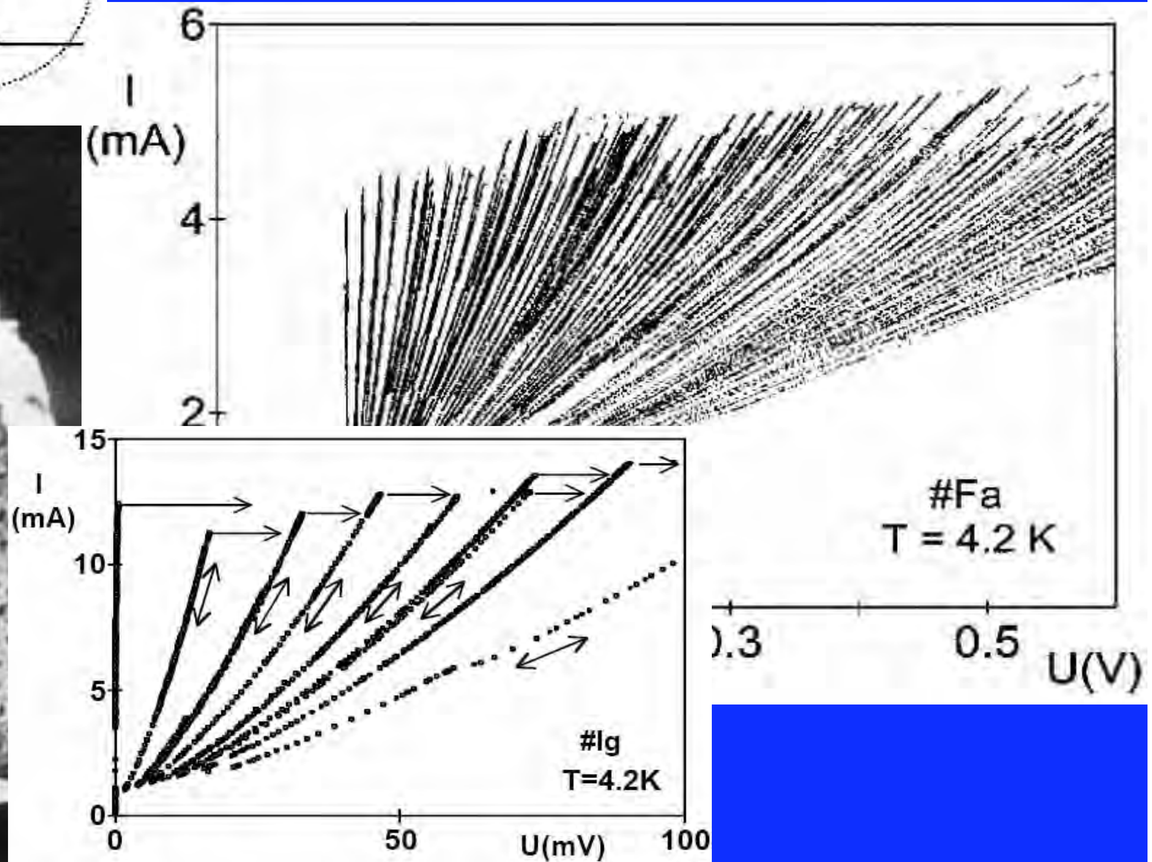

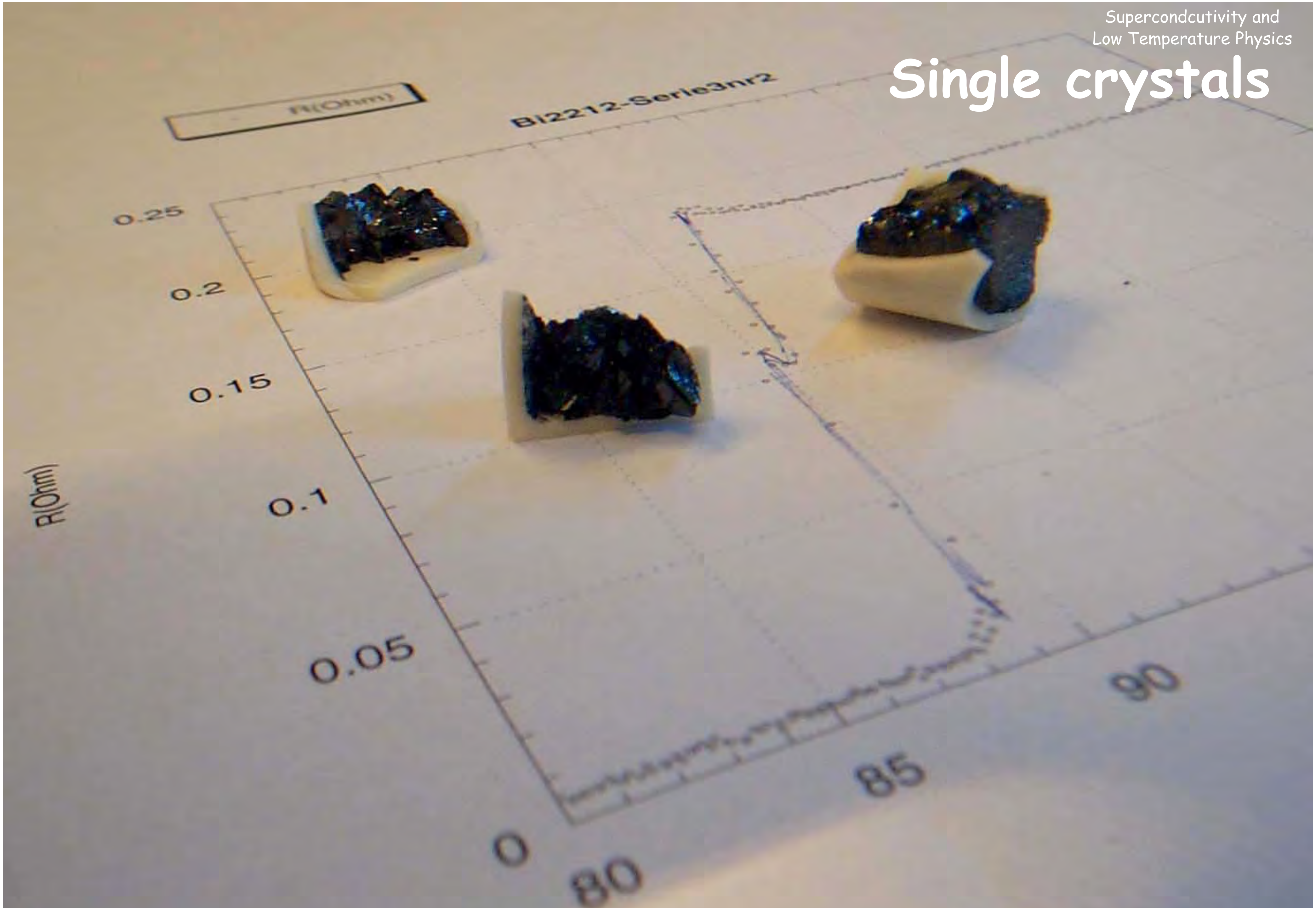
Supercondcutivity and
Low Temperature Physics
Single crystals
Bi2212-Serie3nr2
R(Ohm)
R(Ohm)
0.25
0.2
0.15
0.1
0.05
0
80
85
90

MESA STRUCTURES
– using photolithography

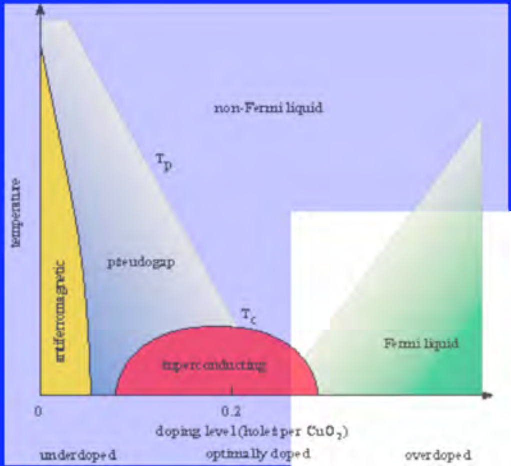

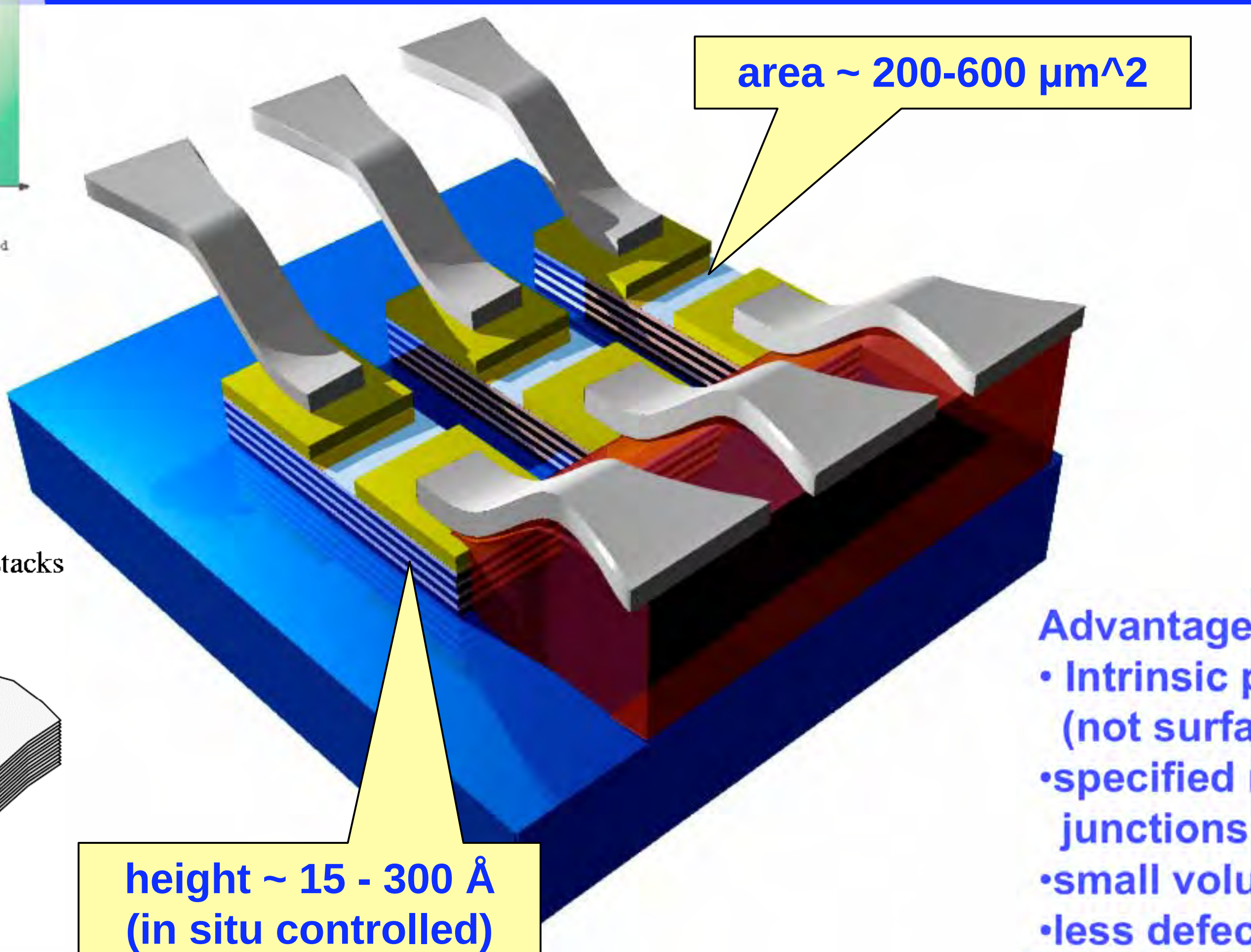

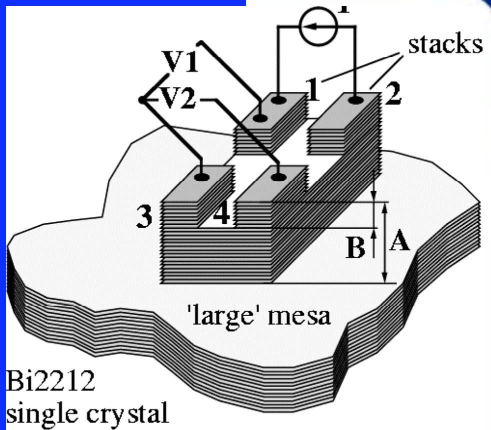

Advantages:
- Intrinsic properties (not surface)
- specified number of junctions
- small volume
- less defects
- less heating

Yurgens et al.

Appl. Phys. Lett. 70, 1760 (1997)

Ar ion etching or

Chemical etching (EDTA)

TUNNELING SPECTROSCOPY...

Superconductor-Insulator-Normal metal

SIN

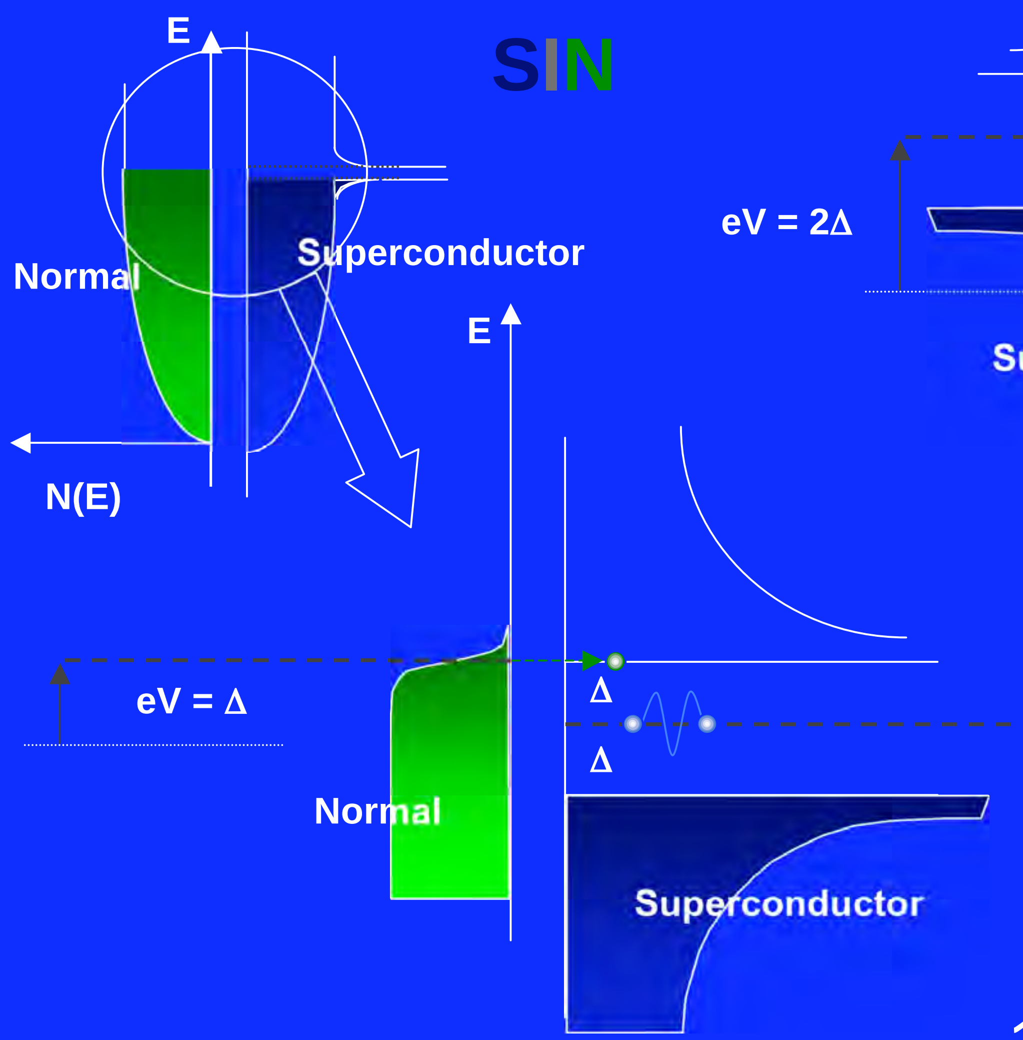

Superconductor-Insulator- Superconductor

SIS

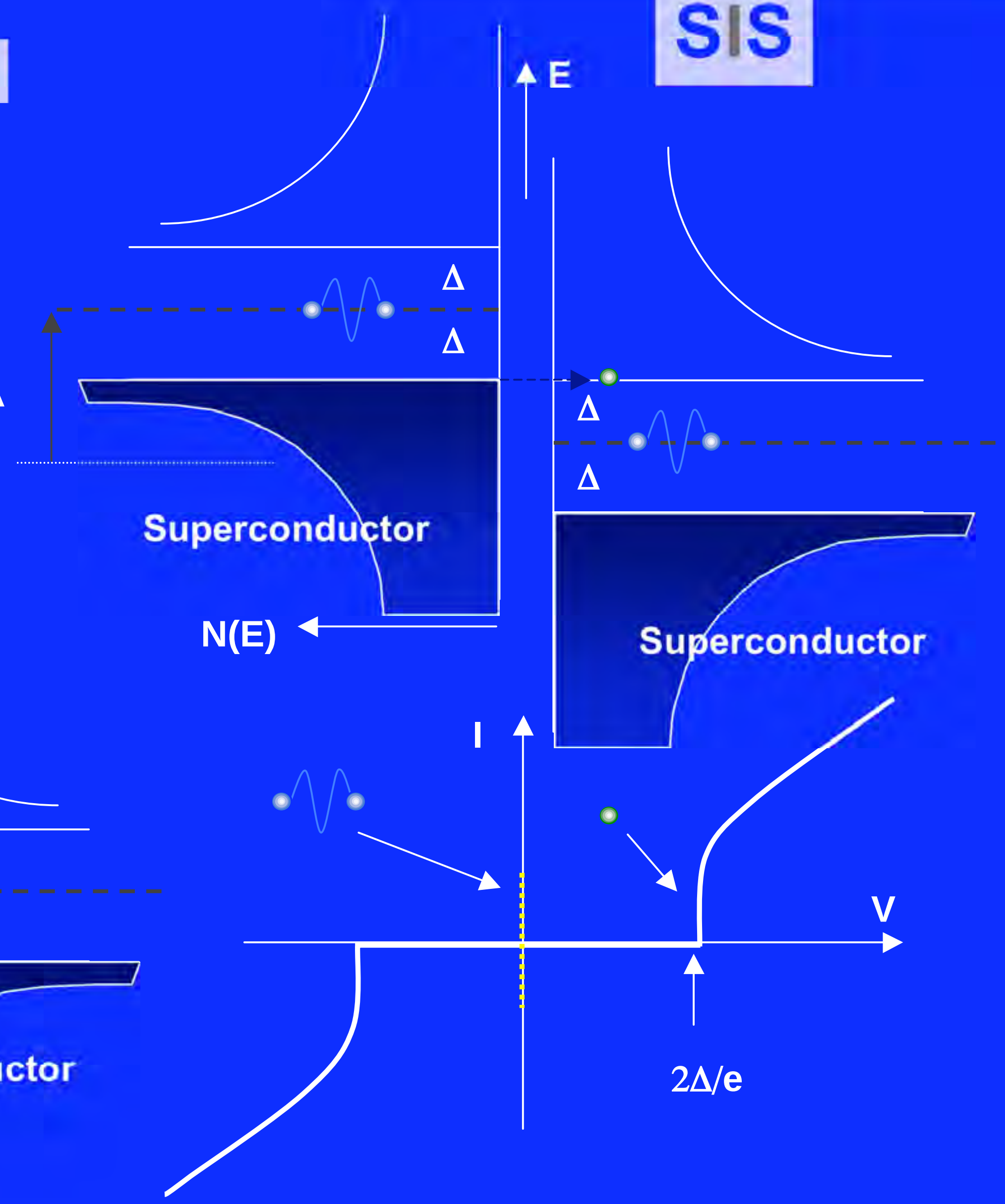

Superconductivity and Low Temperature Physics

INTRINSIC JOSEPHSON JUNCTIONS

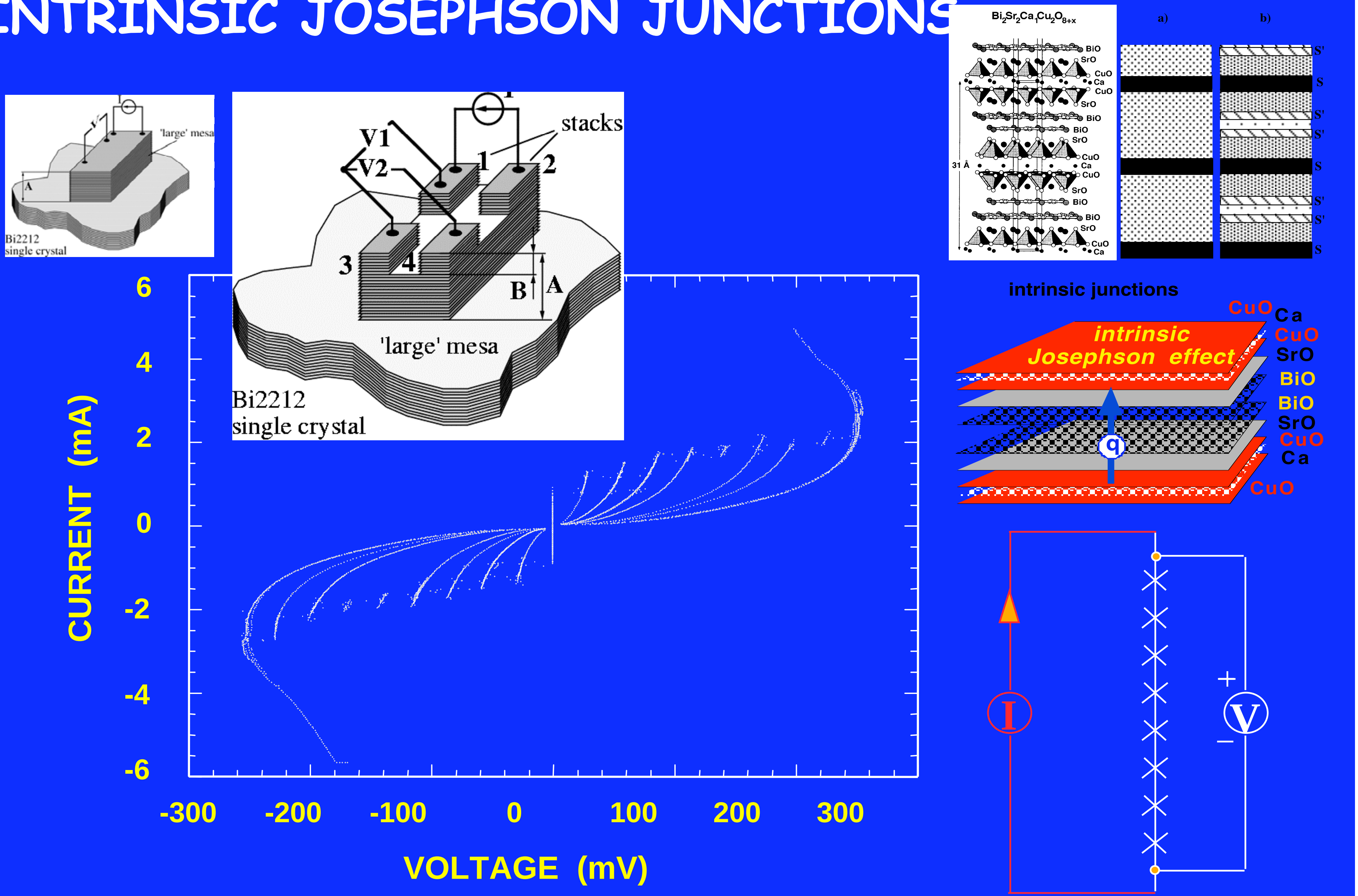

The phenomena

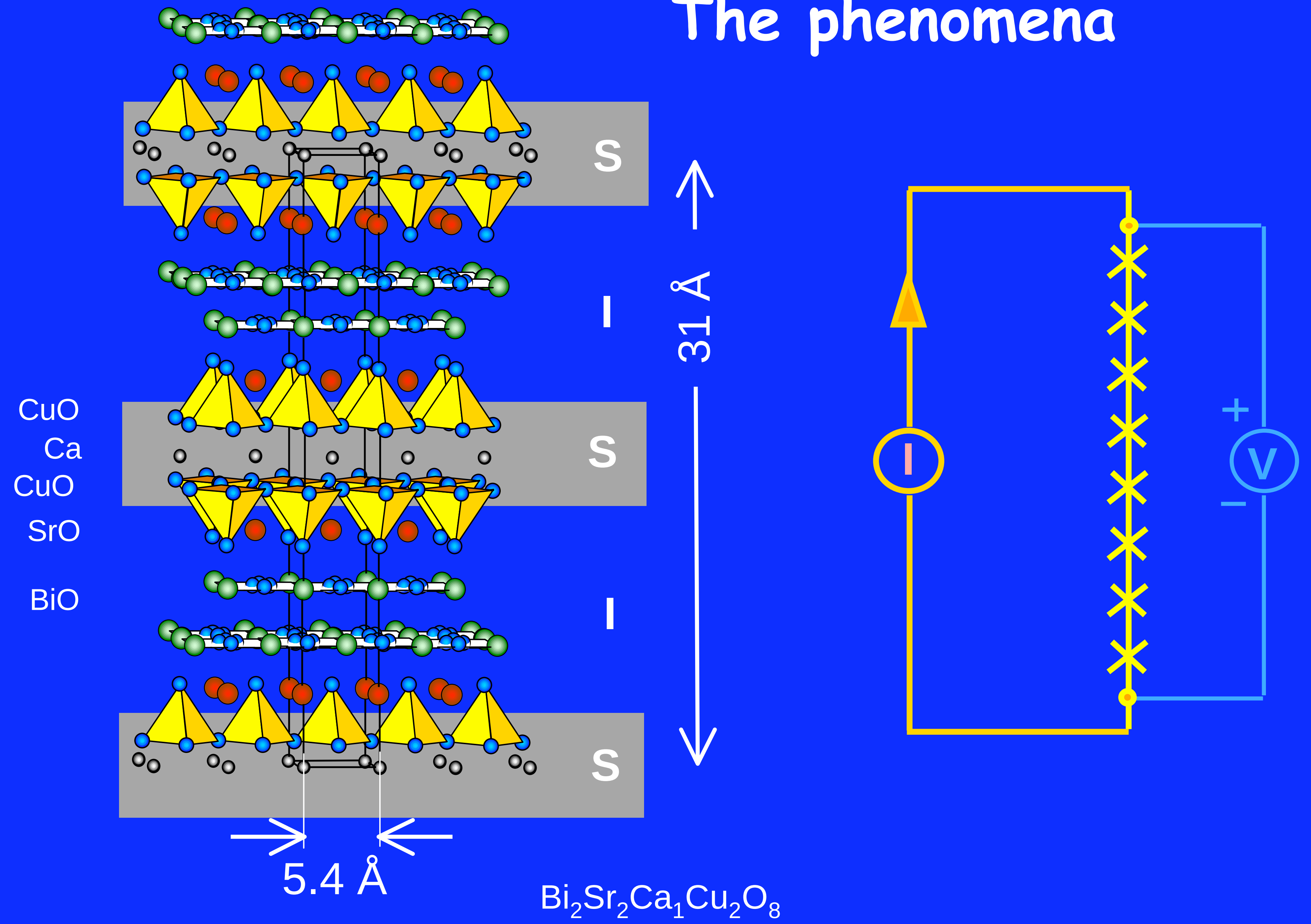

Superconducting gap vs Pseudogap

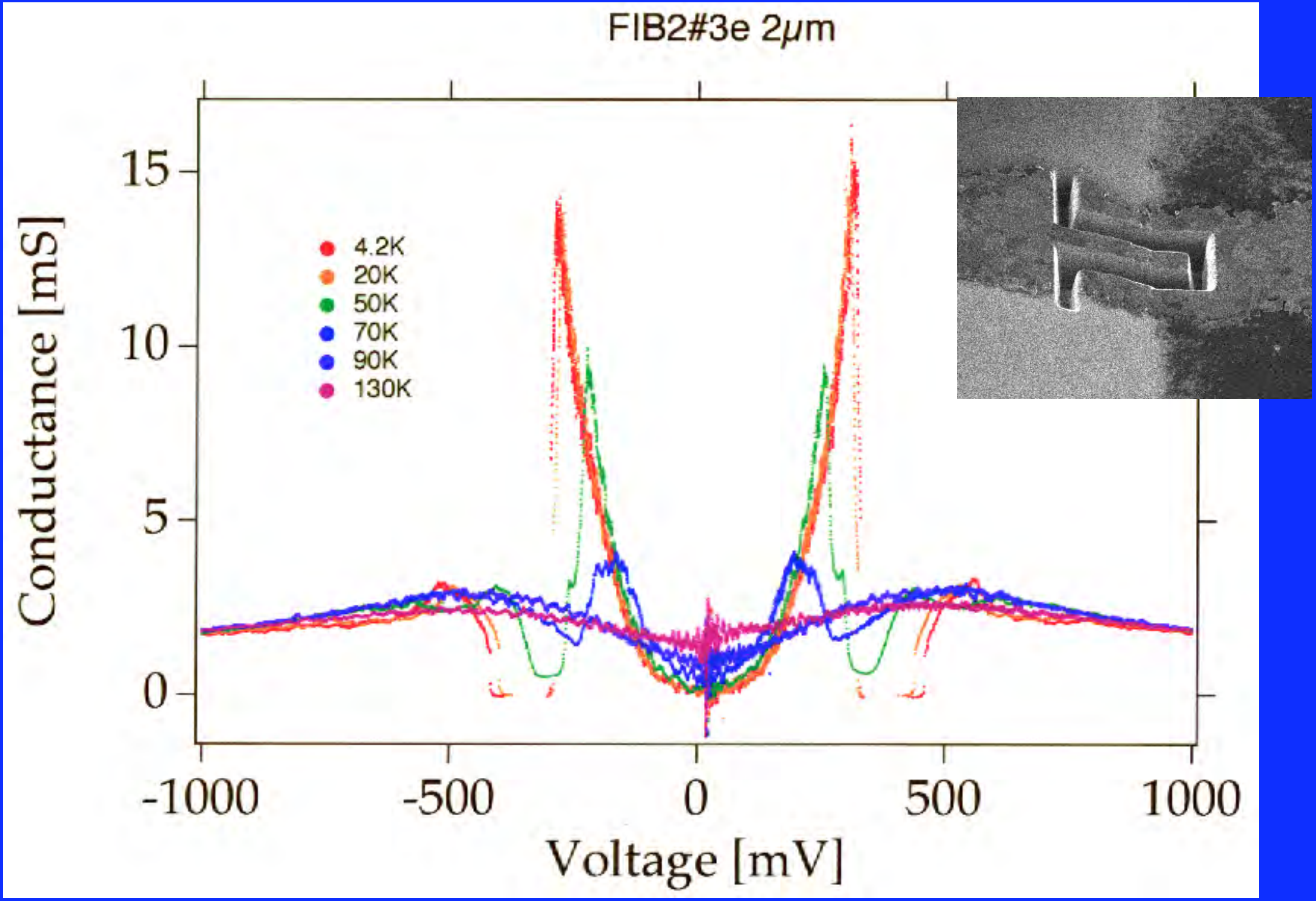

D. Winkler, *et al.*, Superconductor Science & Technology **12**, 1013 (1999)

THE PSEUDOGAP...

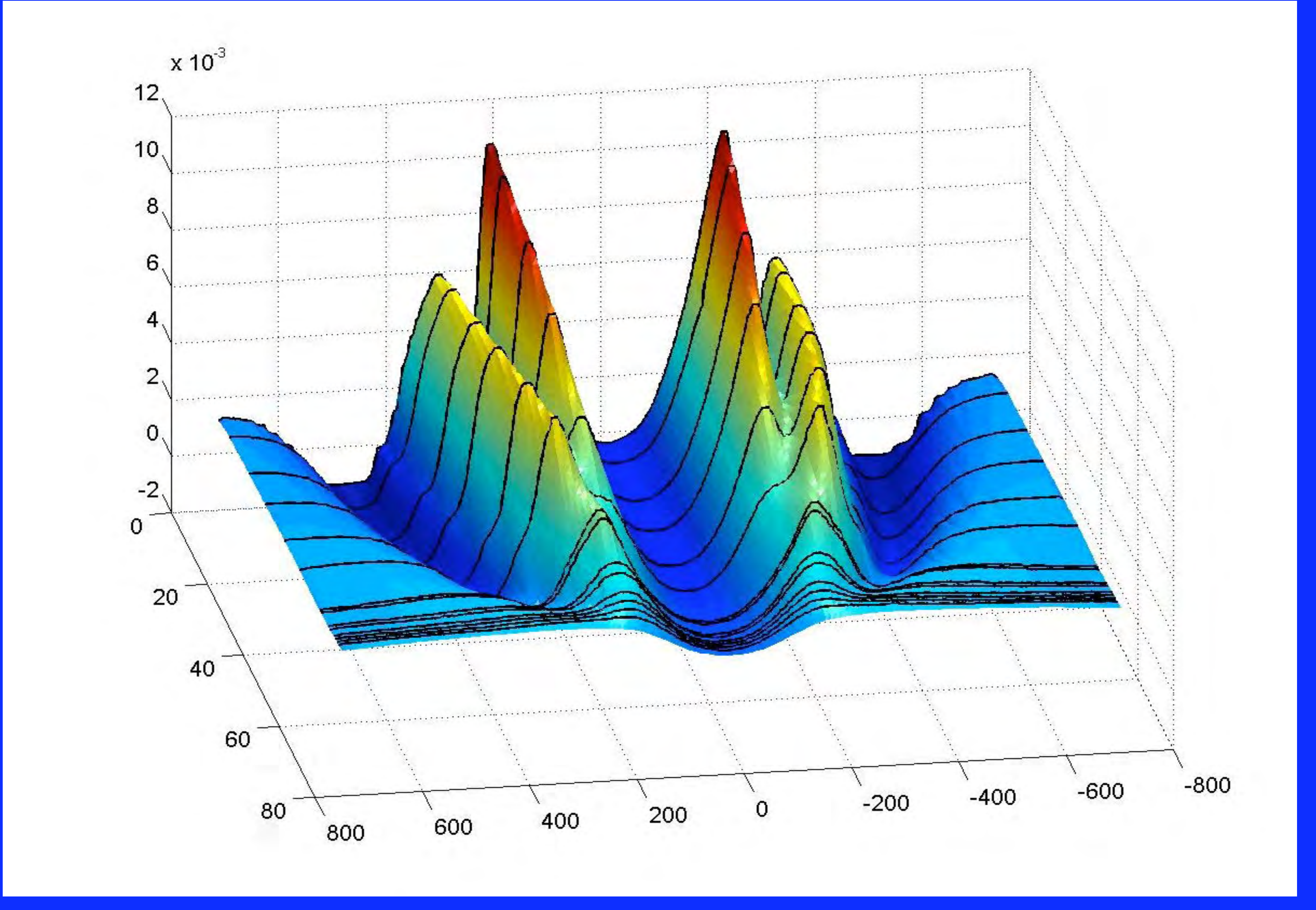

Yurgens et al.

Anisotropy and consequences

Magnetic behaviour

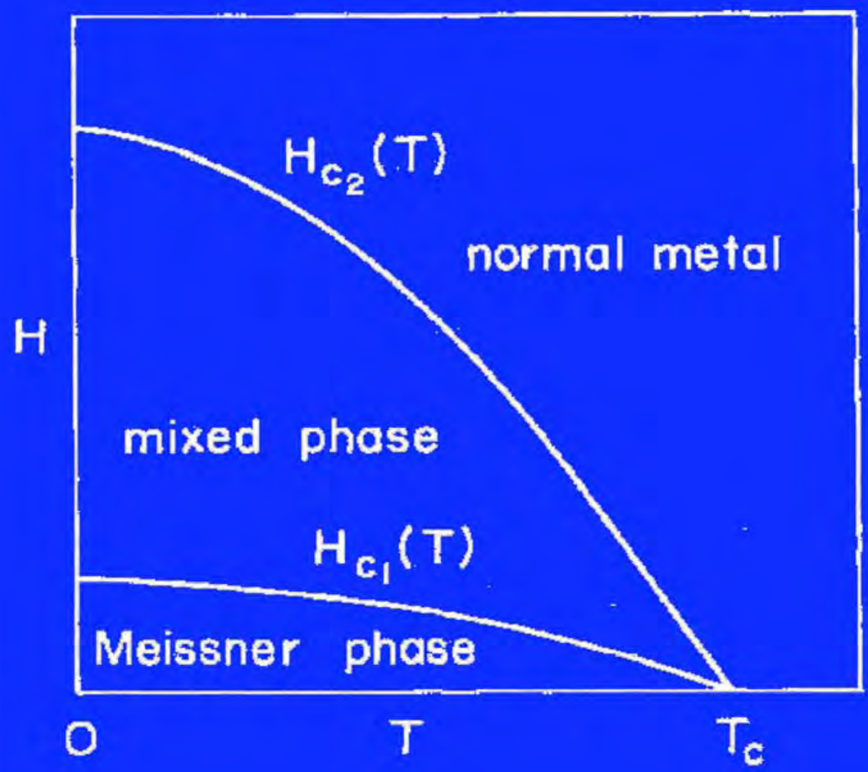

FIG. 1. Mean-field phase diagram comprising a normal-metallic phase at high fields and temperatures, separated by the upper critical-field line $H_{c_2}(T)$ from the mixed or Shubnikov phase, which in turn is separated by the lower critical-field line $H_{c_1}(T)$ from the Meissner-Ochsenfeld phase at low temperatures and fields.

G. Blatter et al., Vortices in high-temperature superconductors, Rev. Mod. Phys., **66**, 1994

ρ(T,B) for LTS and HTS

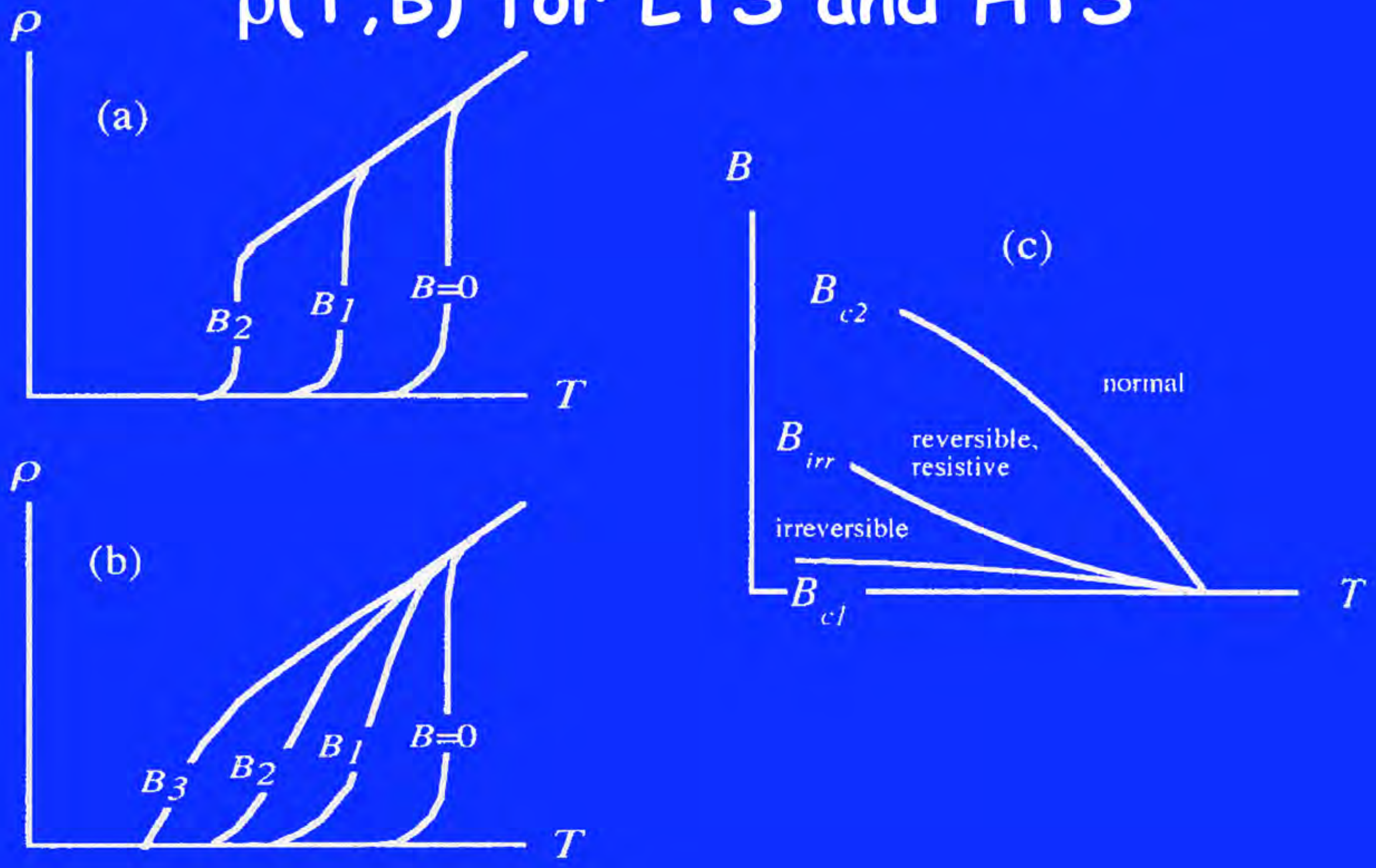

Figure 15.5. Resistive behaviour of type II materials: (a) resistive transitions in a typical conventional superconductor; (b) resistive transitions in a typical cuprate; (c) regions in the B–T plane for a cuprate.

YBCO

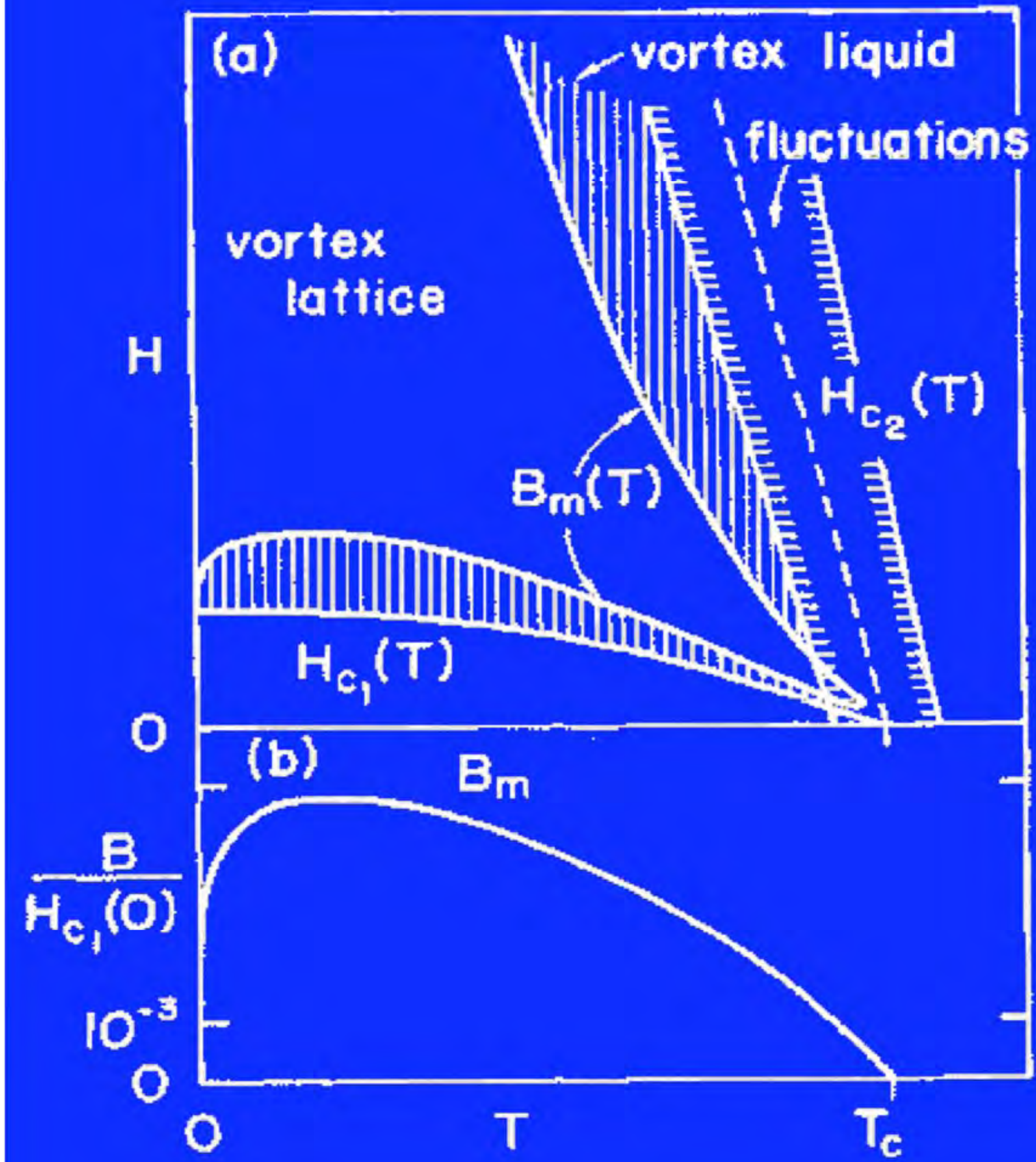

FIG. 2. Phenomenological phase diagram for the anisotropic high-temperature superconductors [parameters for YBCO, $H_{c_1}(0) \approx 730$ G, $H_{c_2}(0) \approx 230$ T, values extrapolated linearly to zero, see also Sec. II.C]: (a) The Abrikosov vortex lattice is melted over a substantial part of the phase diagram. The vortex lattice can melt with increasing temperature (thermal fluctuations) or with decreasing field (exponentially vanishing shear modulus), leading to a reentrant behavior of the melting line $B_m(T)$. The thermodynamic phase transition is shifted to the melting line $B_m(T)$, with the upper critical-field line $H_{c_2}(T)$ marking only a crossover line where the modulus of the order parameter increases rapidly. The regime of large critical fluctuations where the description in terms of vortex (phase) fluctuations breaks down and amplitude fluctuations become important is confined to a rather narrow (~ 1 K wide) region close to $H_{c_2}(T)$. The drawing is not to scale, but emphasizes the main structures appearing in the phase diagram. (b) Shape of the melting line $B_m(T)$ for YBCO with parameters $\xi_{BCS} \approx 16$ Å, $\lambda_L \approx 1400$ Å, and an anisotropy parameter $\varepsilon^2 = M/m \approx 1/25$; drawing is to scale. Note that the extent of the dilute vortex-liquid phase along the field axis is only of the order of a few gauss.

G. Blatter et al., Vortices in high-temperature superconductors, Rev. Mod. Phys., **66**, 1994

BSCCO

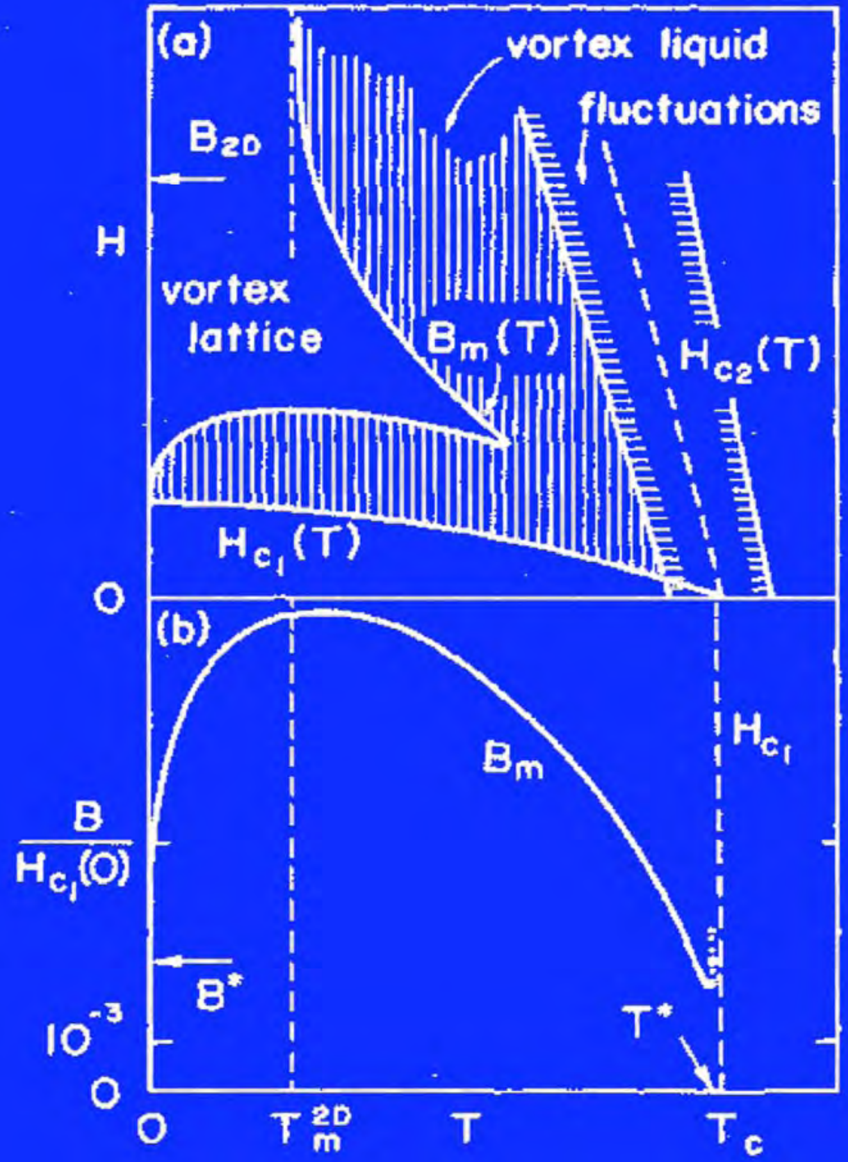

FIG. 3. Phenomenological phase diagram for the strongly layered high-temperature superconductors [parameters for BiSCCO, $H_{c_1}(0)\approx 650$ G, $H_{c_2}(0)\approx 100$ T, values extrapolated linearly to zero, see also Sec. II.C]: (a) The part of the phase diagram occupied by the liquid phase is substantially larger than for the anisotropic YBCO material. Furthermore, the phase diagram separates into two regimes, a low-field regime with $B<B_{2D}$ where the melting process is well described by a 3D continuous anisotropic model, and a high-field region with $B>B_{2D}$, where the melting is quasi-two-dimensional. T_m^{2D} denotes the Berezinskii-Kosterlitz-Thouless dislocation-mediated melting temperature, which is the asymptotic for the melting line $B_m(T)$ at large fields. Drawing not to scale. (b) Shape of the melting lines $B_m(T)$ and the lower critical-field line $H_{c_1}(T)$ for BiSCCO, with parameters $\xi_{BCS}\approx 25$ Å, $\lambda_L\approx 1400$ Å, and an anisotropy parameter $\varepsilon^2=M/m\approx 1/2500$; drawing is to scale. The point (T^*,B^*) denotes the turning point of the lower melting line $B_m(T)$.

G. Blatter et al., Vortices in high-temperature superconductors, Rev. Mod. Phys., **66**, 1994

Abrikosov vortex configurations and Josephson vortices

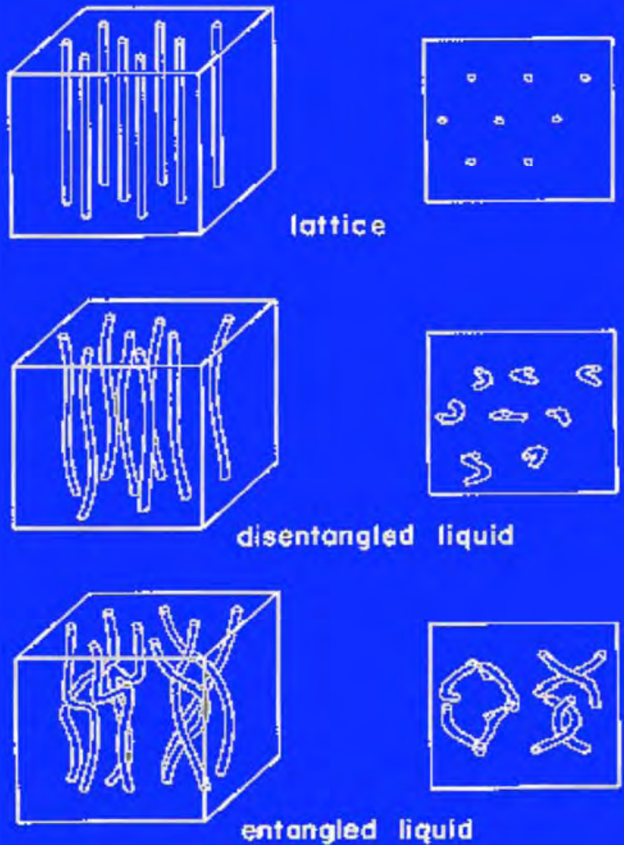

FIG. 23. Various equilibrium phases for a vortex system comprising a vortex-lattice phase (a "Wigner crystal" in the equivalent Bose system), a disentangled vortex-liquid phase (normal ground state), and an entangled vortex-liquid phase (superfluid groundstate) which is equivalent to the normal-metal phase. A vortex-loop excitation (cooperative ring-exchange process) is illustrated in the bottom picture.

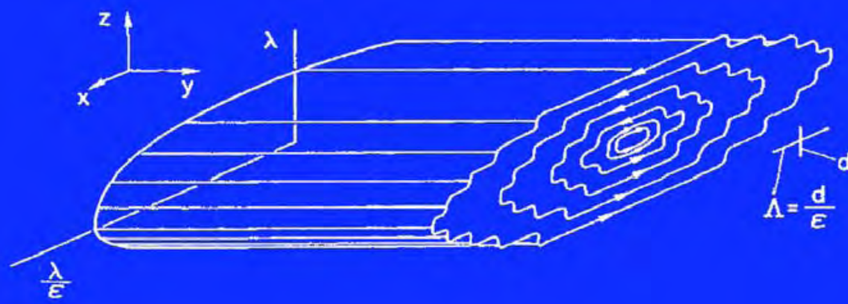

FIG. 31. Josephson vortex in a strongly layered superconductor. The usual normal core of the Abrikosov vortex (dimensions $\varepsilon\xi$ and ξ along z and x, respectively) is replaced by the phase core (dimensions d and $\Lambda = d/\varepsilon$ along z and x, respectively) within which the nonlinearity and the discreteness of the situation are relevant. The region outside the phase core is roughly equivalent to the corresponding regime in an Abrikosov vortex with screening currents extending a distance λ along z and λ/ε along x.

G. Blatter et al., Vortices in high-temperature superconductors, Rev. Mod. Phys., **66**, 1994

Irreversibility lines

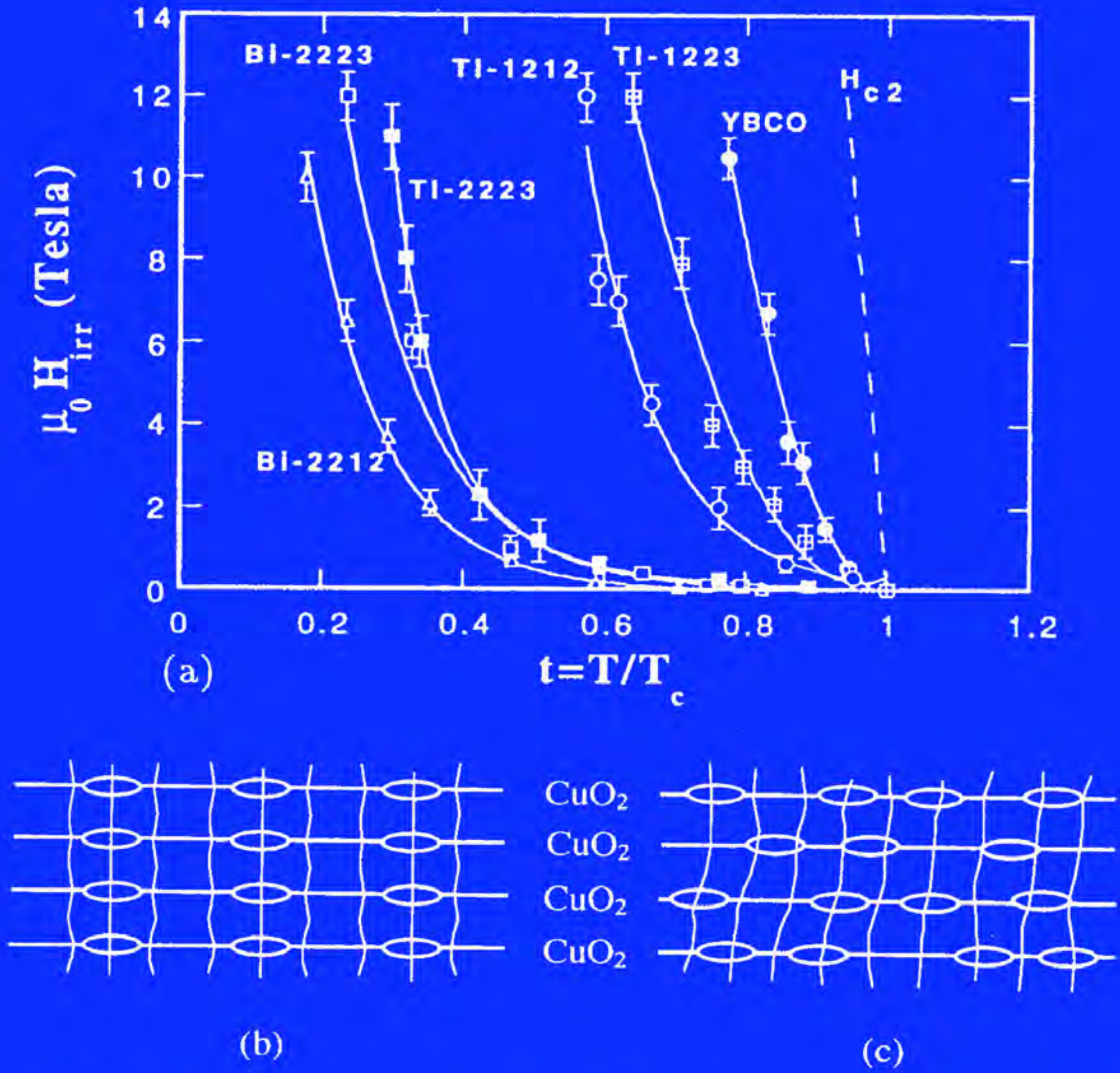

Figure 15.7. (a) The irreversibility line in various cuprates; those with smaller inter-plane couplings lie lower (from Johnson *et al* [9] by permission). (b) Coupled flux pancakes forming extended flux lines. (c) Decoupled flux pancakes.

Experimental phase diagram for vortex matter in BSCCO single crystals

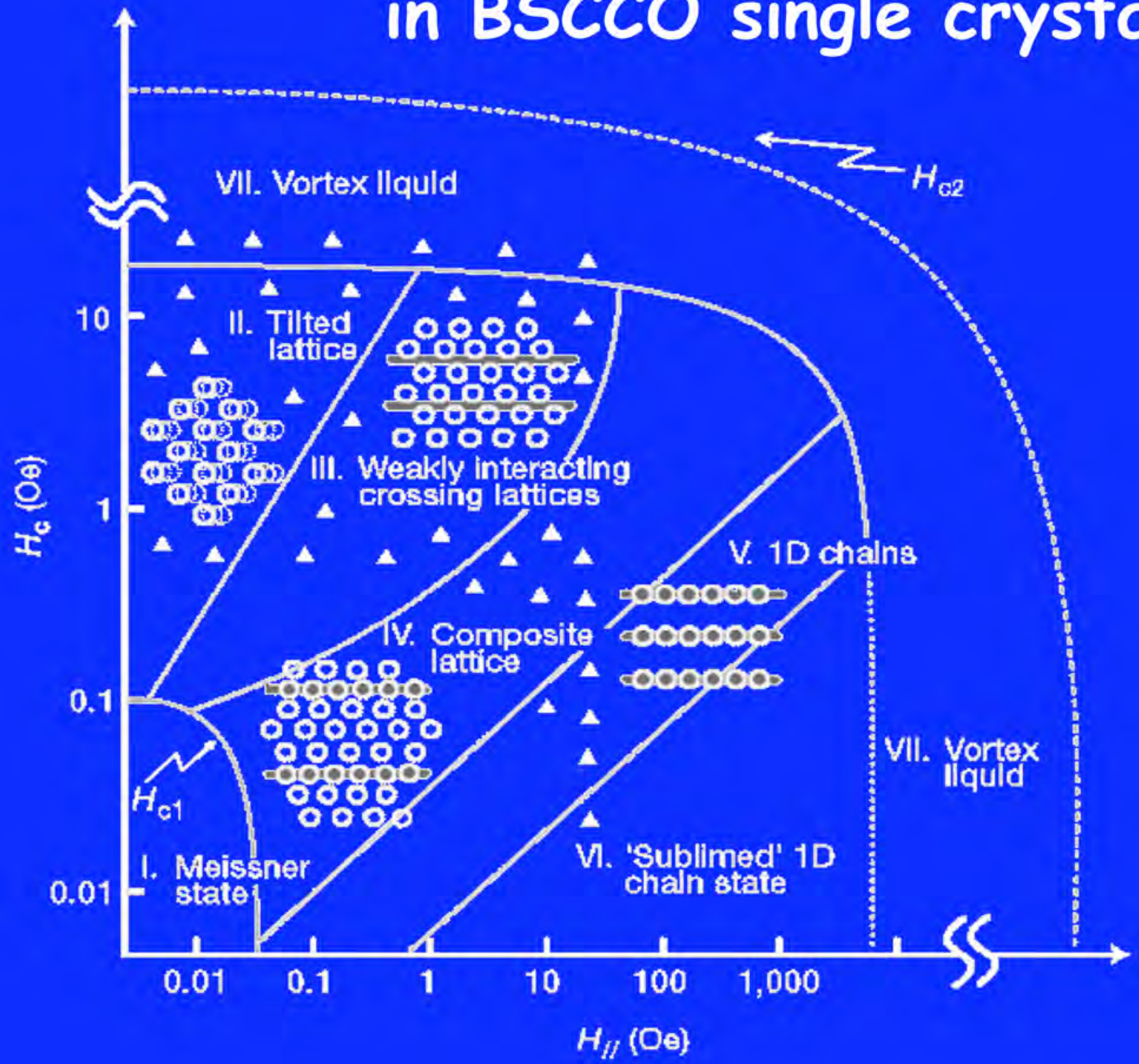

A one-dimensional chain state of vortex matter

Alexander Grigorenko, Simon Bending, Tsuyoshi Tamegai, Shuuichi Ooi and Mohamed Henini

Nature 414, 728-731 (13 December 2001)

Our experimental data (filled triangles) have been used to map out a phase diagram for the different observed states of vortex matter in the Hc–H// domain for the temperature range where this study was performed (77–88 K).

Vortex dynamics

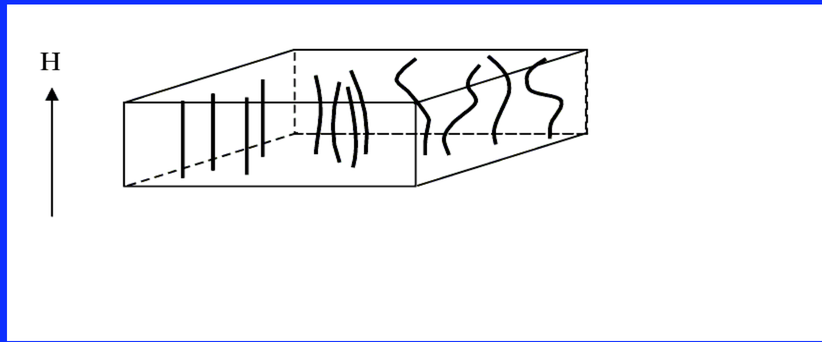

Flux transformer

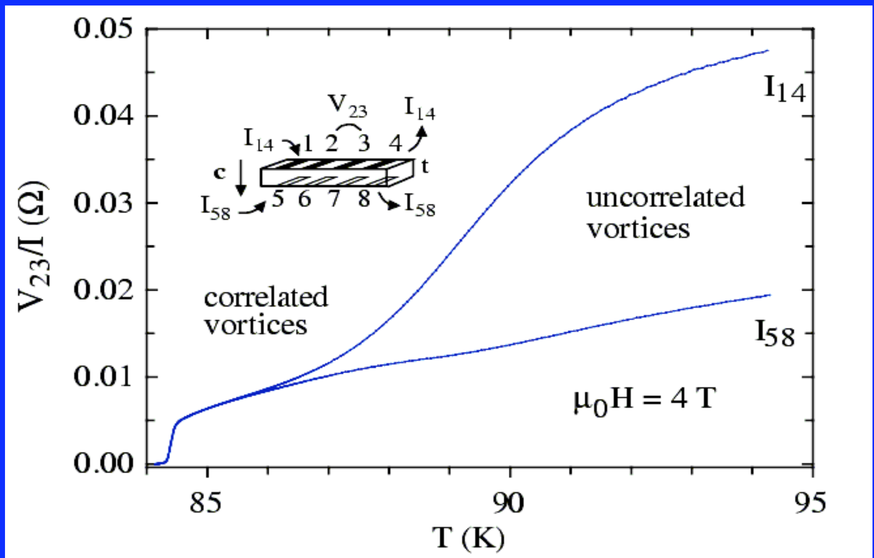

Field independent transition

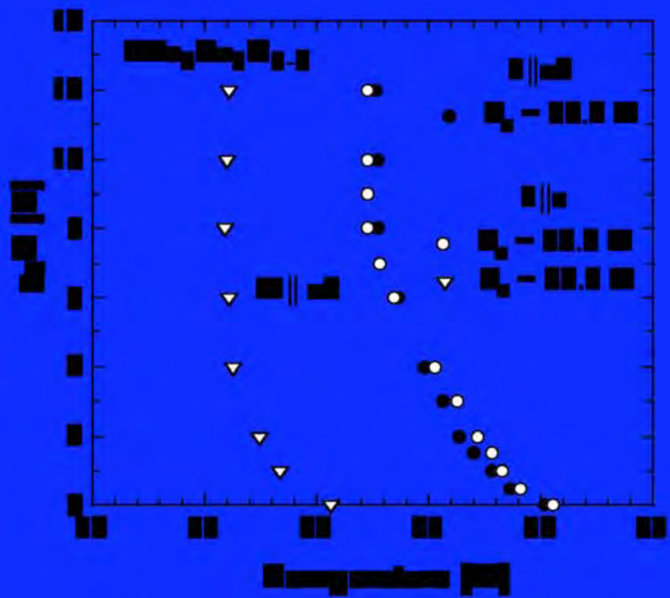

A. Rydh and Ö. Rapp, Phys. Rev. Lett 86 (2001), 1873

B. Lundqvist, Ö. Rapp, and M. Andersson, Phys. Rev. B 64 (2001), 060503R.

Still a puzzle...

17 NOVEMBER 2006 VOL 314 SCIENCE
www.sciencemag.org

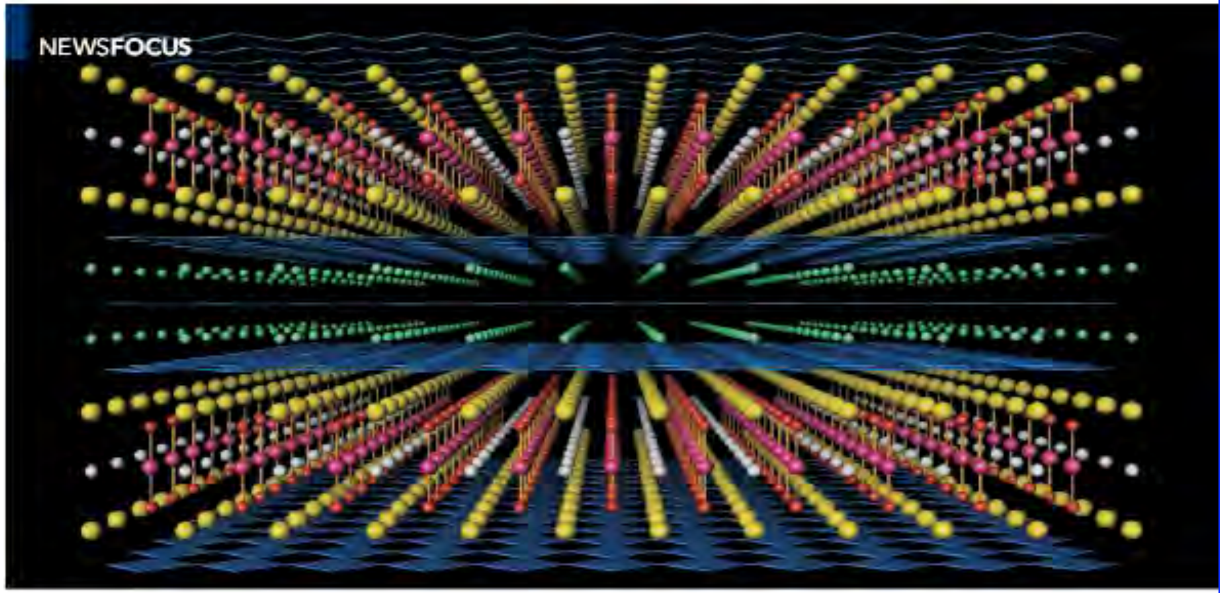

After 2 decades of monumental effort, physicists still cannot explain high-temperature superconductivity. But they may have identified the puzzles they have yet to solve

High T_C: The Mystery That Defies Solution

TWENTY YEARS AGO, A FIRESTORM OF discovery swept through the world of physics. German experimenter J. Georg Bednorz and his Swiss colleague Karl Alexander Müller kindled the flames in September 1986 when they reported that an odd ceramic called lanthanum barium copper oxide carried electricity without any resistance at a temperature of 35 kelvin—12 degrees above the previous record for a superconductor. The blaze ran wild a few months later when Paul Chu of the University of Houston, Texas, and colleagues synthesized yttrium barium copper oxide, a compound that lost resistance at an unthinkable 93 K—conveniently warmer than liquefied air.

A frenzy of slapdash experimenting and sensational claims ensued, says Neil Ashcroft, a theorist at Cornell University. He organized a session on the new high-temperature superconductors at the meeting of the American Physical Society in New York City the following March. The "Woodstock of physics" stretched until 4 a.m. and bubbled over with giddy enthusiasm. "We had prominent people saying it would all be explained quickly and that we would have superconducting power lines and levitating trains," Ashcroft says.

Ashcroft himself had doubts, however, as he told a class of graduate students a few months later. (I was a member of the class.) The materials comprised four and five elements and possessed elaborate layer-cake structures. They broke the rules about what should make a good superconductor. In short, Ashcroft predicted, high-temperature superconductivity would remain the outstanding problem in condensed matter physics for the next 25 years.

That prognostication is coming true. Two decades after high-temperature superconductors were discovered, physicists still do not agree on how electrons within them pair to glide through the materials effortlessly at temperatures as high as 138 K. Researchers haven't failed for lack of trying. According to some estimates, they have published more than 100,000 papers on the materials. Several theorists claim they have deciphered them—although their explanations clash. Still, high-temperature superconductivity has refused to submit to some of the world's best minds.

"The theoretical problem is so hard that there isn't an obvious criterion for *right*," says Steven Kivelson, a theorist at Stanford University in Palo Alto, California. Experimenters are producing a flood of highly detailed data, but physicists struggle to piece the results together, says Joseph Orenstein, an experimenter at the University of California, Berkeley, and Lawrence Berkeley National Laboratory. "It must be close to unique to have so much information and so little consensus on what the questions should be," Orenstein says.

The problem is more than a sliver under the nail. High-temperature superconductivity has shown that physicists' conceptual tools can't handle materials in which electrons shove one another so intensely that it's impossible to disentangle the motion of one from that of the others. Such "strongly correlated" electrons pop up in nanodevices and novel magnets, organic conductors and other exotic superconductors. "High-temperature superconductivity is the stumbling block of the whole discipline of condensed matter physics," says Peter Abbamonte, an experimenter at the University of Illinois, Urbana-Champaign.

In spite of the difficulty of the puzzle, many physicists say they are closing in on a solution. Most now agree on certain key properties of the materials. Precision experiments are

CREDITS (TOP TO BOTTOM): P. EDWARDS AND M. O. JONES/UNIVERSITY OF OXFORD

Published by AAAS

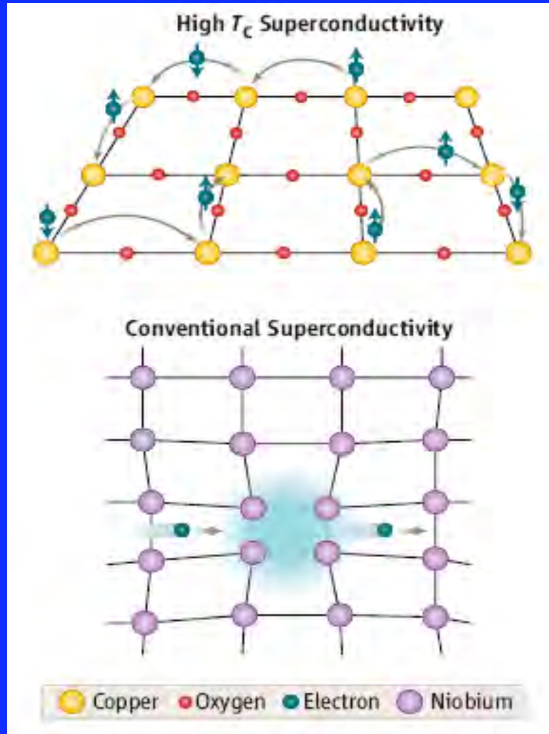

Shall we dance? Instead of the motion of ions, the subtle waltz of electrons along atomic planes may cause pairing in high-temperature materials.

Other bits and pieces in the puzzle…

The pseudogap…

$HgBr_2$-Bi2212

August's pseudogap movie

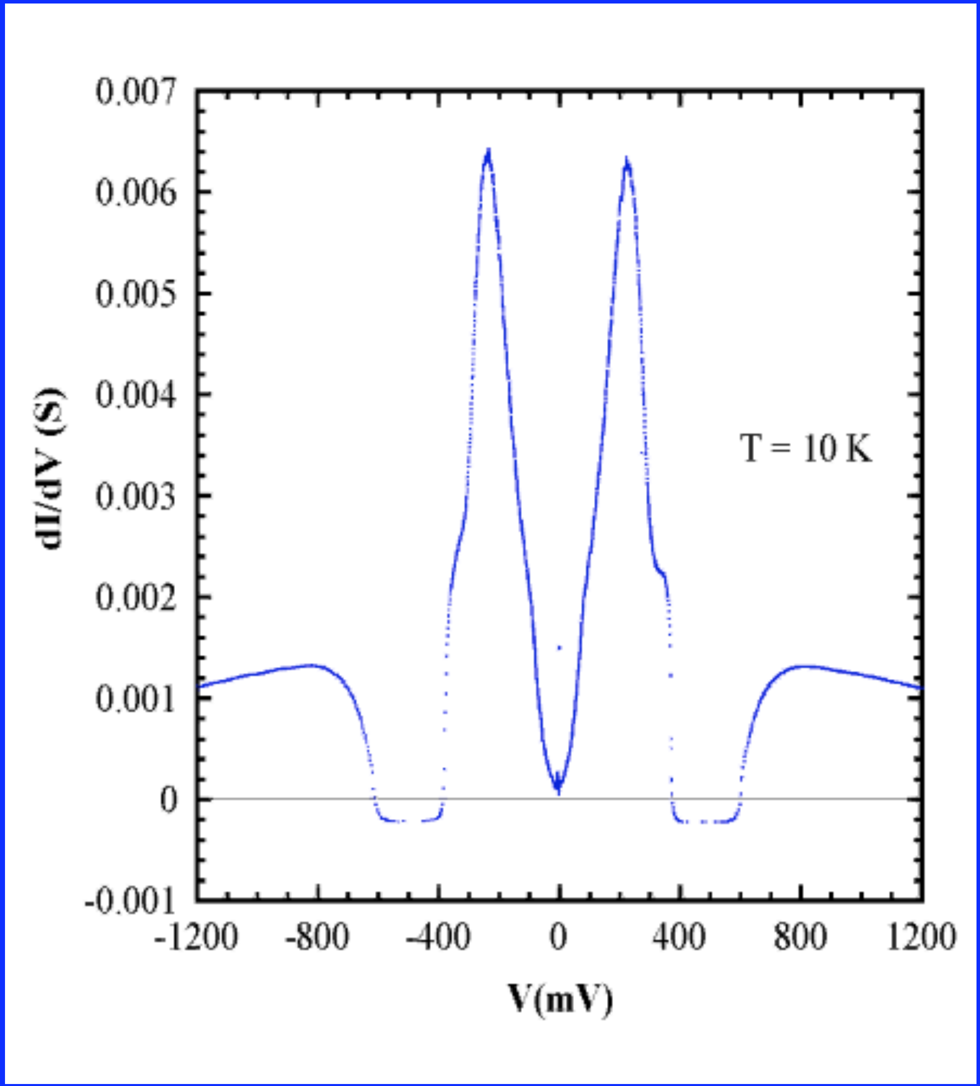

$HgBr_2$- Bi2212

$HgBr_2$- intercalation – see below

The pseudogap

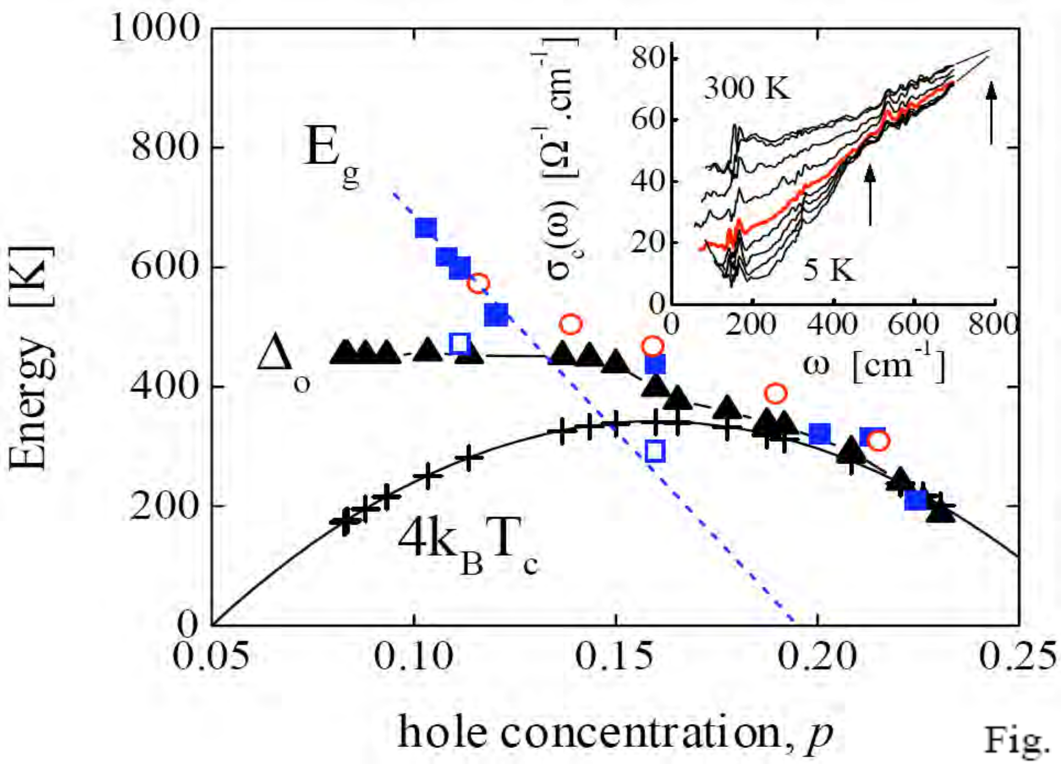

Fig. 8. The p-dependence of the low-temperature spectral gap determined from c-axis IR spectroscopy for Y-123 (○) and SIS tunnelling spectroscopy for Bi-2212 (■) and $4k_BT_c$ for $Y_{0.8}Ca_{0.2}$-123 (crosses). At first sight these appear to confirm a scenario in which T* merges with T_c. Also shown is the SC gap Δ_o determined for $Y_{0.8}Ca_{0.2}$-123 from heat capacity (▲). The open squares are additional second-gap features in the tunnelling spectra that show that the low-doping gap is the pseudogap while the high-doping gap is the SC gap. Inset: the IR conductivity $\sigma_1(\omega)$ for an under-doped sample of Y-123 with T_c= 78 K (see ref. [26]) for different temperatures (T = 300, 200, 150, 100, 80, 70, 55, 450 and 5 K). The highlighted curve (80 K) is close to T_c. The vertical arrows mark the distinct SC gap and pseudo-gap.

The doping dependence of T* - what is the real high-Tc phase diagram?
J. L. Tallona and J.W. Loramb

The pseudogap

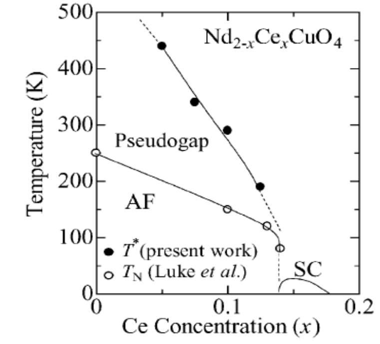

Fig. 4. Electronic phase diagram of $Nd_{2-x}Ce_xCuO_4$. The onset temperature of pseudogap T^* is shown in comparison with the Néel temperature measured previously by Luke et al. [10]. SC and AF stand for the superconducting and antiferromagnetic region, respectively.

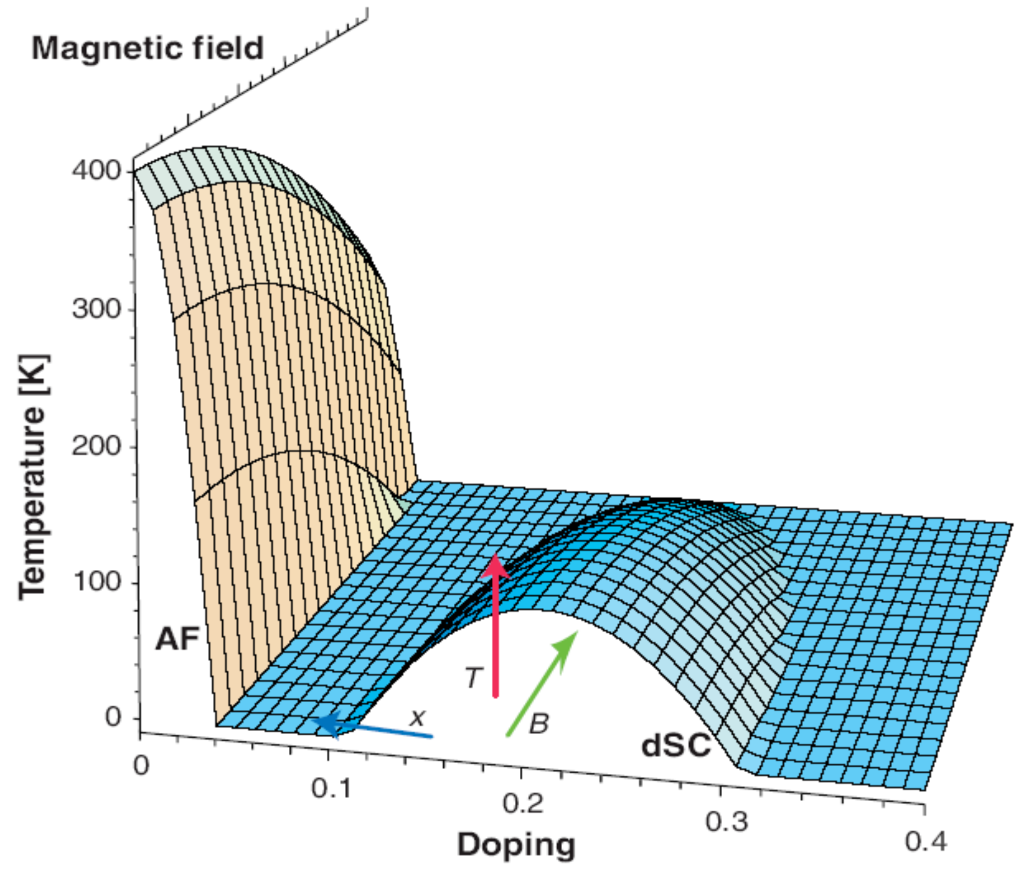

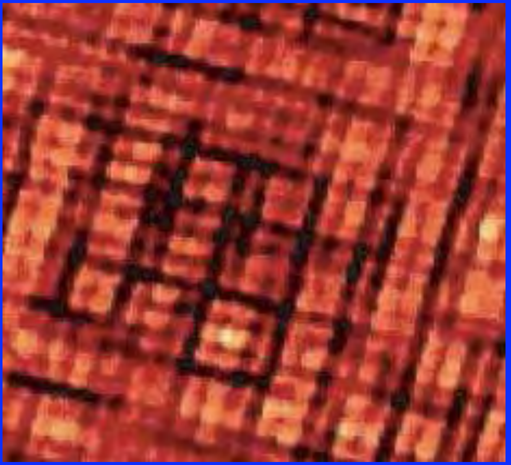

3 SEPTEMBER 2004 VOL 305 p 1410 SCIENCE www.sciencemag.org

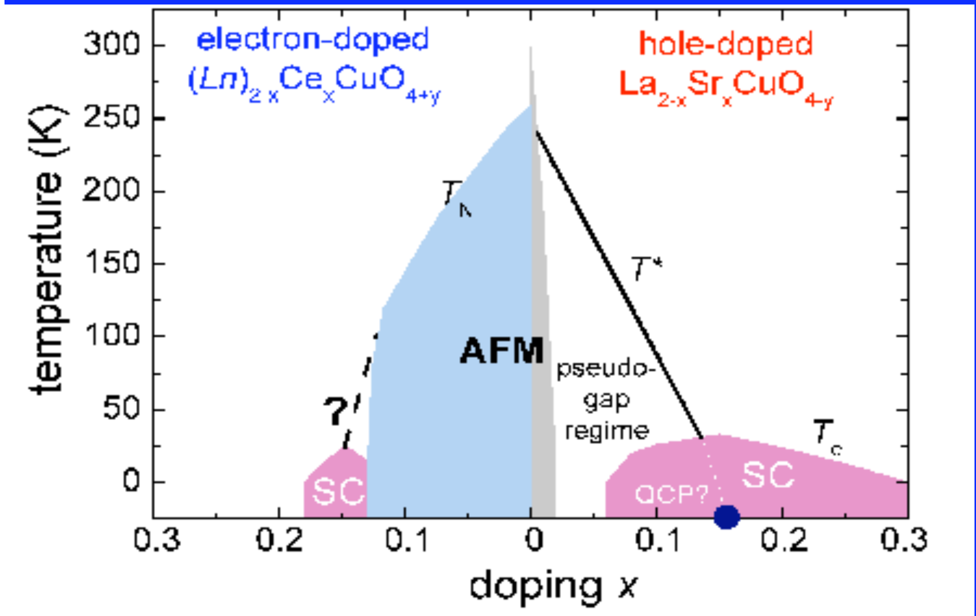

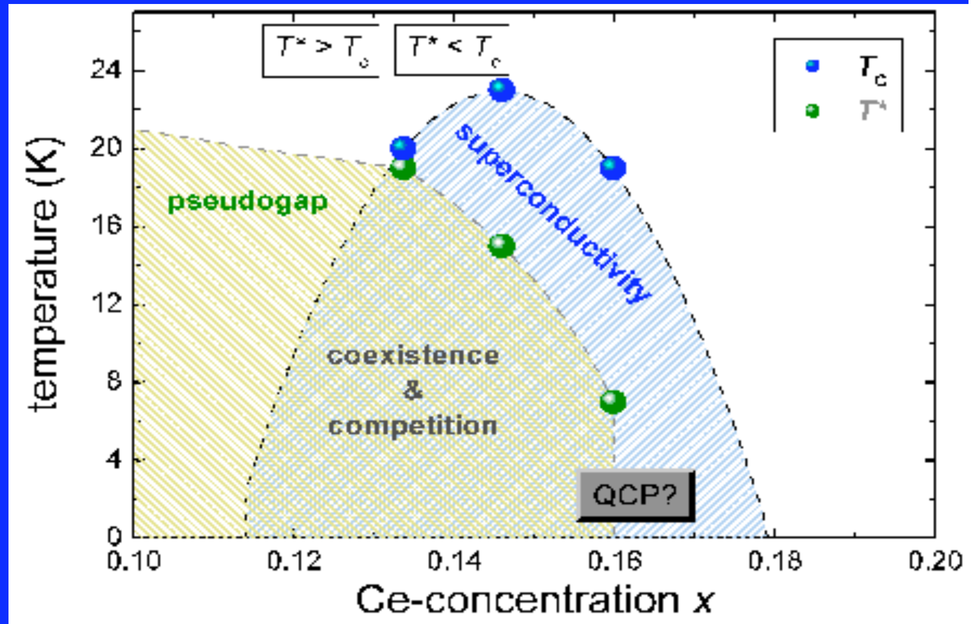

Figure 1: Phase diagram of hole- and electron-doped cuprates.
AFM: Antiferromagnetic region (*TN*: Neel-temperature).
SC: Superconducting region (*TC*: Critical temperature). QCP: Quantum critical point. *T**: Pseudogap temperature.

Figure 2: Coexistence of pseudogap and superconducting phase in electron-doped HTS (from L. Alff *et al.*, Nature **422, 698 (2003)**.

http://www.wmi.badw-muenchen.de/FG538/projects/TP4/TP4.htm

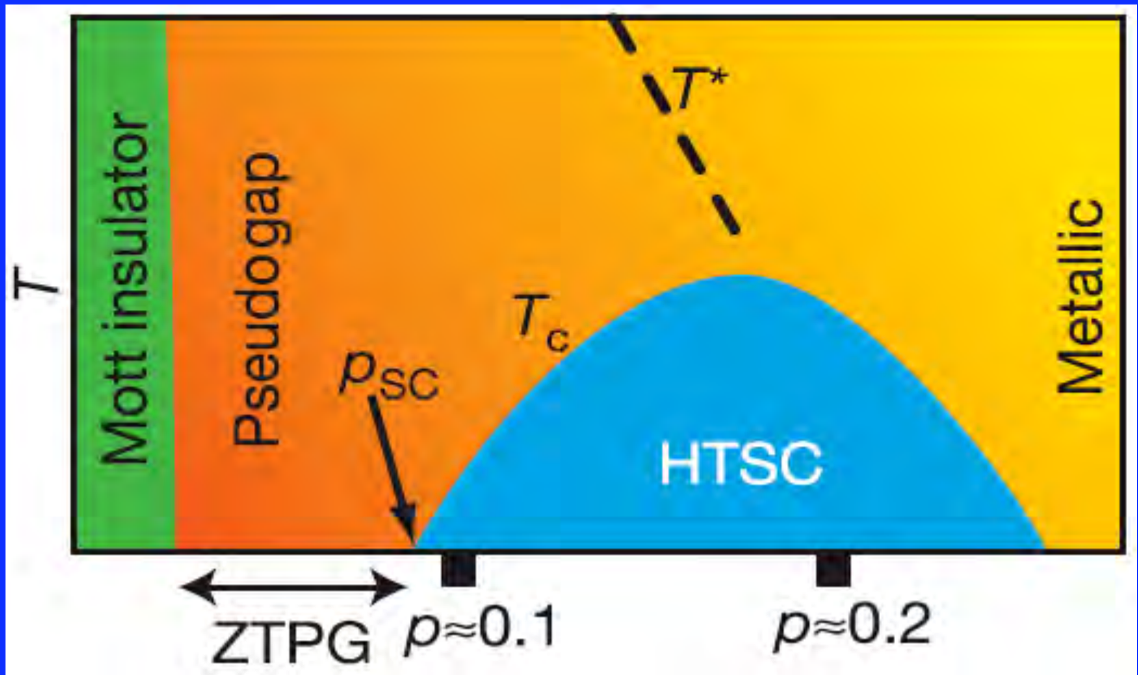

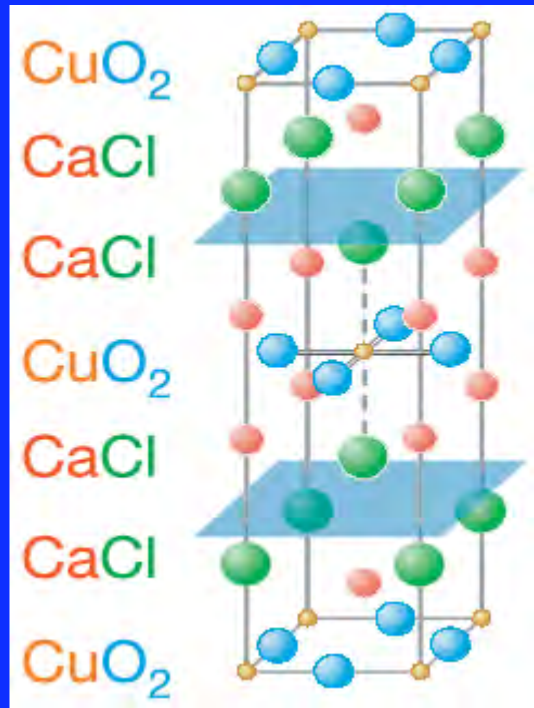

Figure 1 Atomic-scale explorations of electronic states in $Ca_{2-x}Na_xCuO_2Cl_2$. a, A schematic phase diagram of hole-doped copper-oxides showing the Mott insulator, high-T_c superconductor (HTSC) and metallic phases along with the 'pseudogap' regime and the ZTPG line. b, Crystal structure of $Ca_{2-x}Na_xCuO_2Cl_2$. Red, orange, blue and green spheres represent Ca(Na), Cu, O and Cl atoms, respectively. Conducting CuO_2 planes are sandwiched by insulating CaCl layers.

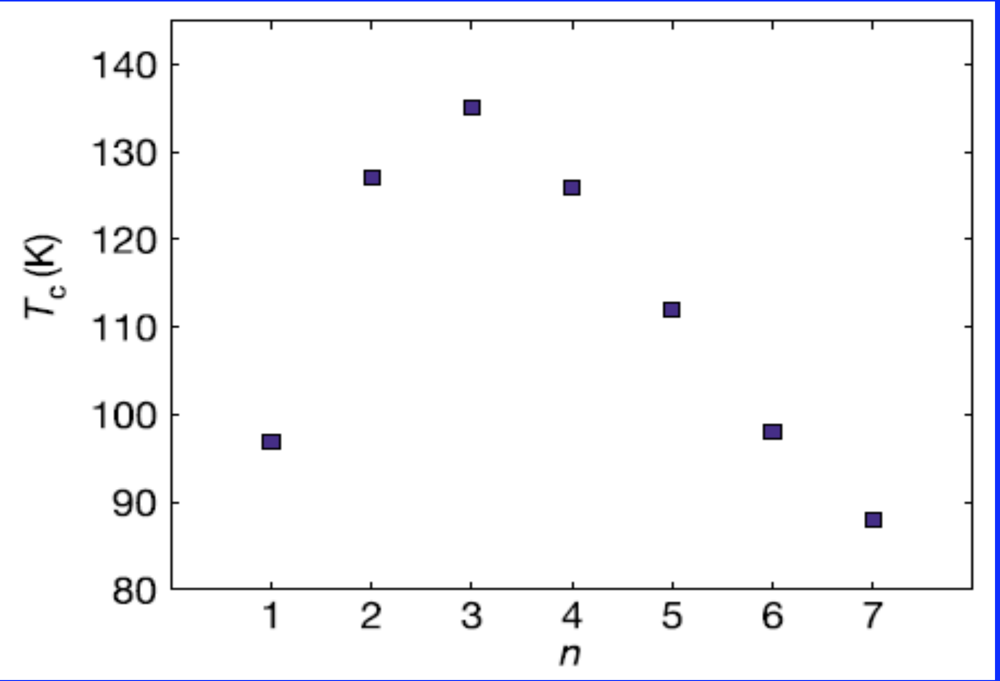

An explanation for a universality of transition temperatures in families of copper oxide superconductors

Sudip Chakravarty[1], Hae-Young Kee[2] & Klaus Völker[2]

[1]*Department of Physics and Astronomy, University of California Los Angeles, Los Angeles, California 90095-1547, USA*
[2]*Department of Physics, University of Toronto, Toronto, Ontario M5S 1A7, Canada*

Figure 1 Transition temperature within a homologous series. A homologous series[29] is a family of compounds having the same charge-reservoir block, but nCuO$_2$-planes in the infinite-layer block, which in turn consists of ($n - 1$) bare cation planes and nCuO$_2$-planes. A good example is the family $HgBa_2Ca_{(n-1)}Cu_nO_{(2n+2+\delta)}$ whose T_c as a function of n, optimized with respect to oxygen concentration, is shown. (The figure is adapted from the data in ref. 30.) Similar results have been known for some time; see ref. 1.

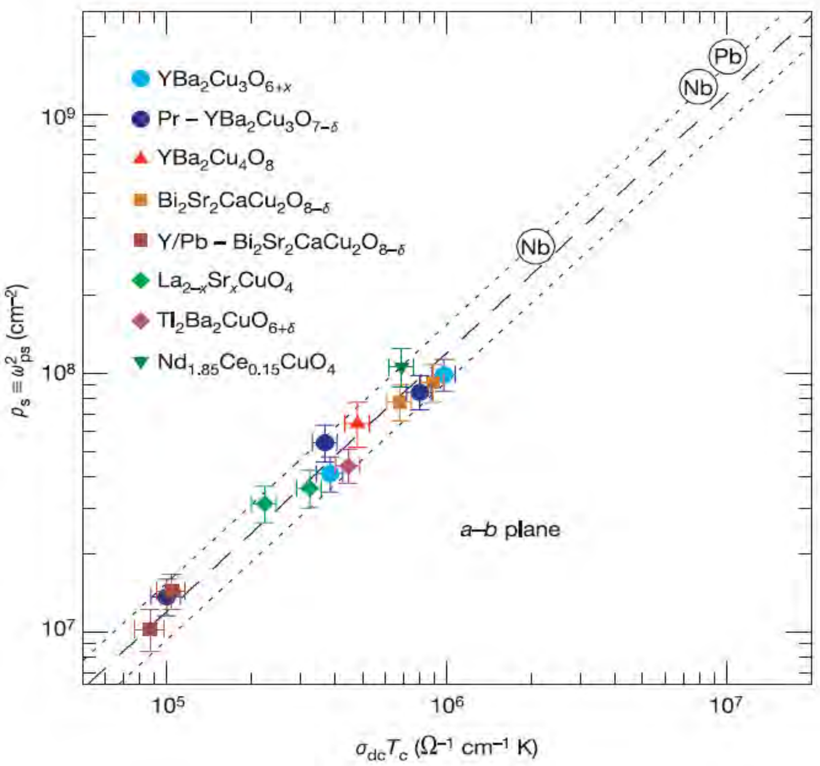

Figure 1 Plot of the superfluid density (ρ_s) versus the product of the d.c. conductivity (σ_{dc}) and the superconducting transition temperature (T_c) for a variety of copper oxides and some simple metals. (σ_{dc} is measured just above the transition, and parallel to the copper–oxygen (*a*–*b*) planes; data are shown on a log–log plot; see Supplementary Table 1 for details, including errors.) The values for σ_{dc} and ρ_s are obtained from optical measurements of the reflectance. The reflectance is a complex quantity consisting of an amplitude and a phase; in an experiment only the amplitude is usually measured. However, if the reflectance is measured over a wide frequency range, the Kramers–Kronig relation may be used to obtain the phase. Once the complex reflectance is known, then other complex optical functions may be calculated (for example, the dielectric function or the conductivity). The σ_{dc} used in this scaling relation has been extrapolated from the real part of the optical conductivity $\sigma_{dc} = \sigma_1(\omega \to 0)$ at $T \approx T_c$. For $T \ll T_c$, the response of the dielectric function to the formation of a condensate is expressed purely by the real part, $\epsilon_1(\omega) = \epsilon_\infty - \omega_{ps}^2/\omega^2$, which allows the superconducting plasma frequency ω_{ps} to be calculated from $\omega_{ps}^2 = -\omega^2\epsilon_1(\omega)$ in the $\omega \to 0$ limit, where $\omega_{ps}^2 = 4\pi n_s e^2/m^*$ is proportional to the number of carriers in the condensate. The strength of the condensate (ρ_s) is simply $\rho_s \equiv \omega_{ps}^2$. The dashed and dotted lines are described by $\rho_s = (120 \pm 25)\sigma_{dc}T_c$. Within error, all the data for the copper oxides are described by the dashed line. The data for the conventional superconductors Nb and Pb, indicated by the atomic symbols within the circles, lie slightly above the dashed line.

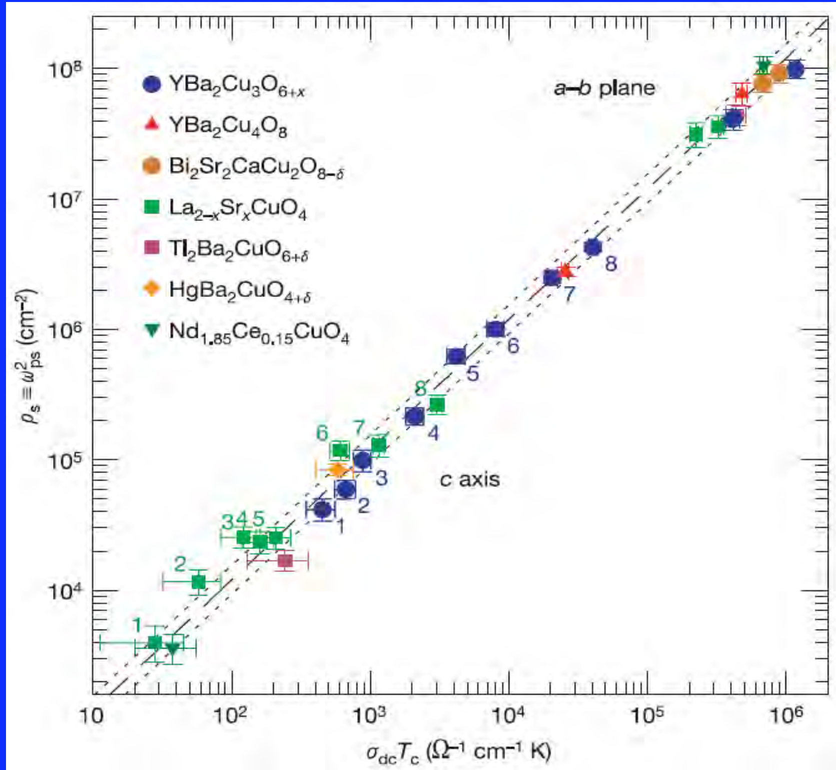

Figure 2 As Fig. 1 but for copper oxides only, and including data for the poorly conducting *c* axis. The values for ρ_s and σ_{dc} are obtained from optical measurements, as described in Fig. 1 legend. In addition to the published results, new data are also included for $HgBa_2CuO_{4+\delta}$ and $La_{2-x}Sr_xCuO_4$. Within error, all of the data fall on the same universal (dashed) line with slope of unity, defined by $\rho_s = 120\sigma_{dc}T_c$; the dotted lines are from $\rho_s = (120 \pm 25)\sigma_{dc}T_c$. See Supplementary Table 2 for details, including errors.

A universal scaling relation in high temperature superconductors
C. C. Homes et al.

NATURE |VOL 430 | 29 JULY 2004 |www.nature.com/nature

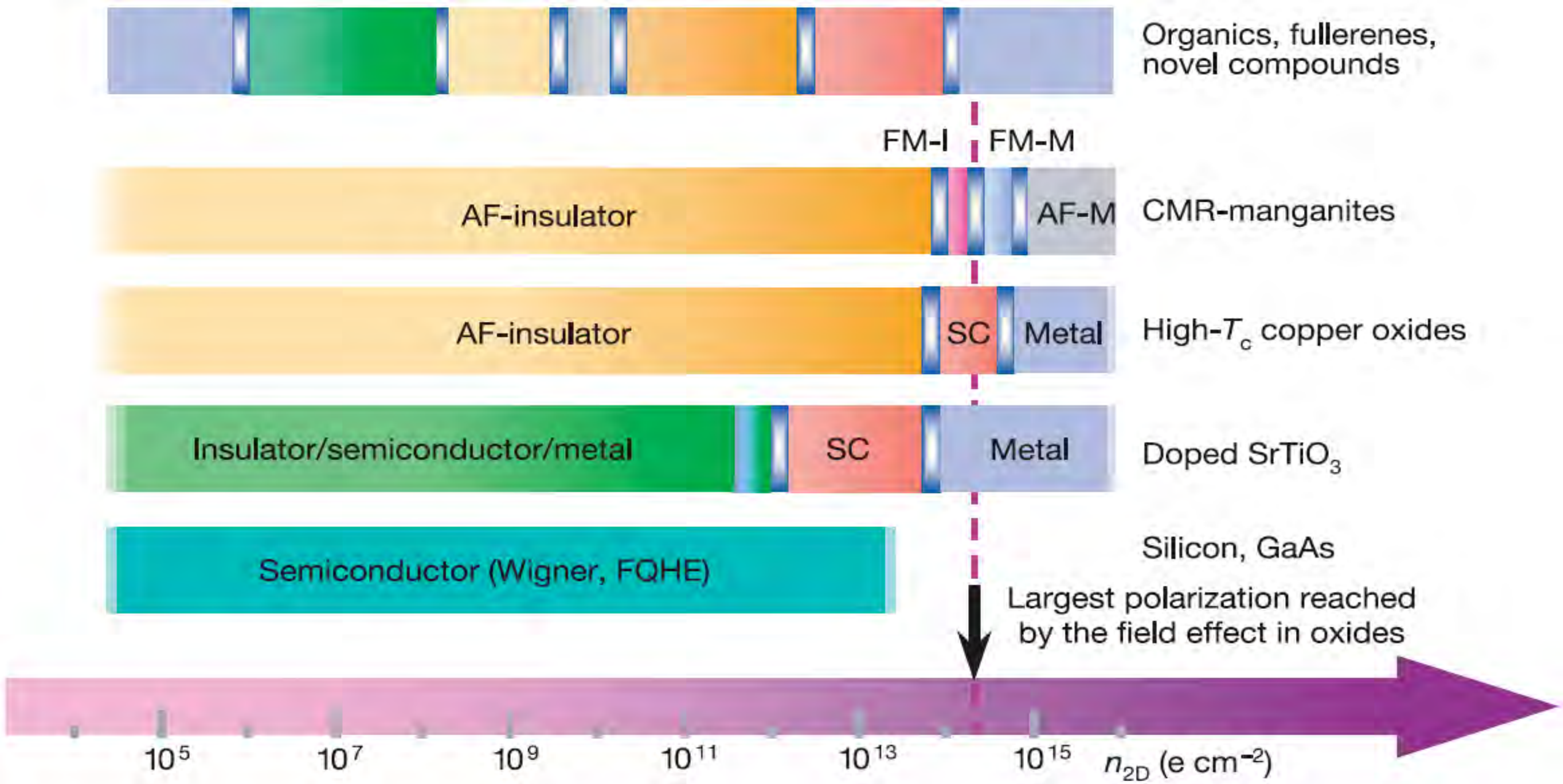

Figure 1 Illustration of the zero-temperature behaviour of various correlated materials as a function of sheet charge density (n_{2D}). Silicon is shown as a reference. The examples for high-T_c superconductors and for colossal magnetoresistive (CMR) manganites reflect $YBa_2Cu_3O_{7-\delta}$ and (La,Sr)MnO_3, respectively. The top bar has been drawn to illustrate schematically the richness of materials available for field-effect tuning and the spectrum of their phases. AF, antiferromagnetic; FM, ferromagnetic; I, insulator; M, metal; SC, superconductor; FQHE, fractional quantum Hall effect; Wigner, Wigner crystal.

Electric field effect in correlated oxide systems
C. H. Ahn, J.-M. Triscone & J. Mannhart

NATURE |VOL 424 | 28 AUGUST 2003 |www.nature.com/nature

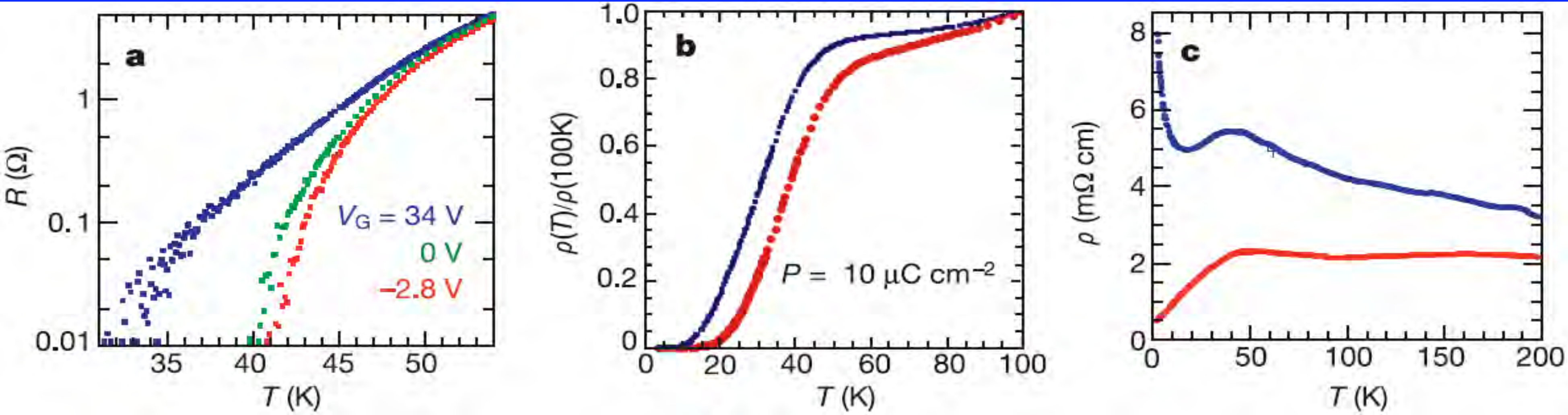

Figure 3 Field effects in superconducting films. In each case, the blue curve corresponds to depletion of the carrier density, and the red curve corresponds to enhancement of the carrier density in the DS (drain–source) channel. **a**, Change of the DS resistance of an ~8-nm-thick $YBa_2Cu_3O_{7-\delta}$ channel with a ~300-nm-thick $Ba_{0.15}Sr_{0.85}TiO_3$ gate insulator. The scatter in the data results from the noise of the measurement system (from ref. 6). **b**, Resistance change of a ~2-nm-thick $GdBa_2Cu_3O_{7-\delta}$ film induced by a 300-nm-thick PZT layer acting as ferroelectric gate. The two curves have been normalized in the normal state. **c**, Resistance change of a ~2-nm-thick $GdBa_2Cu_3O_{7-\delta}$ film whose doping level has been chosen to be close to the superconductor–insulator transition, induced by a 300-nm-thick PZT layer acting as ferroelectric gate. These data have been measured at 1 T (from ref. 18).

MgB_2

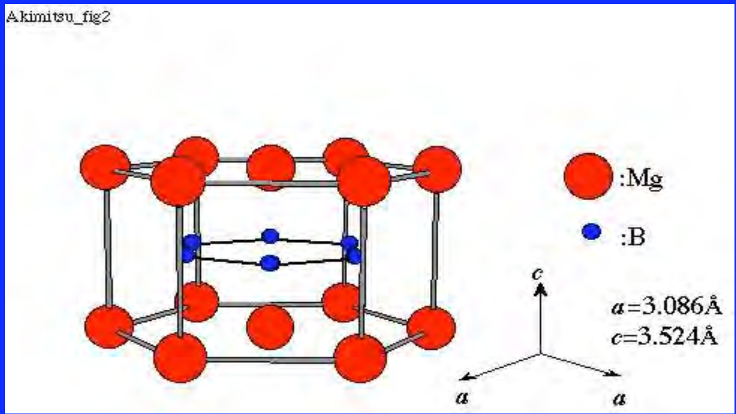

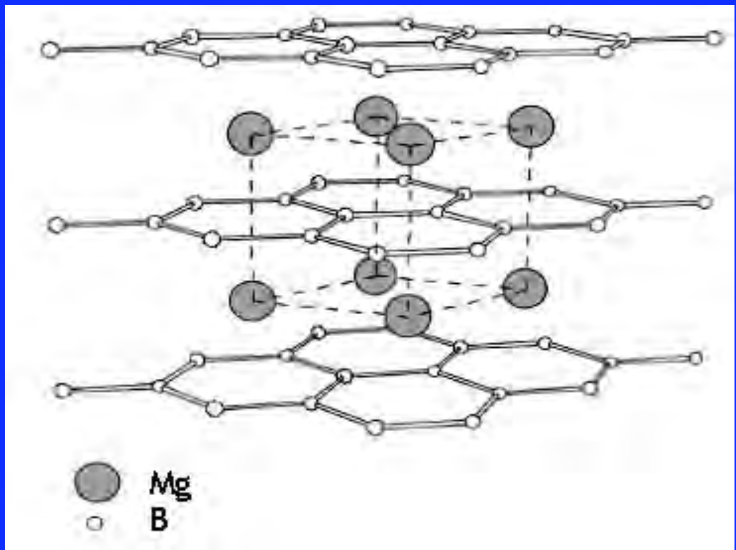

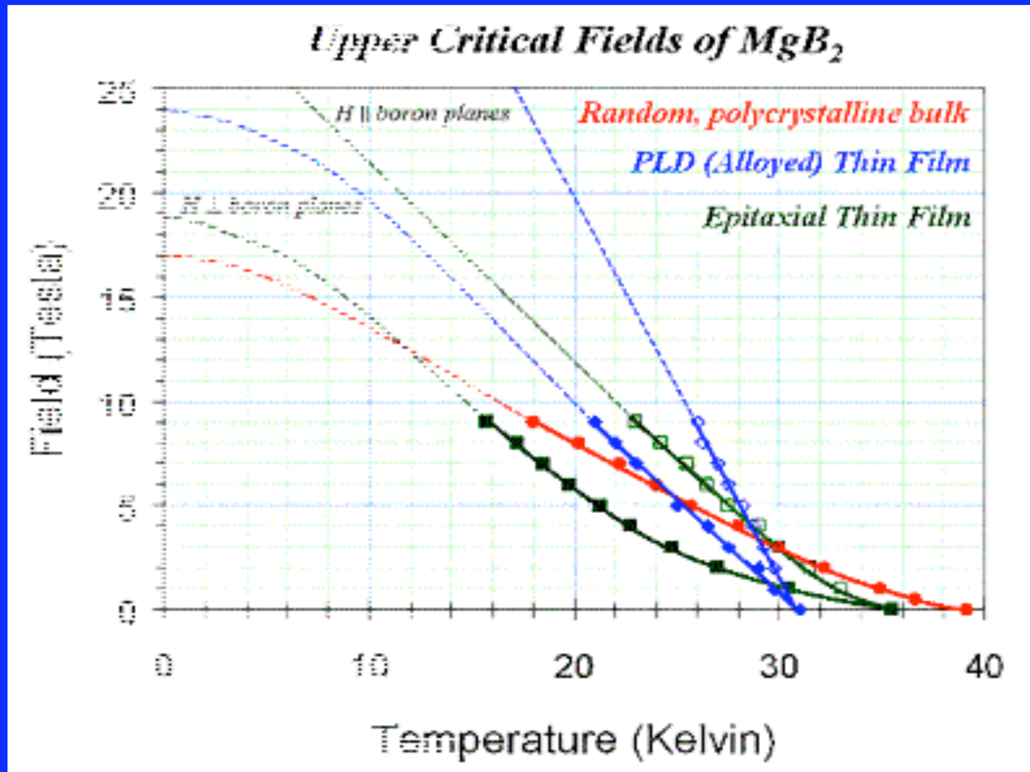

From Jochen Mannhart (Lecture Saas Fee)

Superconductivity in MgB_2

found in 2001 by J. Akimitsu

J. Akimitsu

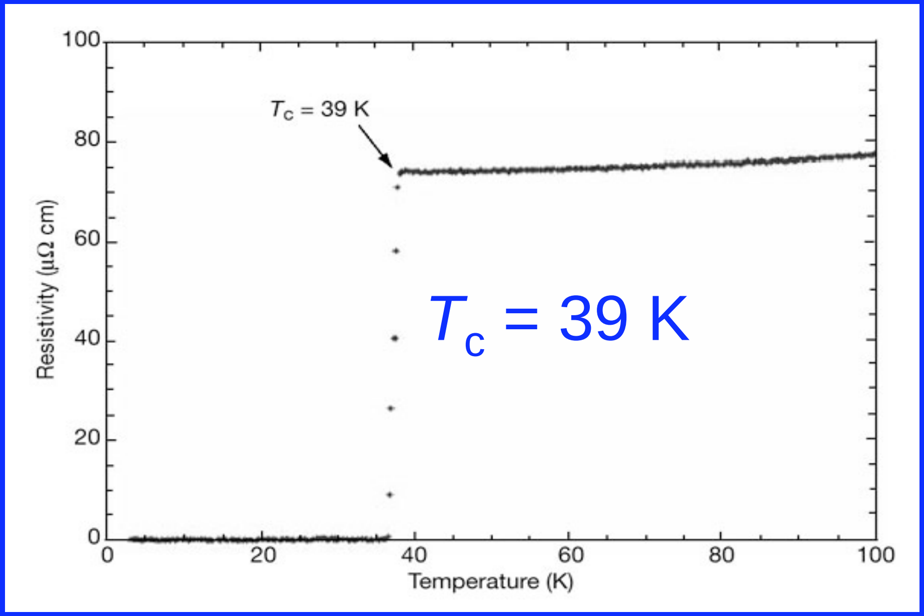

From Jochen Mannhart (Lecture Saas Fee)

MgB_2

From Jochen Mannhart (Lecture Saas Fee)

MgB_2

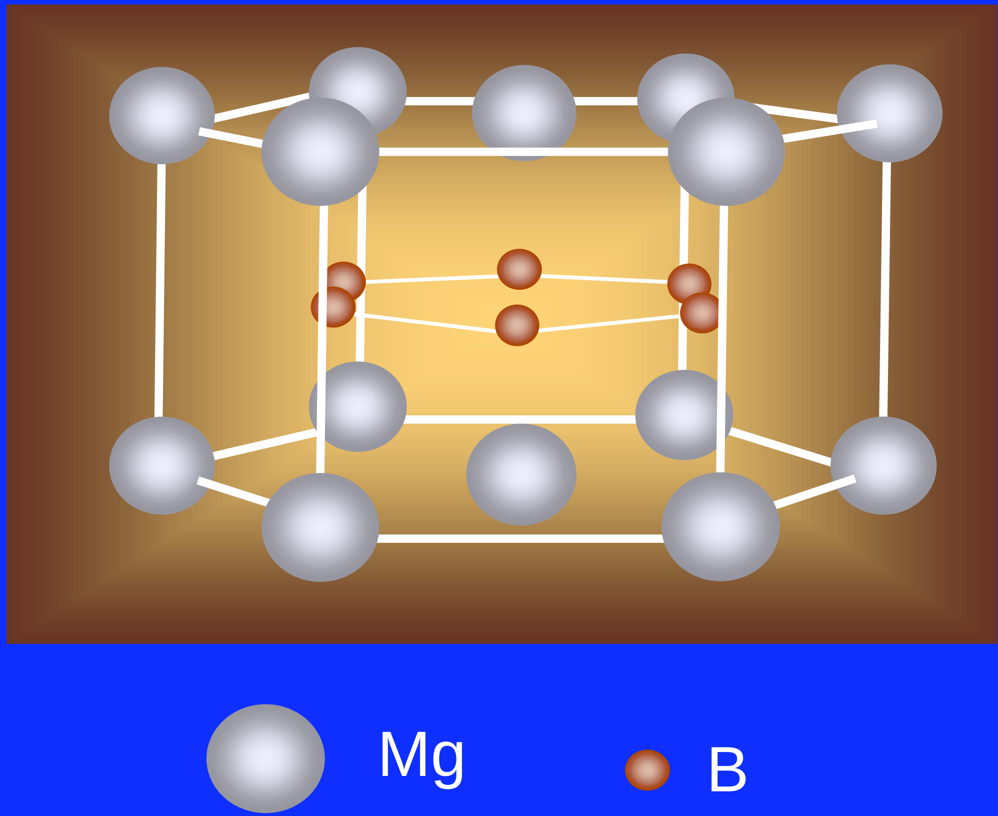

From Jochen Mannhart (Lecture Saas Fee)

MgB_2 Wire

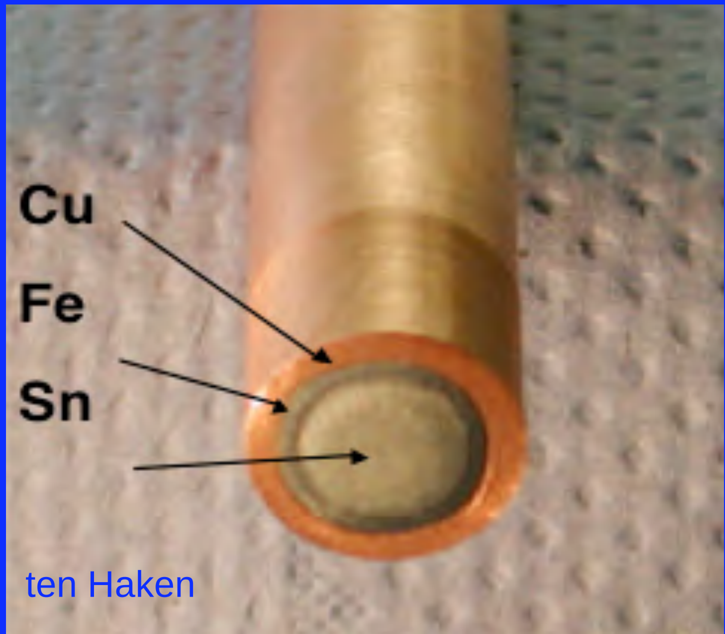

1 mm diameter

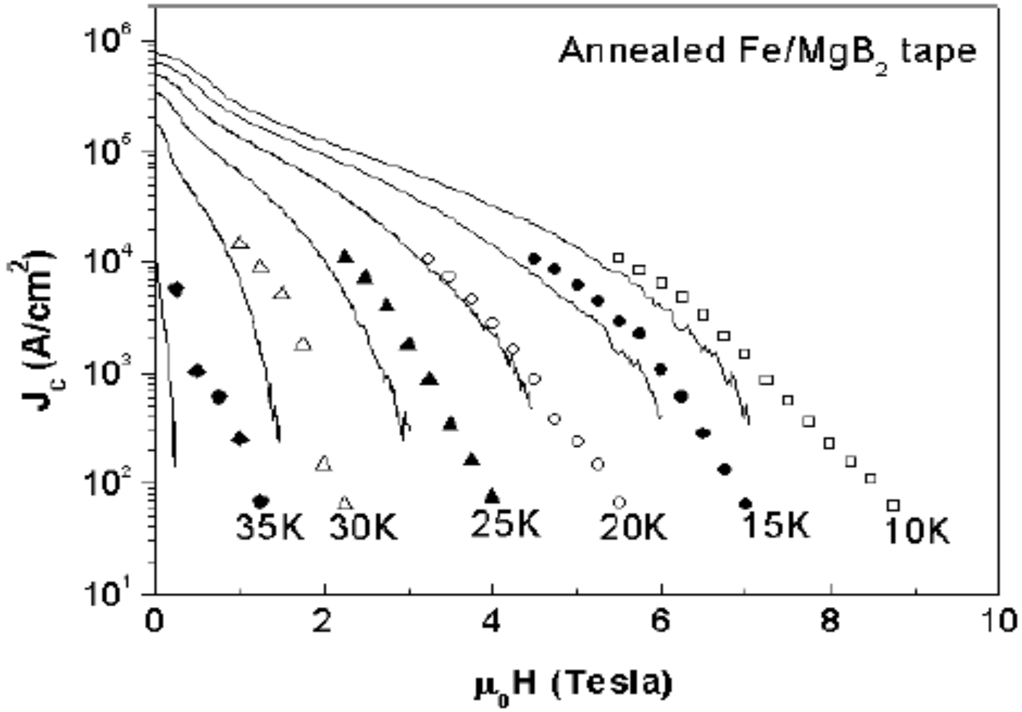

Figure 5. Field dependence of J_c for annealed Fe/MgB_2 tapes, measured every 5 K between 10 and 35 K either inductively (solid lines) or by transport experiments (symbols).

R. Flükiger *et al.*, Supercond. Sci. Techn. 16, 264 (2003)

From Jochen Mannhart (Lecture Saas Fee)

MgB_2 Wire

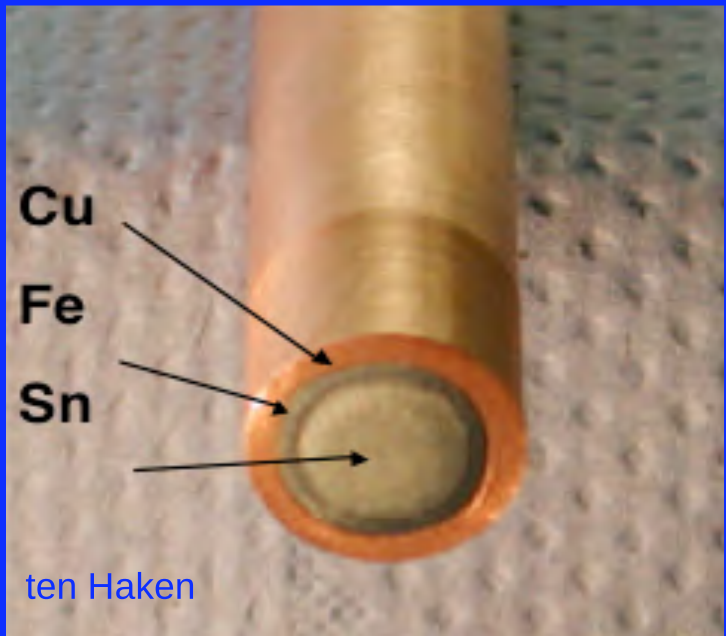

1 mm diameter

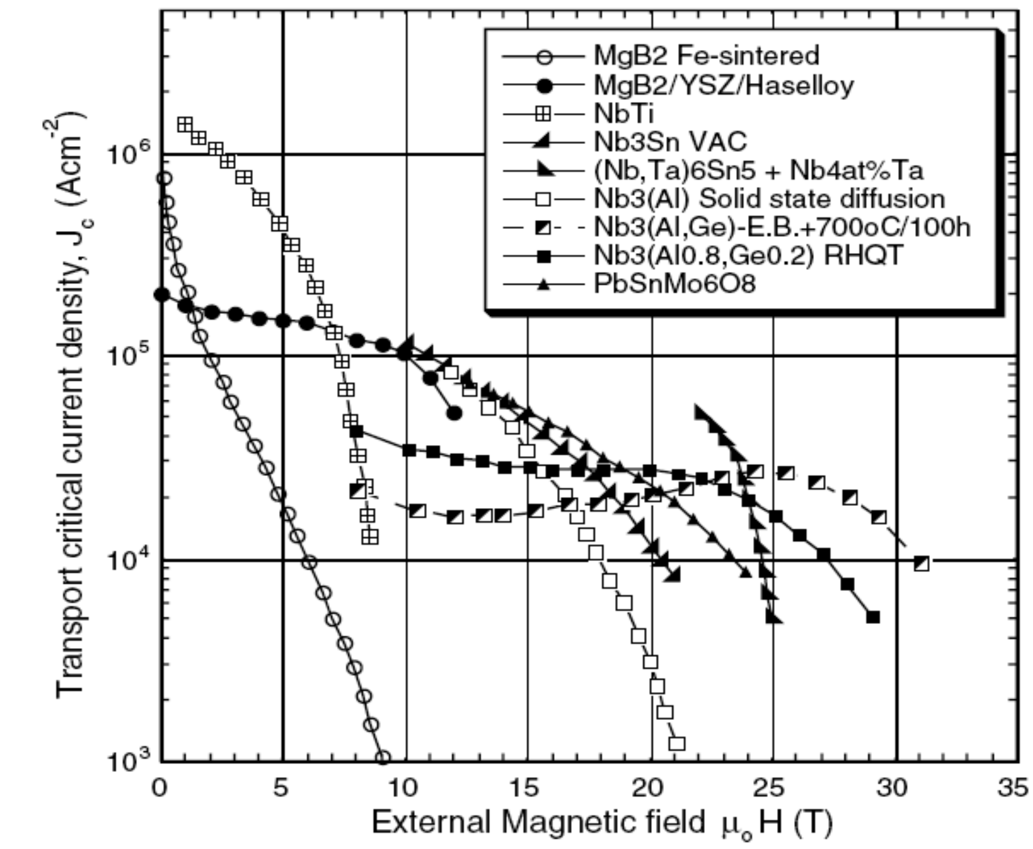

Figure 1. Critical current density versus external magnetic field for the range of superconducting conductors manufactured by different processes as specified in the key. For Nb_3(Al, Ge) tapes formed by liquid quenching processes, and also for MgB_2, the coated conductor magnetic field was parallel to the tape surface. In all cases, the magnetic field was perpendicular to the current [4].

B.A. Glowacki *et al.*, Supercond. Sci. Techn. 16, 297 (2003)

From Jochen Mannhart (Lecture Saas Fee)

Some references

- J R Waldram: Superconductivity of metals and cuprates, (Institute of Physics, Bristol, 1996)
- D. M. Ginsberg, Physical properties of high temperature superconductors (World Scientific, Singapore, 1994)
- C. W. Chu Materials and Physics of High Temperature Superconductors: A Summary, Two Recent Experiments and a Comment
- Physica Scripta. T102, 40-50, 2002
- Robert J. Cava, "Oxide Superconductors" J. Am. Ceram. Soc., 83 [1] 5–28 (2000)
- Jochen Mannhart and Darrell G. Schlom, NATURE|VOL 430 | 5 AUGUST 2004 |www.nature.com/nature
- 17 NOVEMBER 2006 VOL 314 SCIENCE www.sciencemag.org

Materials Processing and Josephson junctions

(additional mtrl)

- This last part was not discussed during the lecture and can be studied on your own if you wish...

LASER DEPOSITION

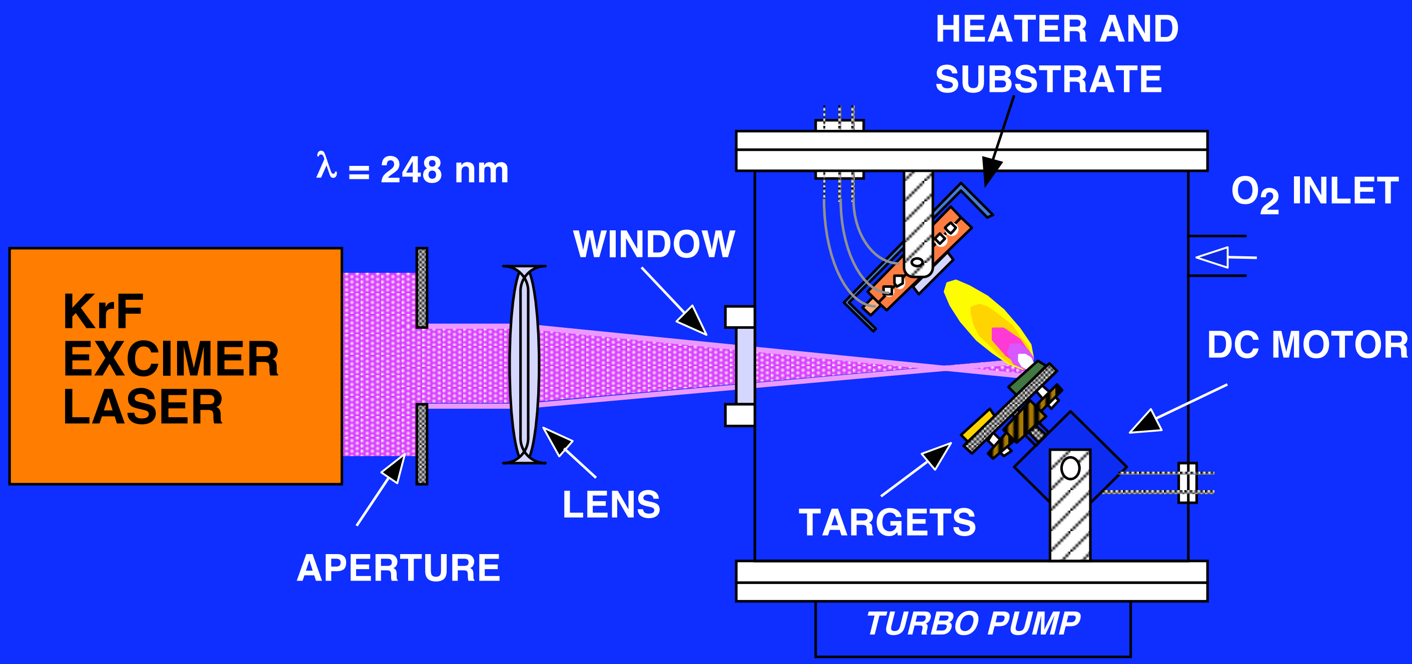

YBCO ARTIFICIAL GRAIN BOUNDARY JUNCTIONS

E. Olsson
J. Alarco

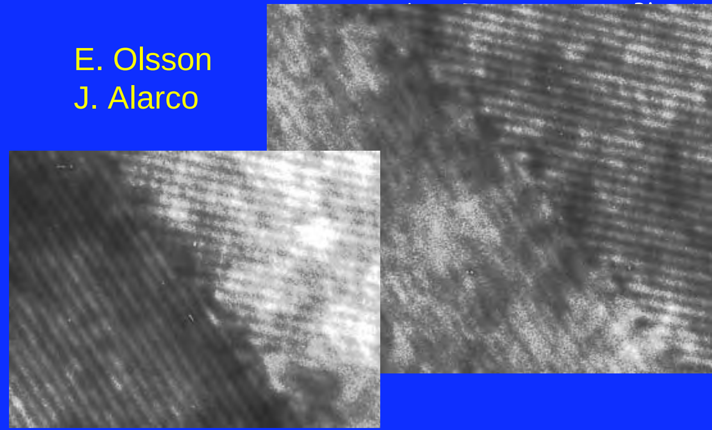

Upper crystal has a c-axis tilt of θ (misorientation angle) relative to the lower part (c-axis is normal to the surface).

The substrate grain boundary is transferred to the YBCO during the thin film growth.

The film grain boundary is usually a Josephson weak link

dc-SQUID

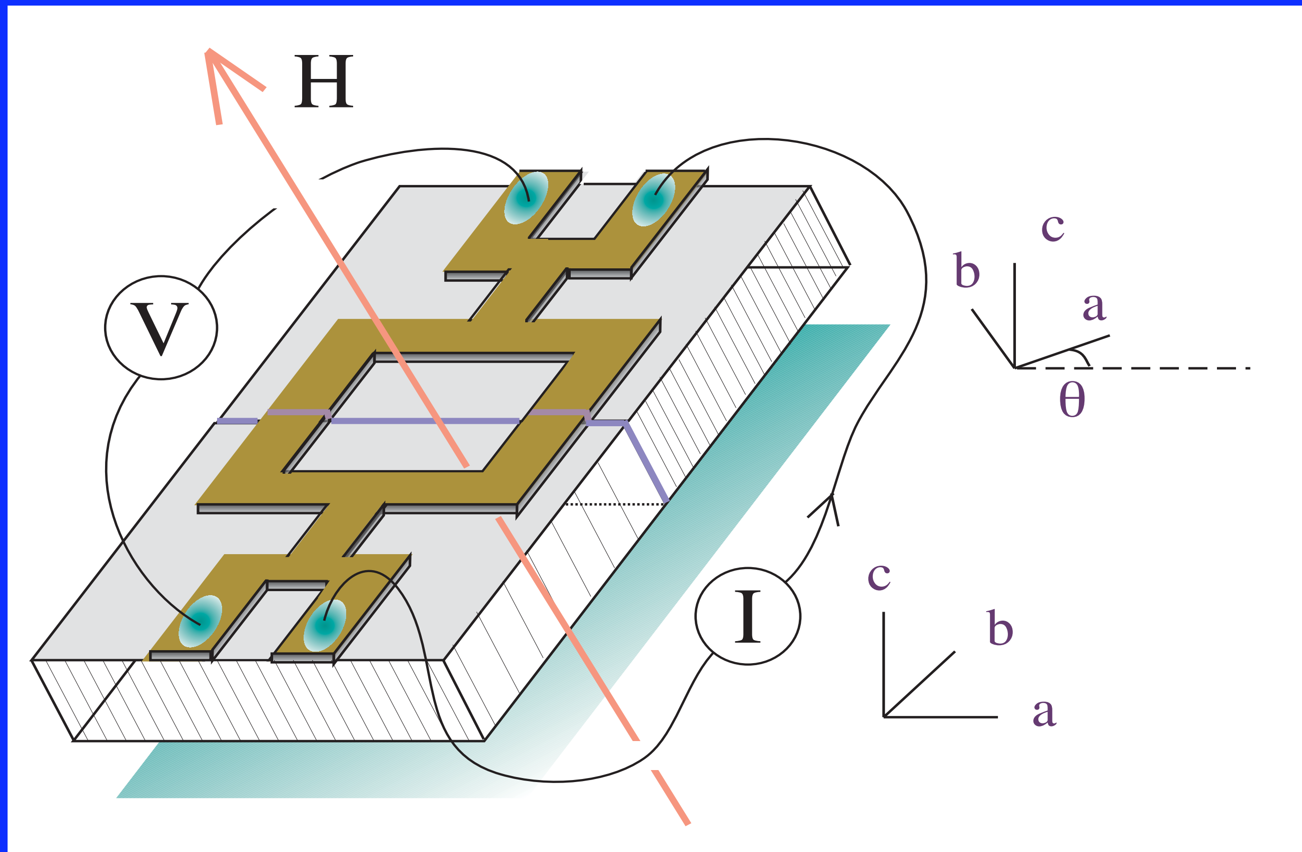

The Josephson effects - shunted junction

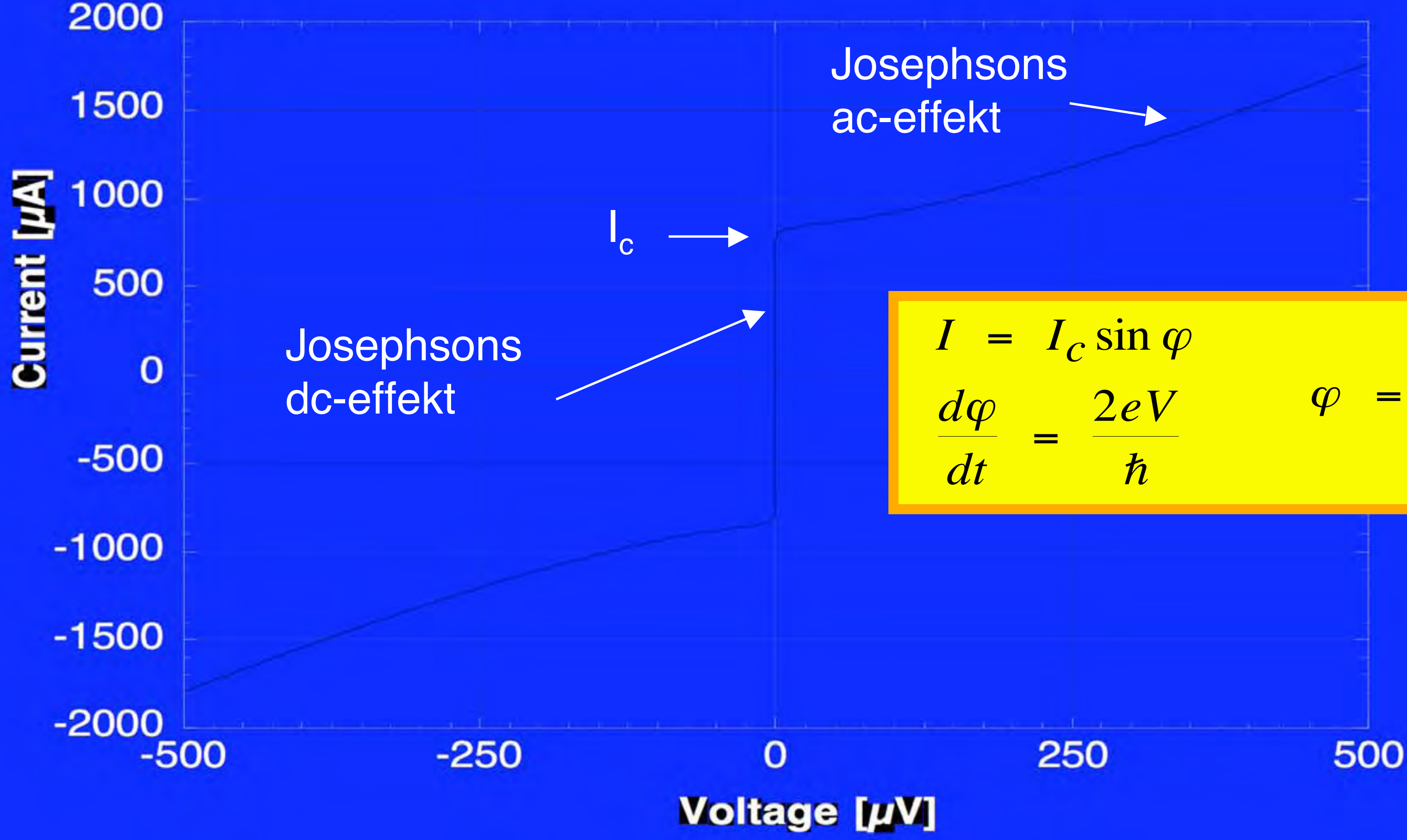

$$I = I_c \sin\varphi$$

$$\frac{d\varphi}{dt} = \frac{2eV}{\hbar} \qquad \varphi = \varphi_2 - \varphi_1$$

The Bicrystal Technology

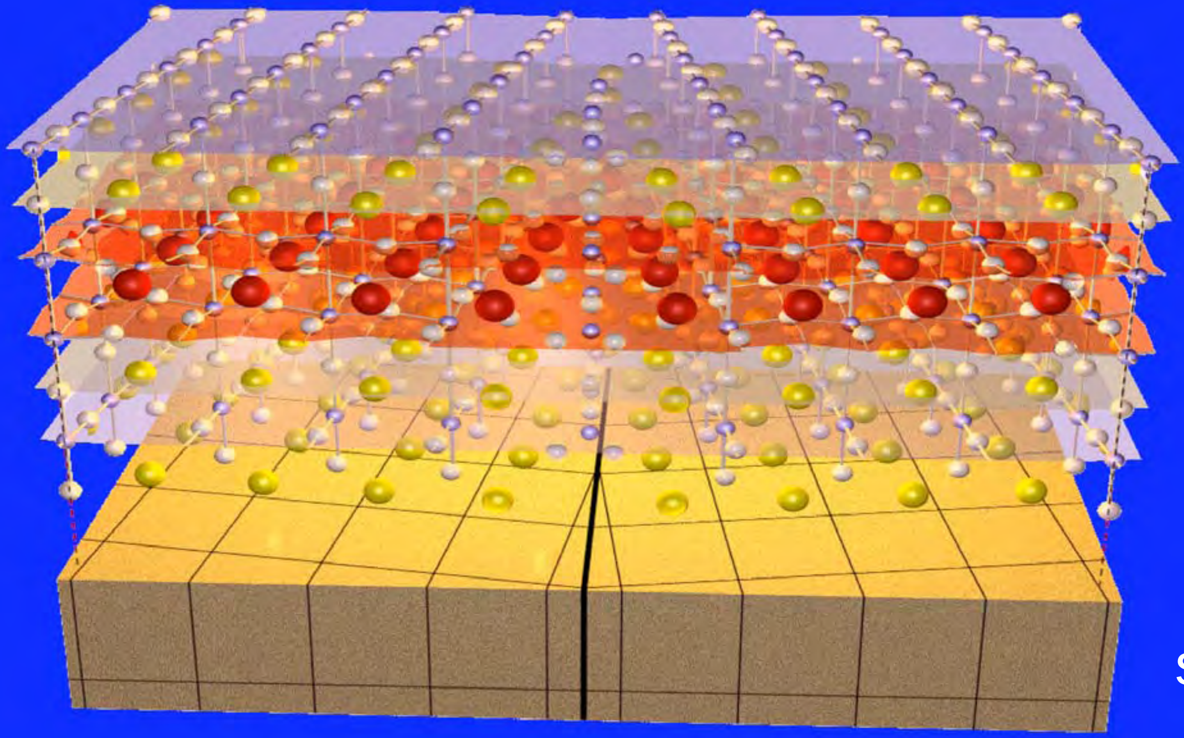

D. Dimos, P. Chaudhari, and J. Mannhart, Phys. Rev. B 41, 4038 (1990)

Physics Today 11, 48 (2001)

H. Hilgenkamp and J. Mannhart, Rev Mod Phys 74, p 485, APRIL 2002

Superconductivity and
Low Temperature Physics

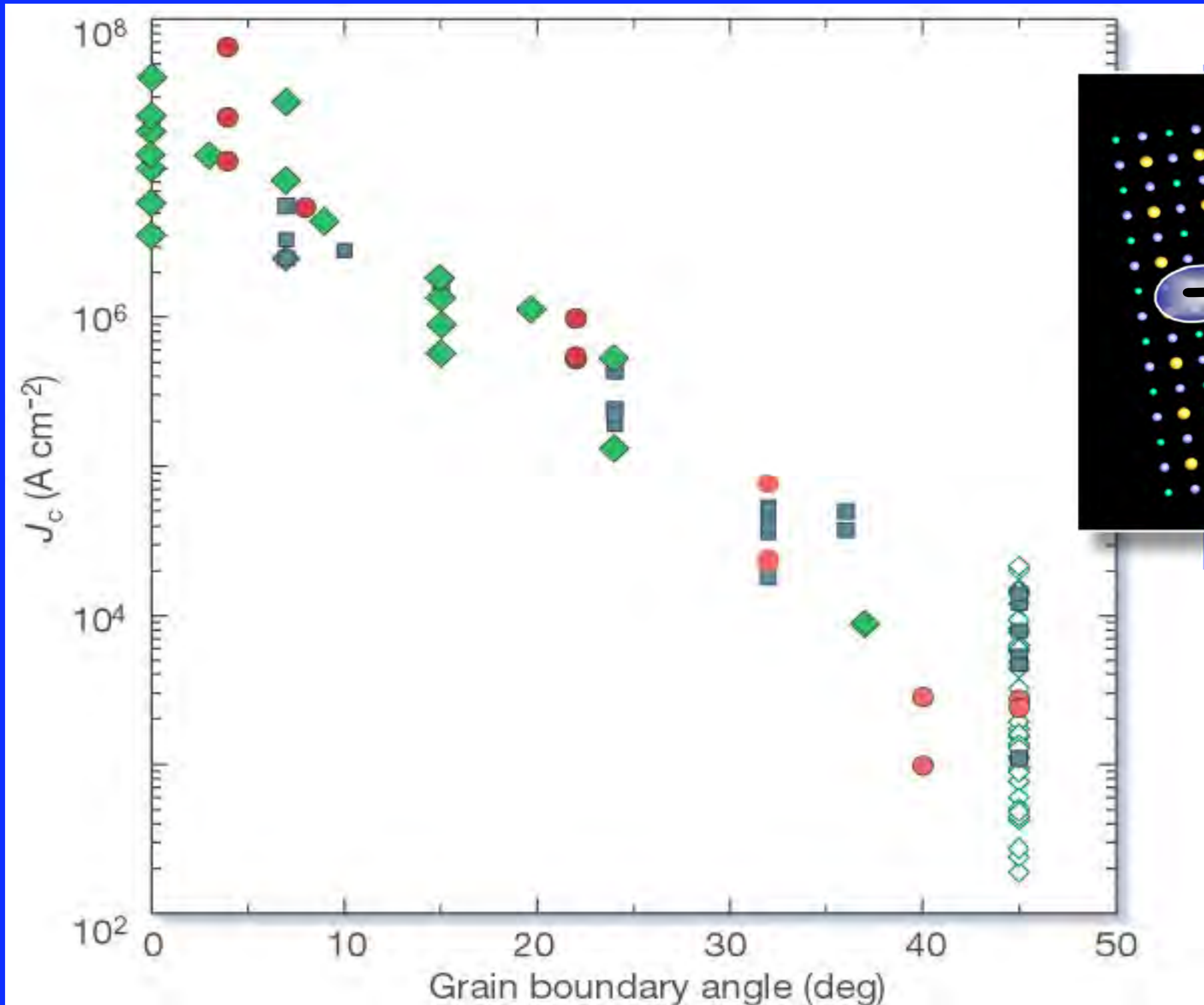

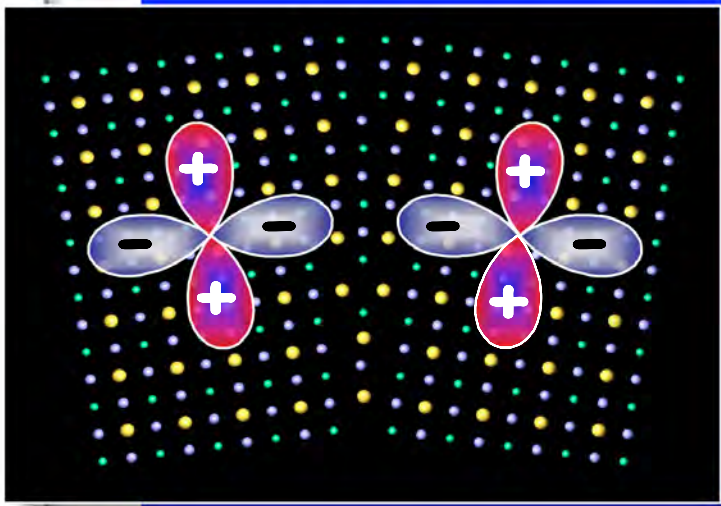

H. Hilgenkamp and J. Mannhart, Rev Mod Phys 74, p 485, APRIL 2002

Figure 4 Transport critical current density at 4.2 K measured in thin films of YBCO grown on [001] tilt bicrystal substrates of $SrTiO_3$ (squares[37] and filled diamonds[44]), Y_2O_3-stabilized ZrO_2 (circles[97]), and bi-epitaxial junctions (open diamonds[98]) of varying misorientation angle . Data of refs 97 and 44 were taken at 77 K and have been multiplied by a factor of 10.9 to make them comparable with the data at 4.2 K. Despite a significant scattering, $J_c(\Theta)$ exhibits a universal exponential dependence on. Data compilation courtesy of J. Mannhart[37].

KLEINER AND MÜLLER

VOLUME 68, NUMBER 15 PHYSICAL REVIEW LETTERS 13 APRIL 1992

Intrinsic Josephson Effects in $Bi_2Sr_2CaCu_2O_8$ Single Crystals

R. Kleiner, F. Steinmeyer, G. Kunkel, and P. Müller
Walther-Meissner-Institut, Walther-Meissner-Strasse 8, W-8046 Garching, Germany
(Received 21 August 1991; revised manuscript received 11 February 1992)

PHYSICAL REVIEW B VOLUME 49, NUMBER 2 1 JANUARY 1994-II

Intrinsic Josephson effects in high-T_c superconductors

R. Kleiner and P. Müller

FIG. 1. Superposition of the BSCCO crystal structure and a stack of Josephson junctions, whose electrodes are formed by CuO_2 double layers.

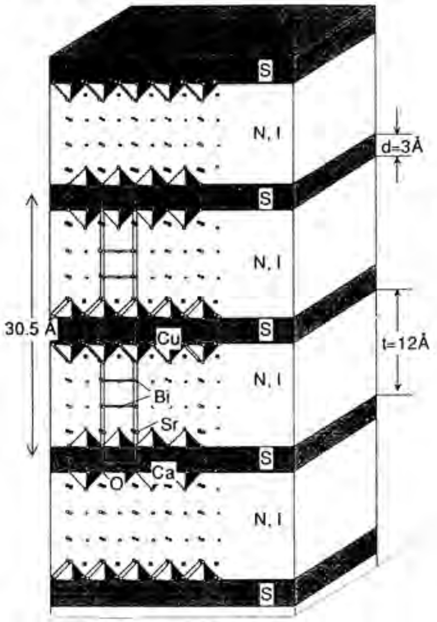

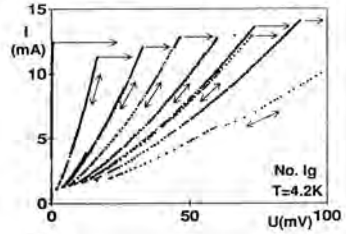

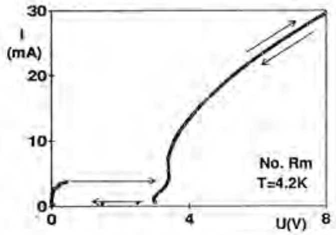

FIG. 5. *I-V* characteristics of Ar-annealed BSCCO crystals at different voltage scales. The multiple branches shown in the upper figure have not been traced out in the lower figure. The annealing conditions of the samples are 12 h, 600 °C (No. Ig) and 10 h, 550 °C (No. Rm). Contact resistances have been subtracted. Details of the *I-V* characteristics are described in the text.

VOLUME 68, NUMBER 15 PHYSICAL REVIEW LETTERS 13 APRIL 1992

2394 – 2397

Intrinsic Josephson Effects in $Bi_2Sr_2CaCu_2O_8$ Single Crystals

R. Kleiner, F. Steinmeyer, G. Kunkel, and P. Müller
Walther-Meissner-Institut, Walther-Meissner-Strasse 8, W-8046 Garching, Germany
(Received 21 August 1991; revised manuscript received 11 February 1992)

We have observed Josephson coupling between CuO double layers in $Bi_2Sr_2CaCu_2O_8$ single crystals by direct measurements of ac and dc Josephson effects with current flow along the *c* axis. The results show that a small $Bi_2Sr_2CaCu_2O_8$ single crystal behaves like a series array of Josephson junctions which can exhibit mutual phase locking.

PACS numbers: 74.50.+r, 74.60.Jg, 74.70.Jm

PHYSICAL REVIEW B VOLUME 49, NUMBER 2 1 JANUARY 1994-II

1327 – 1341

Intrinsic Josephson effects in high-T_c superconductors

R. Kleiner and P. Müller
Walther-Meissner-Institut, D-85748 Garching, Germany
(Received 19 July 1993)

We have investigated the coupling between CuO_2 layers in high-T_c superconductors by direct measurements of all dc and ac Josephson effects with current flow in the c-axis direction. The measurements have been performed on small single crystals of $Bi_2Sr_2CaCu_2O_8$, $(Pb_yBi_{1-y})_2Sr_2CaCu_2O_8$, $Tl_2Ba_2Ca_2Cu_3O_{10}$, and $YBa_2Cu_3O_{7-\delta}$ and on *a*-axis-oriented $YBa_2Cu_3O_7$ thin films. The results clearly show that all materials behave like stacks of superconductor-insulator-superconductor Josephson junctions. The current-voltage characteristics exhibit large hystereses and multiple branches, which can be explained by a series connection of highly capacitive junctions. From the modulation of the critical current in a magnetic field parallel to the layers, we infer a junction thickness of approximately 15 Å. In our microwave emission experiments we were able to prove explicitly that every pair of CuO_2 double or triple layers forms a working Josephson contact. An exception is $YBa_2Cu_3O_7$, where only flux-flow behavior has been observed.

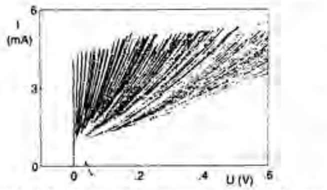

FIG. 1. *I-V* characteristic of sample *Fa* at $T = 4.2$ K. The contact resistance of 18 Ω is subtracted.

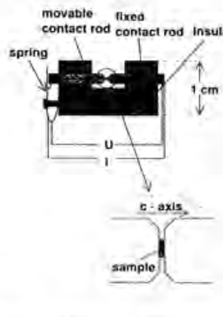

FIG. 4. Schematic view of the sample holder.

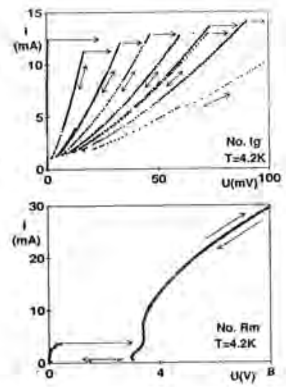

FIG. 5. *I-V* characteristics of Ar-annealed BSCCO crystals at different voltage scales. The multiple branches shown in the upper figure have not been traced out in the lower figure. The annealing conditions of the samples are 12 h, 600 °C (No. Ig) and 10 h, 550 °C (No. Rm). Contact resistances have been subtracted. Details of the *I-V* characteristics are described in the text.

VORTEX DYNAMICS

VOLUME 79, NUMBER 25 PHYSICAL REVIEW LETTERS 22 DECEMBER 1997

Relationship between the Out-Of-Plane Resistance and the Subgap Resistance of Intrinsic Josephson Junctions in $Bi_2Sr_2CaCu_2O_{8+\delta}$

A. Yurgens,[1,2] D. Winkler,[1] N. V. Zavaritsky,[2,*] and T. Claeson[1]
[1]*Department of Microelectronics and Nanoscience, Chalmers University of Technology, S-41296, Göteborg, Sweden*
[2]*P. L. Kapitza Institute for Physical Problems, ul. Kosygina 2, Moscow, 117334, Russia*
(Received 2 June 1997)

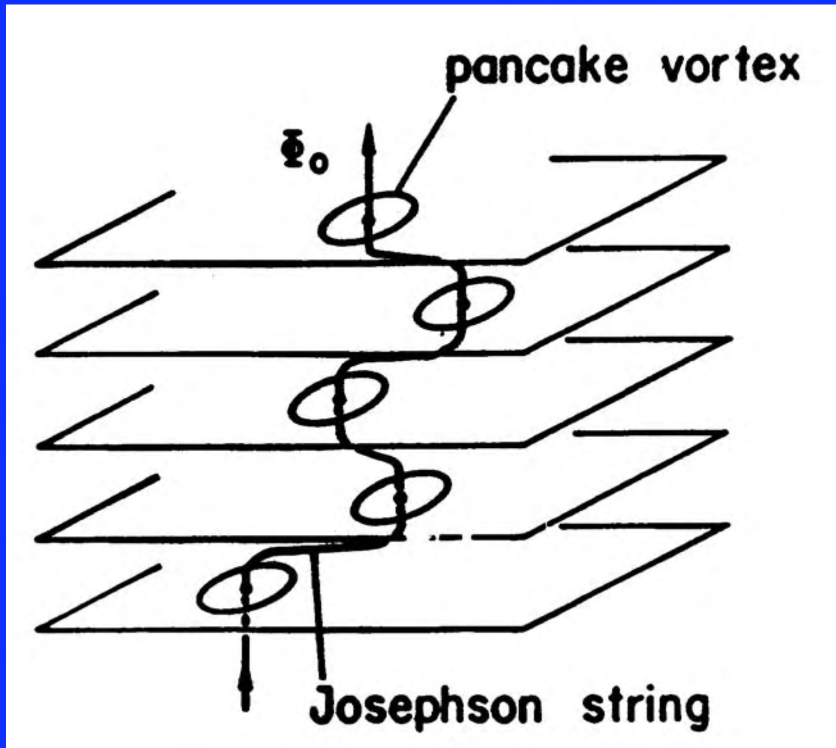

Electrotechnical applications

- What are the problems
- What is needed
- To what cost

High T_c superconductors—composite wire fabrication

S. Jin, R. C. Sherwood, R. B. van Dover, T. H. Tiefel, and D. W. Johnson, Jr.
AT&T Bell Laboratories, Murray Hill, New Jersey 07974

(Received 13 April 1987; accepted for publication 22 May 1987)

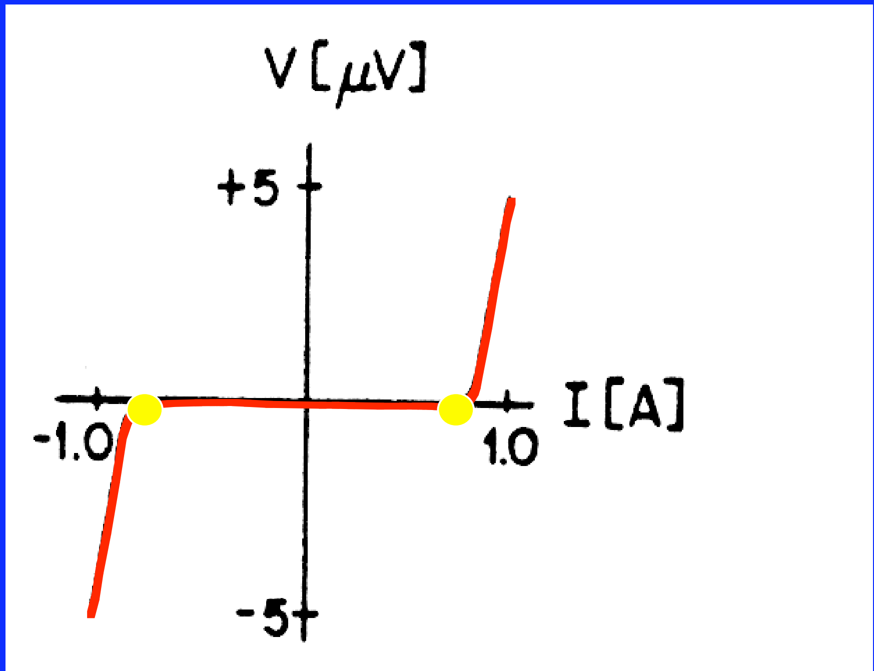

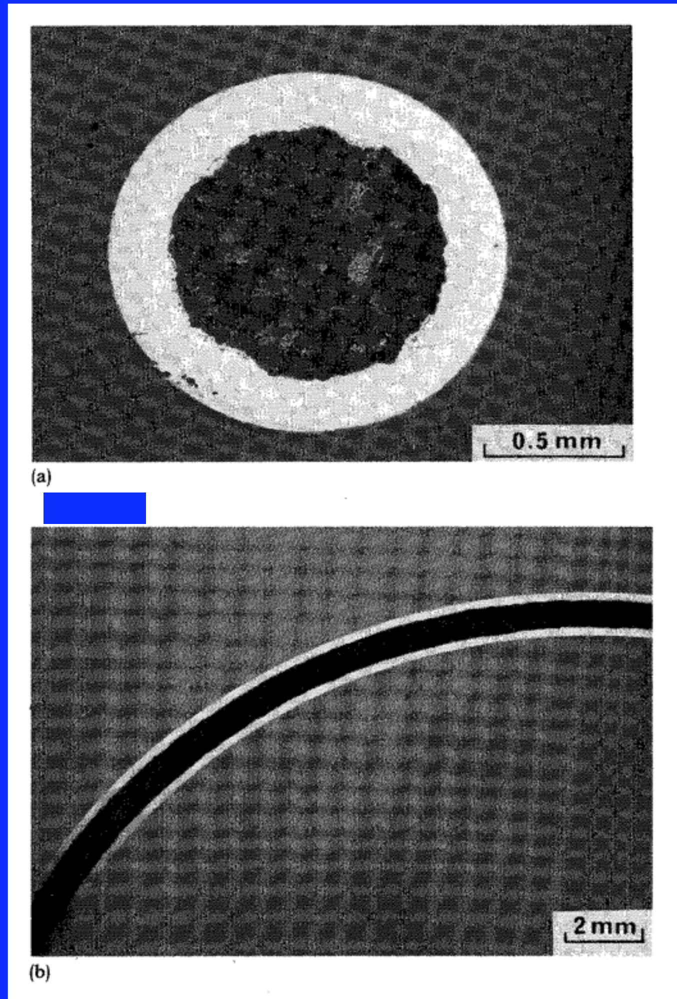

$YBa_2Cu_3O_{7-\delta}$ / Ag - wire

- J_c (77 K, 1987) = 175 A/cm^2

From Jochen Mannhart (Lecture Saas Fee)

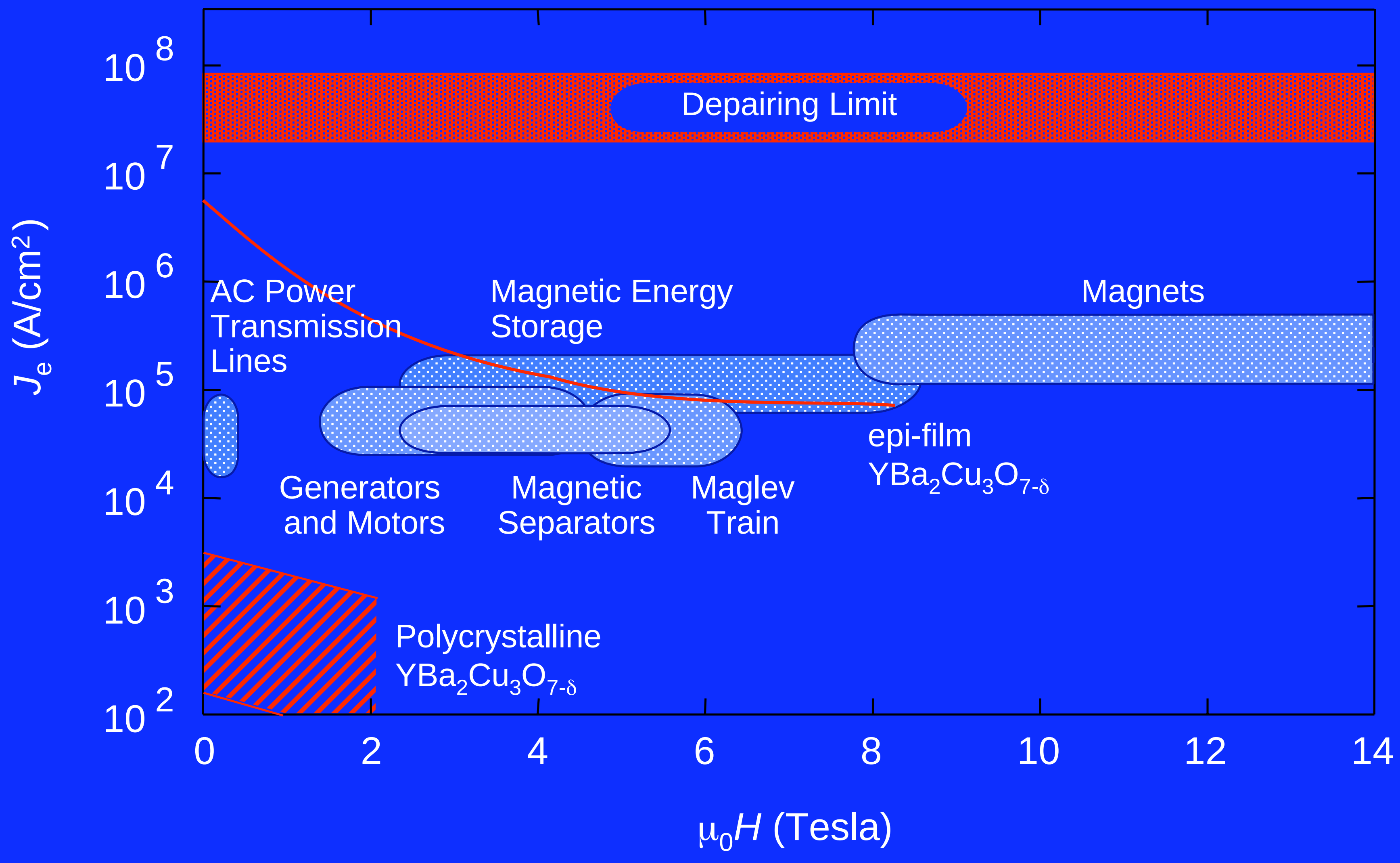

From Jochen Mannhart (Lecture Saas Fee)

Melt Textured Superconductors to Avoid Boundaries

GdBCO
5 cm diameter
3 cm thick

Nexans

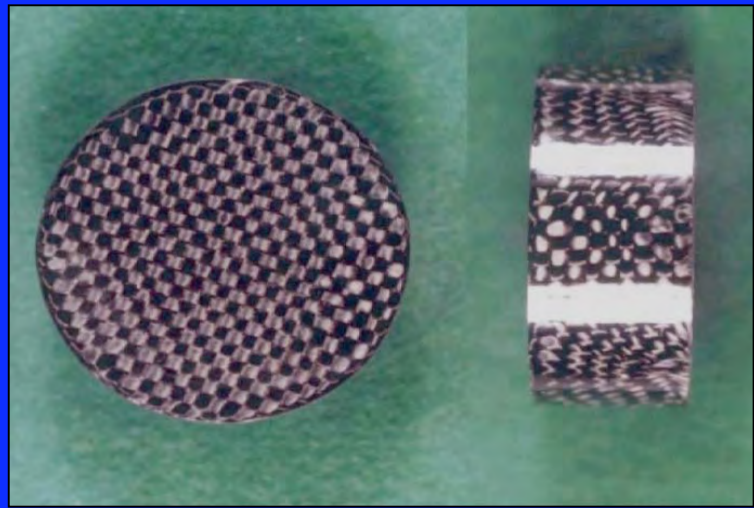

YBCO
2.6 cm diameter
resin impregnated

ISTEC

From Jochen Mannhart (Lecture Saas Fee)

Melt Textured Superconductors to Avoid Grain Boundaries

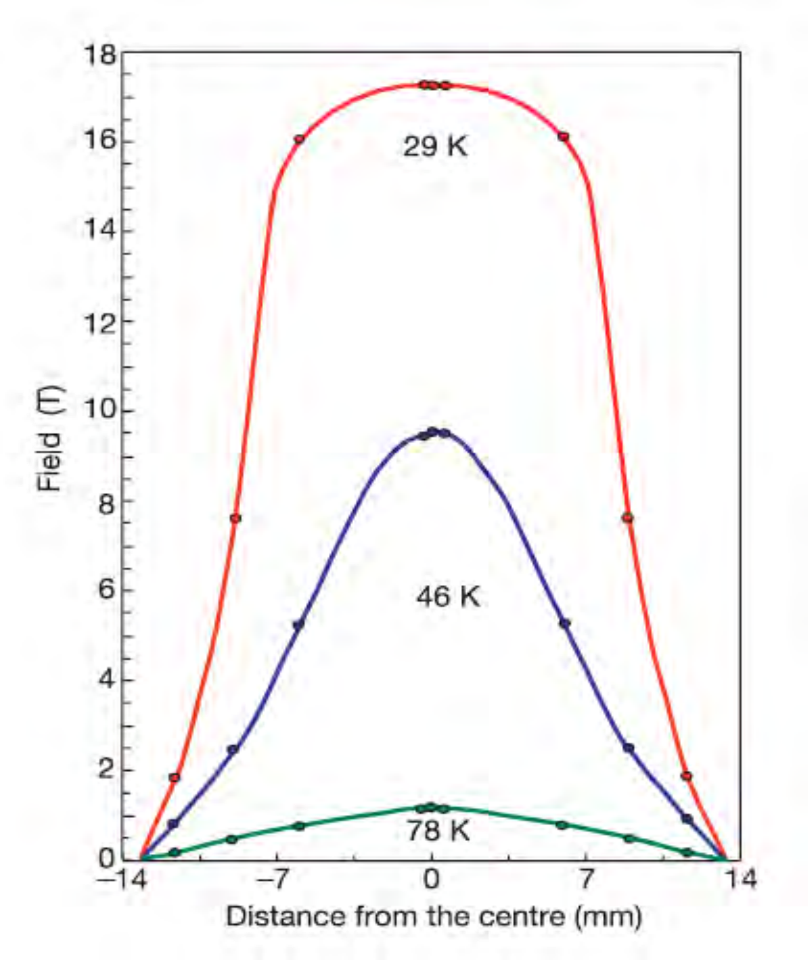

Applications :

- levitation
- bearings (e.g. for flywheels)
- magnetic separators
- water cleaning

Trapped field between two YBCO disks

M. Tomita and M. Murakami, Nature 421, 519 (2003)

From Jochen Mannhart (Lecture Saas Fee)

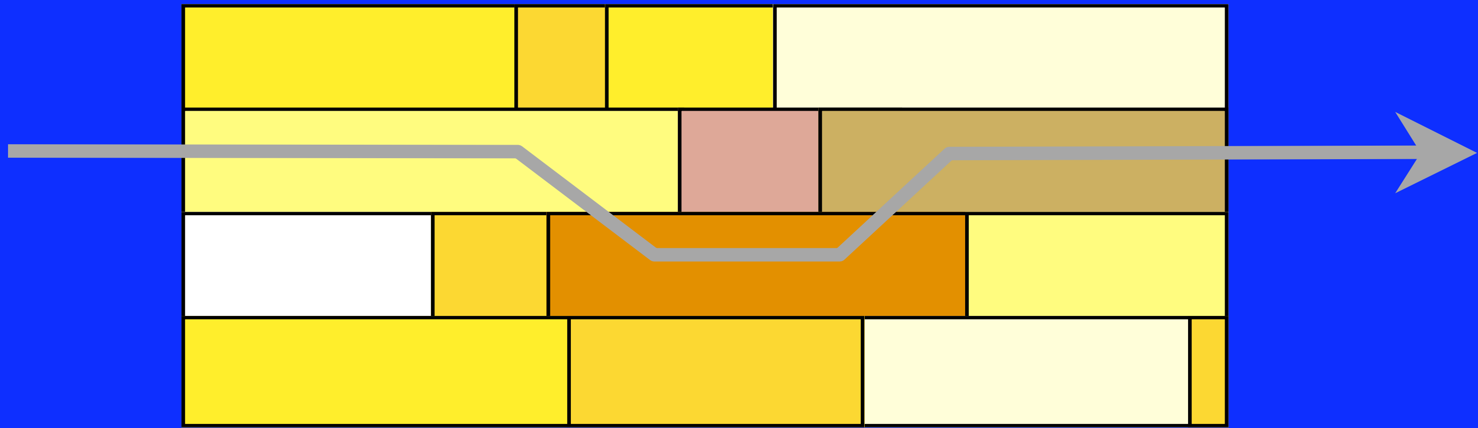

J. Mannhart and C.C. Tsuei, Z. Phys. B 77, 53 (1989)

BSCCO ($Bi_2Sr_2Ca_2Cu_3O_{10}$) Powder in Tube Technology

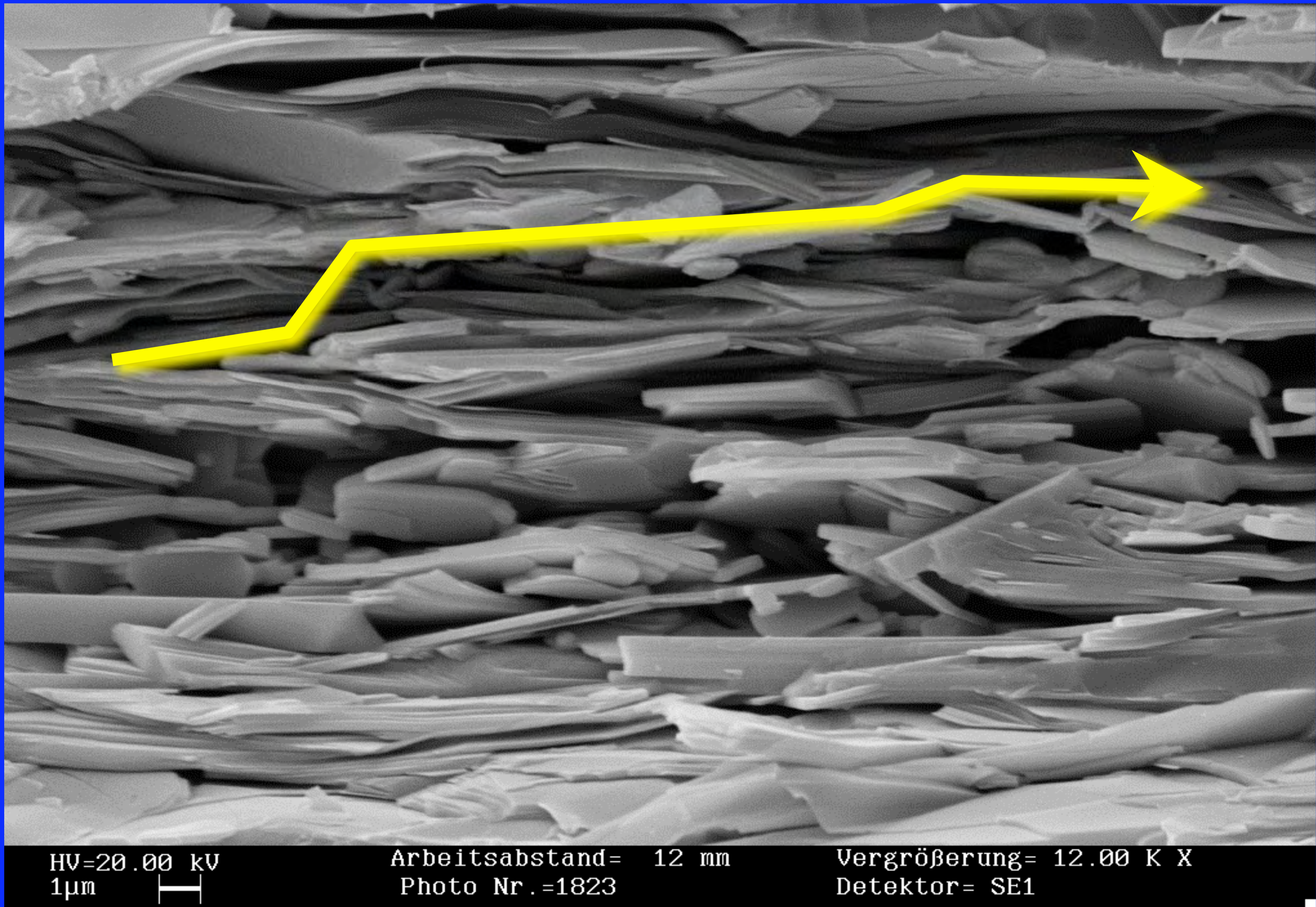

From Jochen Mannhart (Lecture Saas Fee)

American Superconductors, and others, ...

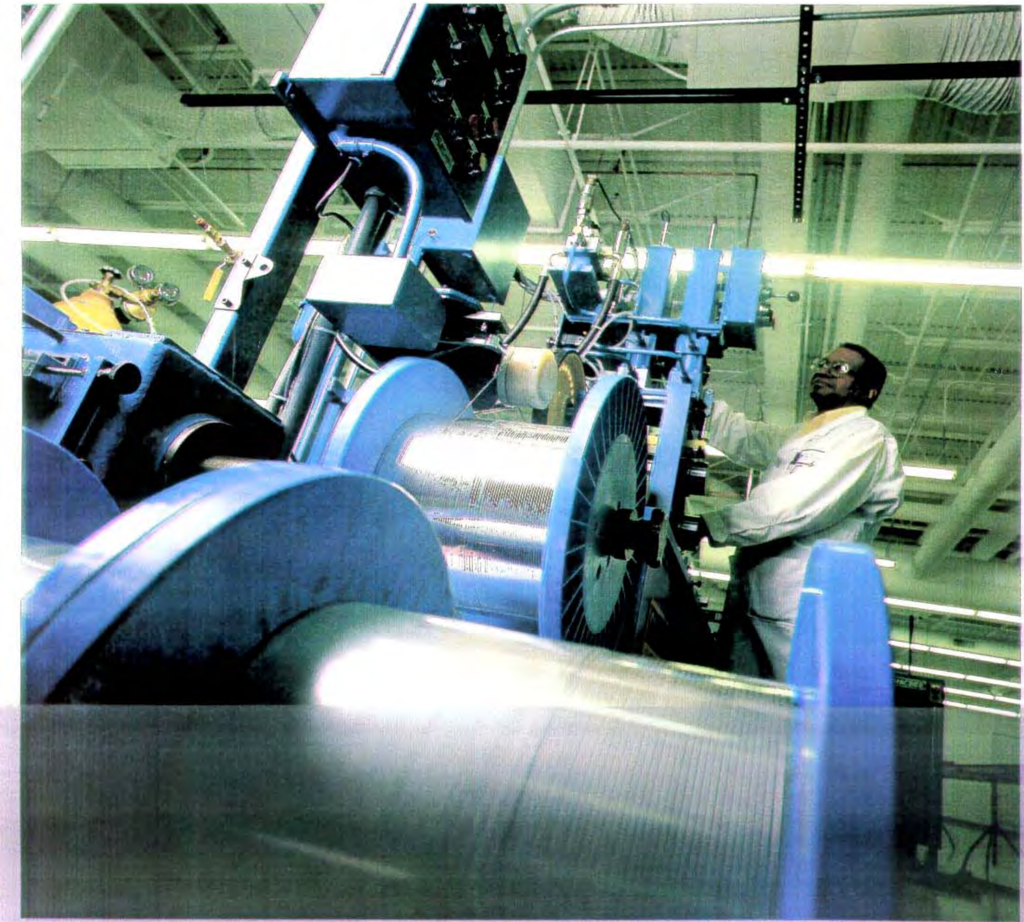

American Superconductor established the world's first pilot manufacturing line for HTS wires, a critical step in transitioning from its achievements in R&D to meeting the challenges of manufacturing. The company's manufacturing technologies, based on metal deformation processes such as wire drawing, are fully scalable to low-cost, high-volume production. The rolling mill, shown here, is used to create the internal architecture and external shape that is part of the process of transforming HTS material into usable wire. ASC currently produces approximately 900-foot lengths of wire on a day-to-day basis and has demonstrated lengths up to 3,800 feet.

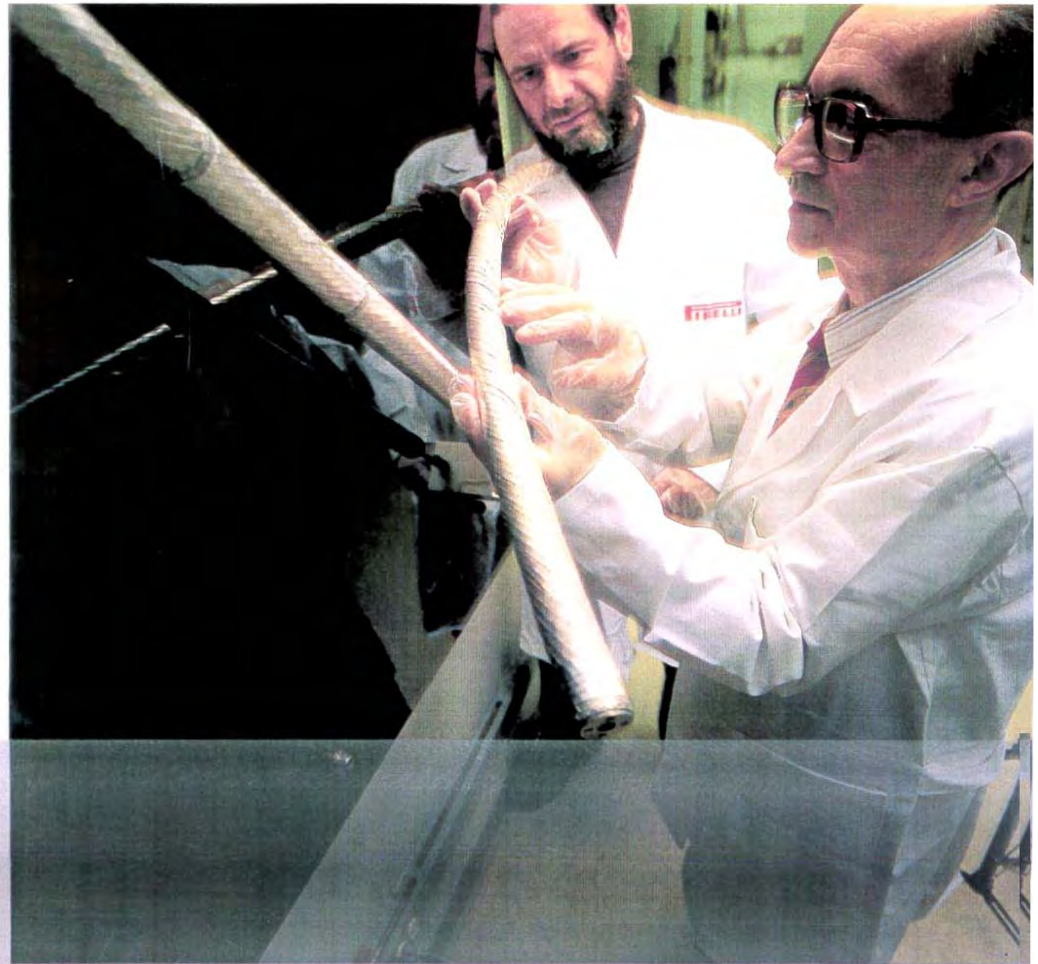

Strategic alliances have helped American Superconductor to accelerate the development of its HTS technology and to t relationships with prospective end-use customers. ASC is working closely with Pirelli Cavi SpA, one of the world's lea manufacturers of power transmission cables, on the development of HTS technology for superconducting power cable syst The three-foot-long, 4,200 amp prototype HTS cable conductor shown above is a step toward reaching the goal of testing scale prototype HTS power cables at electric utilities within the next three years.

BSCCO Powder in Tube Technology - Cables


Pirelli

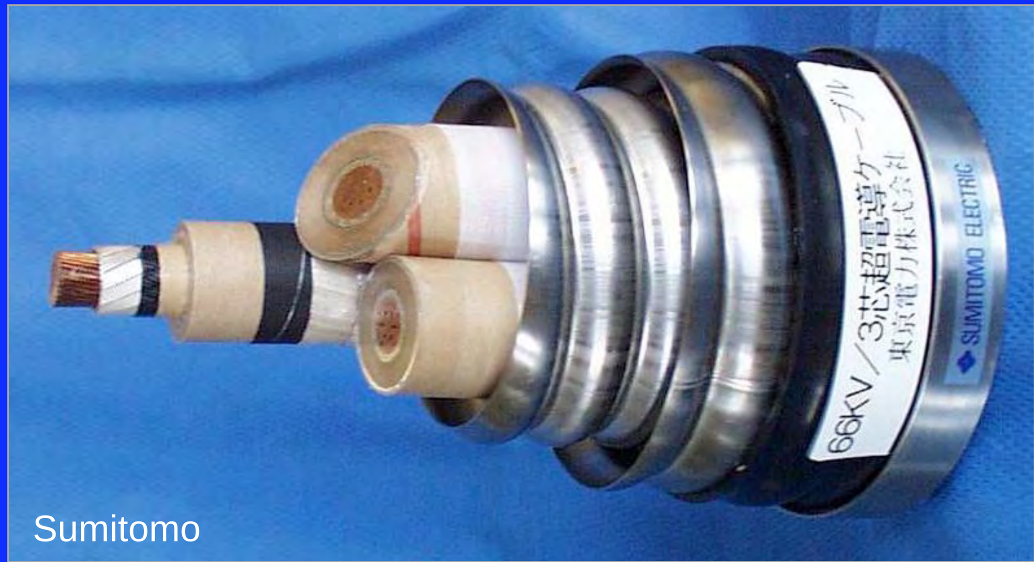

Sumitomo

Sumitomo

100 m, 114 MVA, 1000 A

cold dielectric design, 3-phase

From Jochen Mannhart (Lecture Saas Fee)

BSCCO Powder in Tube Technology - Problems

1) Operation at 77 K in magnetic fields hopeless

Reason: thermally activated flux motion due to pancake structure of vortices

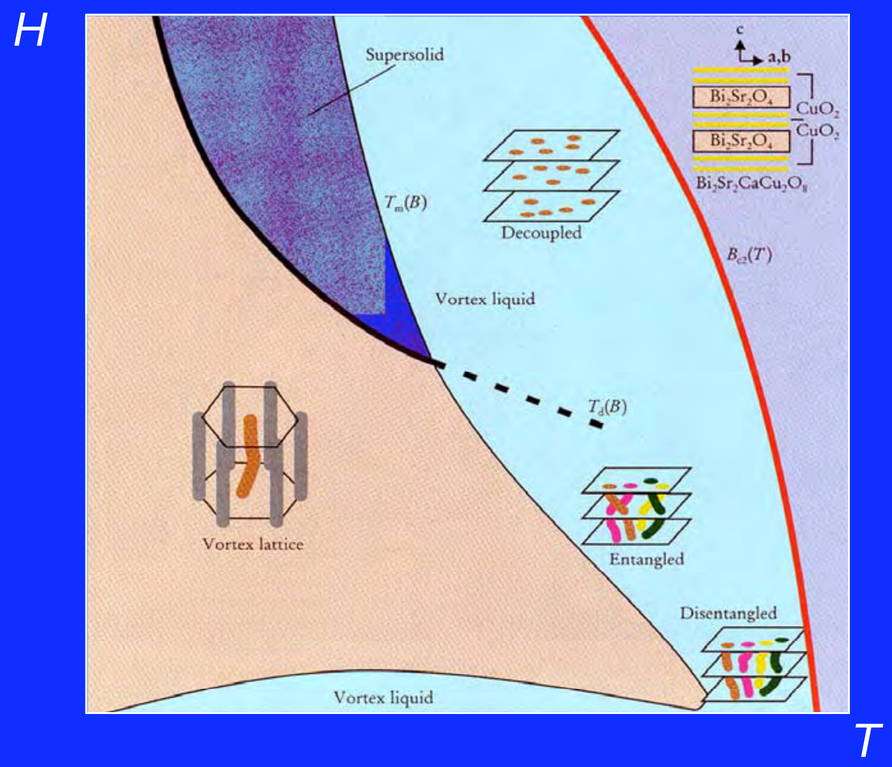

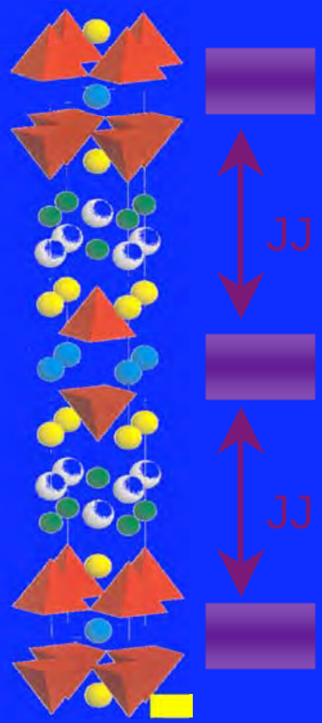

2) Too expensive! Cost of material (silver) too high

Coated Conductors

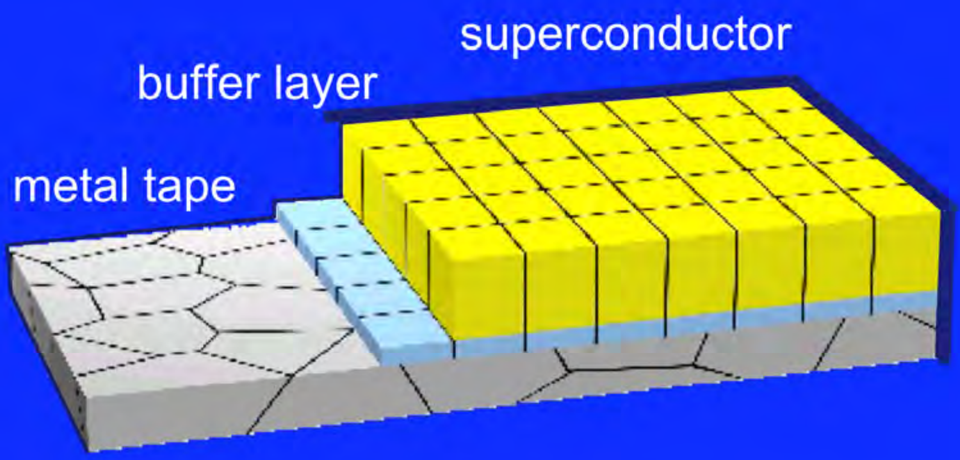

RABiTS - IBAD - ISD

I_c = 4200 A

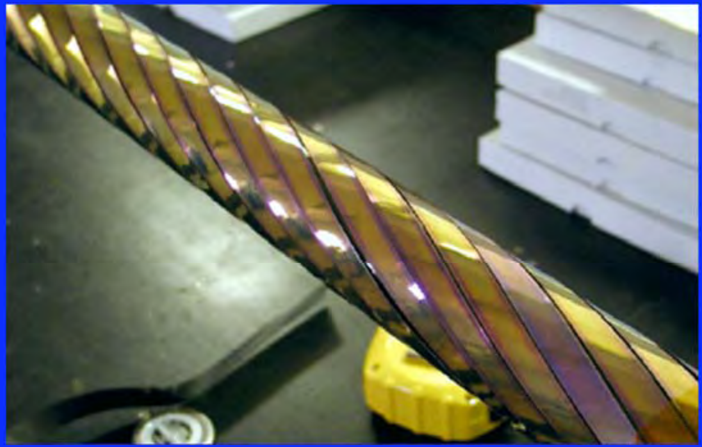

Southwire, ORNL, AMSC

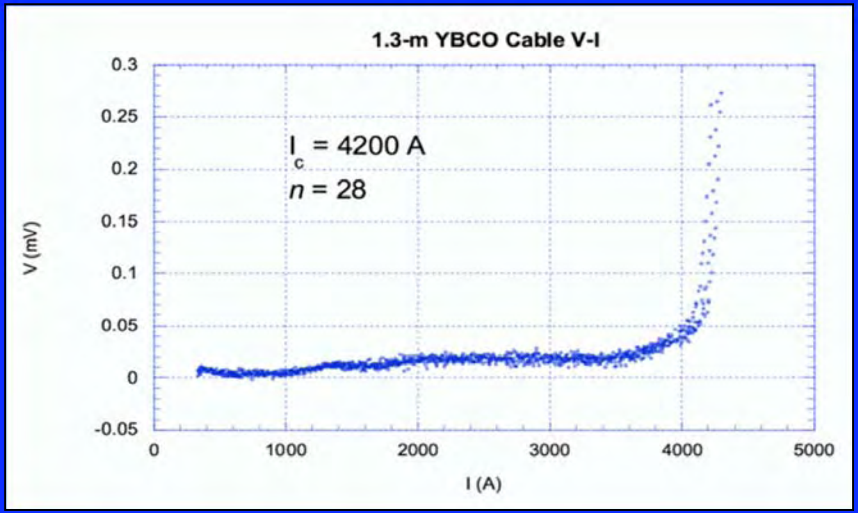

77 K

From Jochen Mannhart (Lecture Saas Fee)

Chemical Solution Deposition

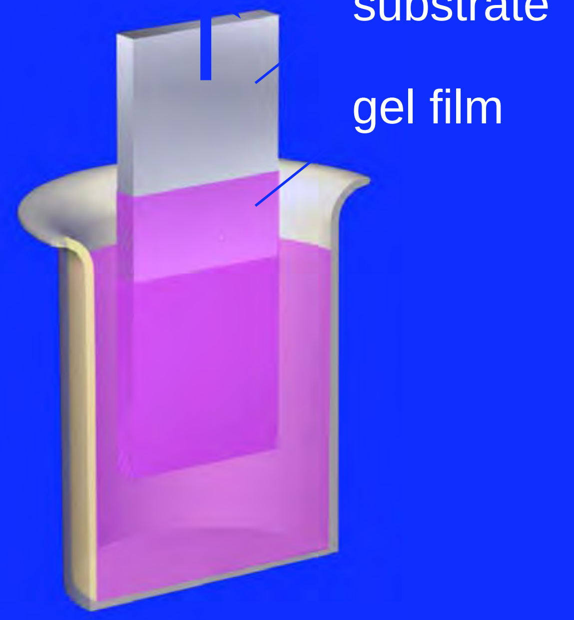

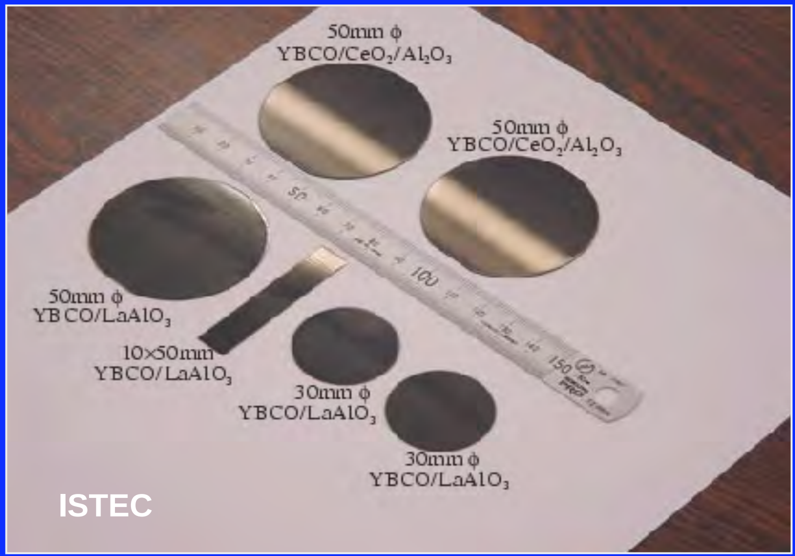

dip coating

J_c = 6-7 x 10^6 A/cm^2 (77 K) on Al_2O_3

J_c > 1 x 10^6 A/cm^2 (77 K) on buffered metal tapes

From Jochen Mannhart (Lecture Saas Fee)

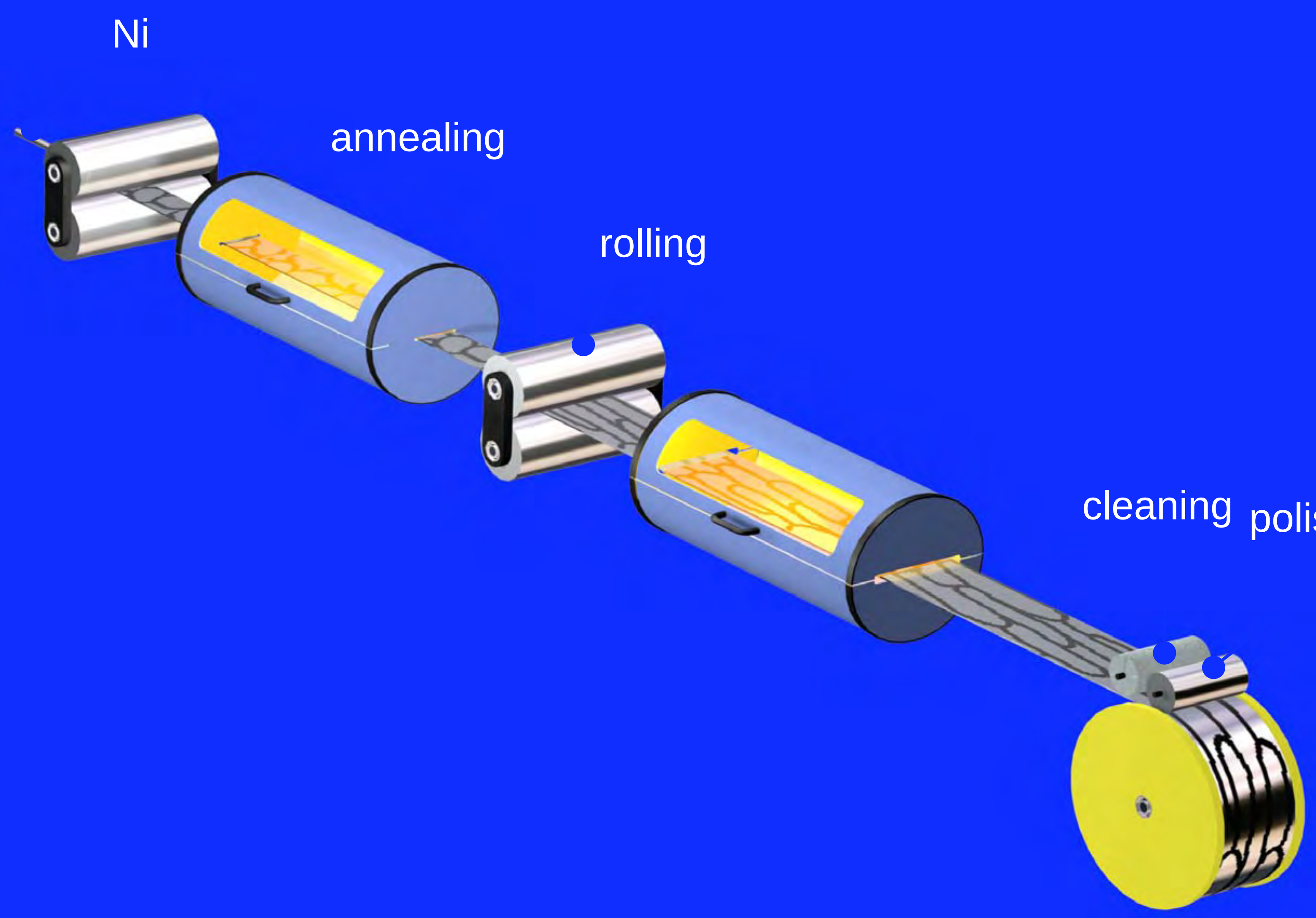

G. Hammerl *et al.*, APL 81, 3209 (2002)

From Jochen Mannhart (Lecture Saas Fee)

buffer layer deposition

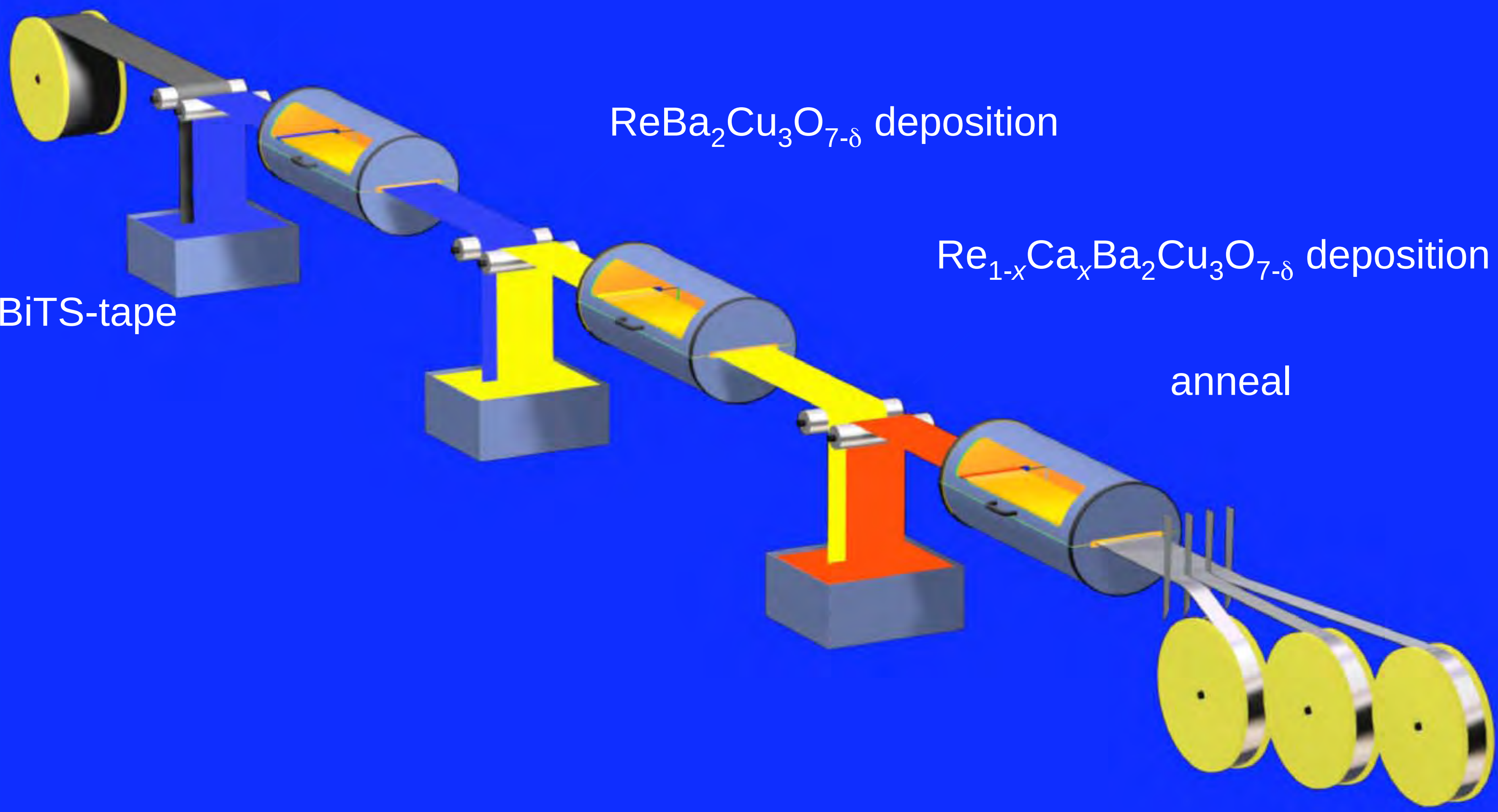

$ReBa_2Cu_3O_{7-\delta}$ deposition

$Re_{1-x}Ca_xBa_2Cu_3O_{7-\delta}$ deposition

anneal

RABiTS-tape

G. Hammerl *et al.*, APL 81, 3209 (2002)

From Jochen Mannhart (Lecture Saas Fee)

SOME ISSUES IN HTS

- FUNDAMENTAL PROBLEMS:
  - Spin gap, Pseudo gap
  - Wave symmetry, pairing state
  - Theory
  - Irreversibility line and vortex dynamics
  - Andreév states and tunneling

- MATERIAL PROBLEMS AND TECHNICAL ISSUES:
  - Ways of making : *Microstructure*
  - Josephson weak links *Epitaxy*
  - Josephson *tunnel* junction *Multilayers*
  - long conductors:
  - with large j_c and j_e in moderate fields

Eg. Neglected Enablers: Low Thermal Load Input-Output Cabling

Andrew Smith
TRW Space & Electronics
Redondo Beach, California

Technical Challenge:
- Superconducting electronic systems need A of dc I & high speed cabling, especially from 4-70 Kelvin
- In normal metals low electrical resistance comes with low thermal resistance and therefore high thermal loads

Approach:
- Thermal conductance break: Insert High temperature superconductor (HTS) on thin substrate into leads
- High density connector

Status:
- Design and connectorization complete
- HTS manufacturing and mounting incomplete

H. Harshavardhan
Neocera, Beltsville MD

HTS on flexible YSZ substrate
SBIR phase 1: YBCO on YSZ
SBIR phase 2: pulsed e beam dep.

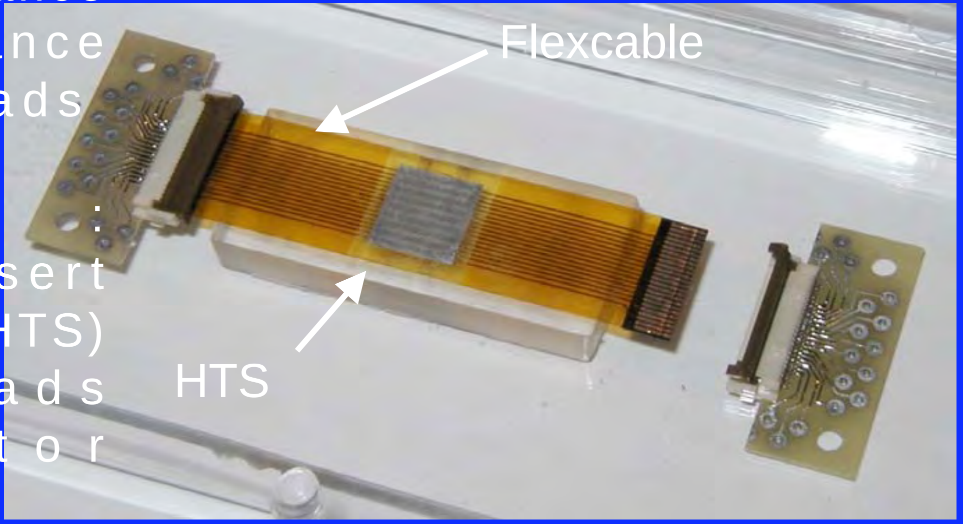

Prototype flexible cable with HTS thermal block

From Jochen Mannhart (Lecture Saas Fee)

Low Heat-Load, Wide Band Microwave Leads For RT to 70K

Andrew Smith
NG Space Technology
Redondo Beach, California

TRW patented design concept before beginning work

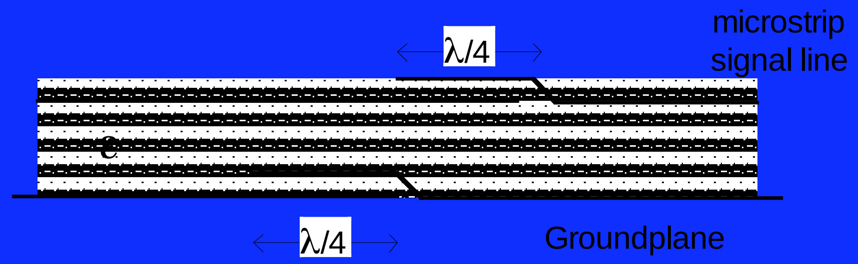

Technical Challenge:

- Cryogenic microwave systems (filters, low noise amplifiers) must connect room temperature signals to a cryogenic stage
- Low electrical resistance comes with low thermal resistance and therefore high thermal loads

Approach:

- Multli-layer flexible cable
- Quarter-wavelength resonators break thermal path

Progress

- Prototype developed and tested
- Most useful > 10 GHz

Prototype flexible microwave cable

From Jochen Mannhart (Lecture Saas Fee)

Deborah Van Vechten ONR